Investigation of Monoclonal Antibodies Generated against the Growth Hormone Receptor on Growth Hormone Signaling

Inaugural-Dissertation

zur

Erlangung des Doktorgrades

Dr. rer. nat.

der Fakultät für

Biologie

an der

Universität Duisburg-Essen

vorgelegt von

Esra Guen

aus Werne, Deutschland

April 2018

DOI: 10.17185/duepublico/46490
URN: urn:nbn:de:hbz:465-20220704-104758-8

Die der vorliegenden Arbeit zugrunde liegenden Experimente wurden an der University of Southern California (Los Angeles, Kalifornien, USA) und der Abteilung Molekularbiologie II der Universität Duisburg-Essen (Deutschland) durchgeführt.

1. Gutachter: Prof. Dr. Shirley Knauer
2. Gutachter: Prof. Dr. Perihan Nalbant

Vorsitzender des Prüfungsausschusses: PD Dr. Marc Seifert

Tag der mündlichen Prüfung: 25.06.2018

Table of Contents

1. Introduction

1.1. The Growth Hormone Receptor

The growth hormone receptor (GHR) is ubiquitously expressed on the cell surface of target cells that are generally involved in cell growth, constitutive cell proliferation and cell differentiation (de Vos *et al.,* 1992). Determination of mRNA expression of the GHR on a broad range of human tissues and cell lines shows that it is mostly enriched in the liver, adipose tissue, muscle cells and the kidney (Ballesteros *et al.,* 2000) (Fig. 1.1.).

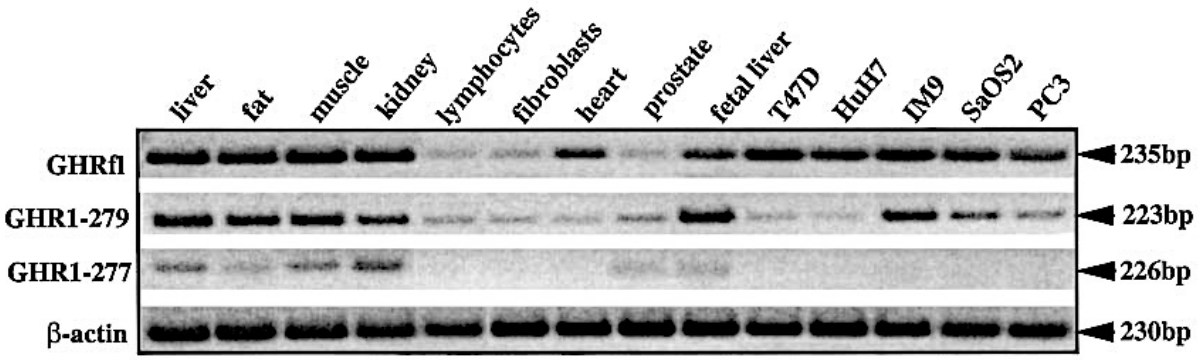

Fig. 1.1. Relative abundance and distribution of the GHR in human tissues and cell lines (modified from Ballesteros *et al.,* 2000).

RT-PCR products of three GHR isoforms were analyzed by agarose gel electrophoresis and exposure to UV after staining with ethidium bromide. The relative molecular sizes of the products are depicted in base pairs (bp). GHR1-279 and GHR1-277 represent alternatively spliced transcripts at exon 9 of the full-length GHR (GHRfl) gene. The GHR1-279 transcript lacks 26 base pairs at exon 9, whereas for GHR1-277 exon 9 is fully deleted (Dastot *et al.,* 1996; Ross *et al.,* 1997).

Important physiological functions mediated through the GHR include the regulation of postnatal growth, metabolism of bone, cartilage and muscle cells, regulation of lactation, hematopoiesis, immune function, cognition, gut function, and contribution to oncogenesis (de Vos *et al.,* 1992; Brooks *et al.,* 2014; Waters, 2016). These functional properties are the result of GHR activation, which involves binding and association of the GHR with its ligand, the growth hormone (GH). It further requires sequential receptor homodimerization, and conformational changes within the receptor that result in the conversion of the extracellular signal to an intracellular signal, and thus exertion of the implications mentioned above.

1.2. Structural Properties of the Growth Hormone Receptor

The GHR belongs to the superfamily of hematopoietic receptors, which is more commonly known as class I cytokine receptors (Cosman *et al.,* 1990; KI *et al.,* 1990; Bazan, 1990). These receptors represent transmembrane receptors, which recognize, bind and respond to cytokines comprised of four α-helices. The GHR was the first receptor from this family to be cloned and characterized. Therefore, it served as an archetype for the remaining 30 receptors of this family for cytokine signaling. Other members of this superfamily include receptors for erythropoietin, prolactin, leptin, thrombopoietin, LIF, CTNF, oncostatin-M, cardiotropin-1, a majority of the interleukins and hematopoietic colony-stimulating factors (Waters, 2016) (Fig. 1.2.).

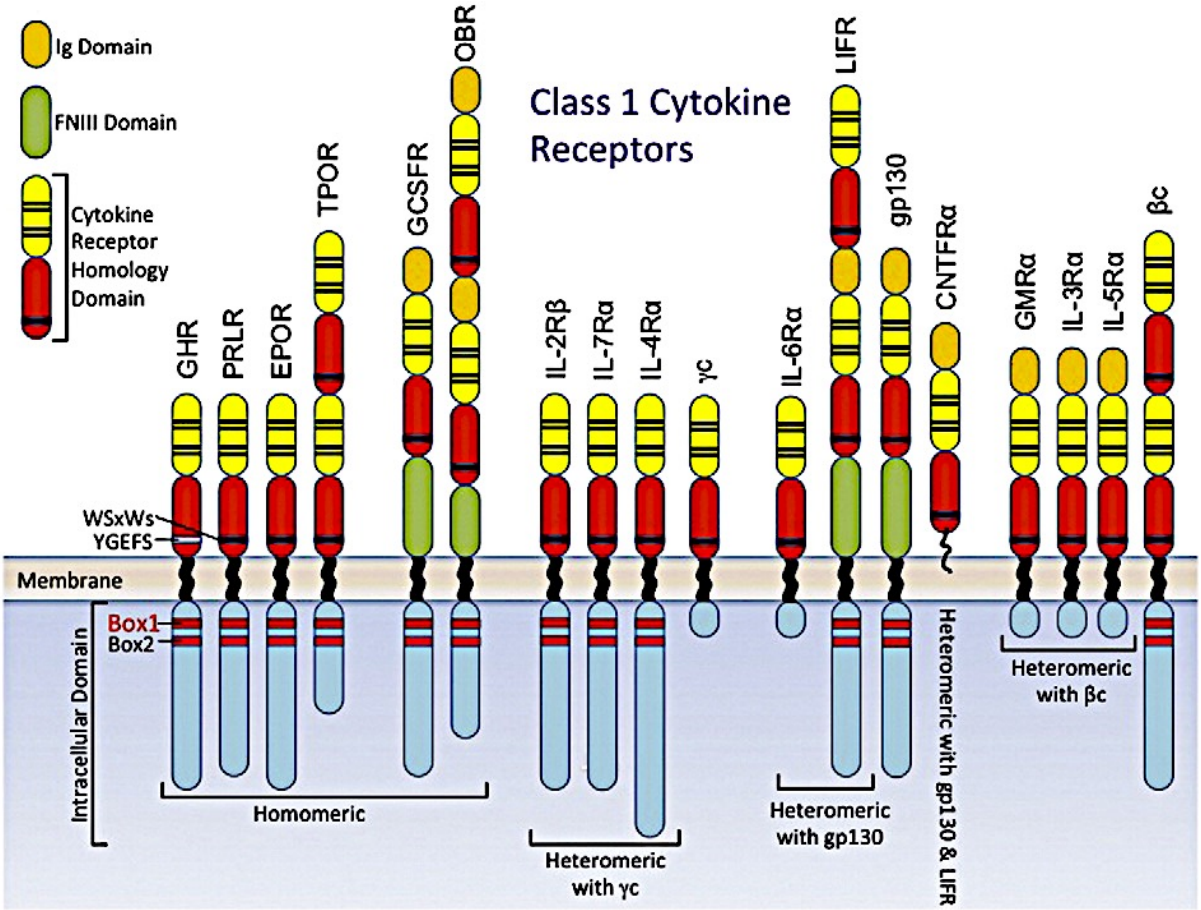

Fig. 1.2. Schematic representation of the domain structures of class I cytokine receptors (modified from Waters, 2016).

Commonly shared features of homomeric and heteromeric class I cytokine receptors include disulfide bonded domain I (yellow) and domain II (red) within the cytokine receptor homology domain. Evolutionarily conserved sequences within Box 1 and Box 2, as well as the WSxWS motif (YGEFS motif for the GHR) also present hallmarks, which are common for this particular superfamily of receptors.

Structurally, the class I cytokine receptors are all single transmembrane pass receptors, which can form homodimers or heterodimers with accessory proteins (Waters *et al.,* 1999). They bear a three-domain organization consisting of an extracellular ligand binding domain, a single transmembrane domain and an intracellular domain (de Vos *et al.,* 1992). The cytokine receptor homology domain is a core component of the extracellular portion and consists of two fibronectin III like modules (FNIII). Each of these modules is structurally organized in a seven-stranded beta sandwich, which modulates the ligand binding activity of the receptors (Waters, 2016). Furthermore, an evolutionary conserved WSxWS motif is present in the lower FNIII module, which is responsible for the stability and structural integrity of the receptors. However, for the GHR, the YGeFS motif represents the equivalent for the WSxWS motif. The core component and structurally characteristic feature of these receptors is the conserved proline-rich Box 1 domain, which is crucial for the association with accessory proteins such as tyrosine Janus kinases (JAK). These accessory proteins are located closer to Box 2, a domain rich in aromatic and acidic amino acids. The Janus kinases phosphorylate tyrosine residues within the intracellular domain of the receptors as well as other cytosolic substrates and therefore promote the activity of the receptors. For the GHR, the phosphorylated tyrosine residues within the intracellular domain serve as a docking platform for SH2 (Src Homology 2) domain-containing proteins such as STAT5a and STAT5b (Waters, 2016). The anchoring process to the GHR facilitates their phosphorylation through structural proximity, followed by STAT5 dimer formation and nuclear translocation where it functions a transcription factor for the regulation of target genes (Lichanska and Waters, 2008).

Understanding of signal transduction through the GHR is tied to a deep knowledge of the three-dimensional structure of the GHR itself. As previously mentioned, the GHR is structurally and functionally divided into an extracellular domain (ECD; residues 19-262), a transmembrane domain (TMD; residues 263-288) and an intracellular domain (ICD; residues 289-638) (de Vos *et al.,* 1992; Lichanska and Waters, 2008) (Fig. 1.3.).

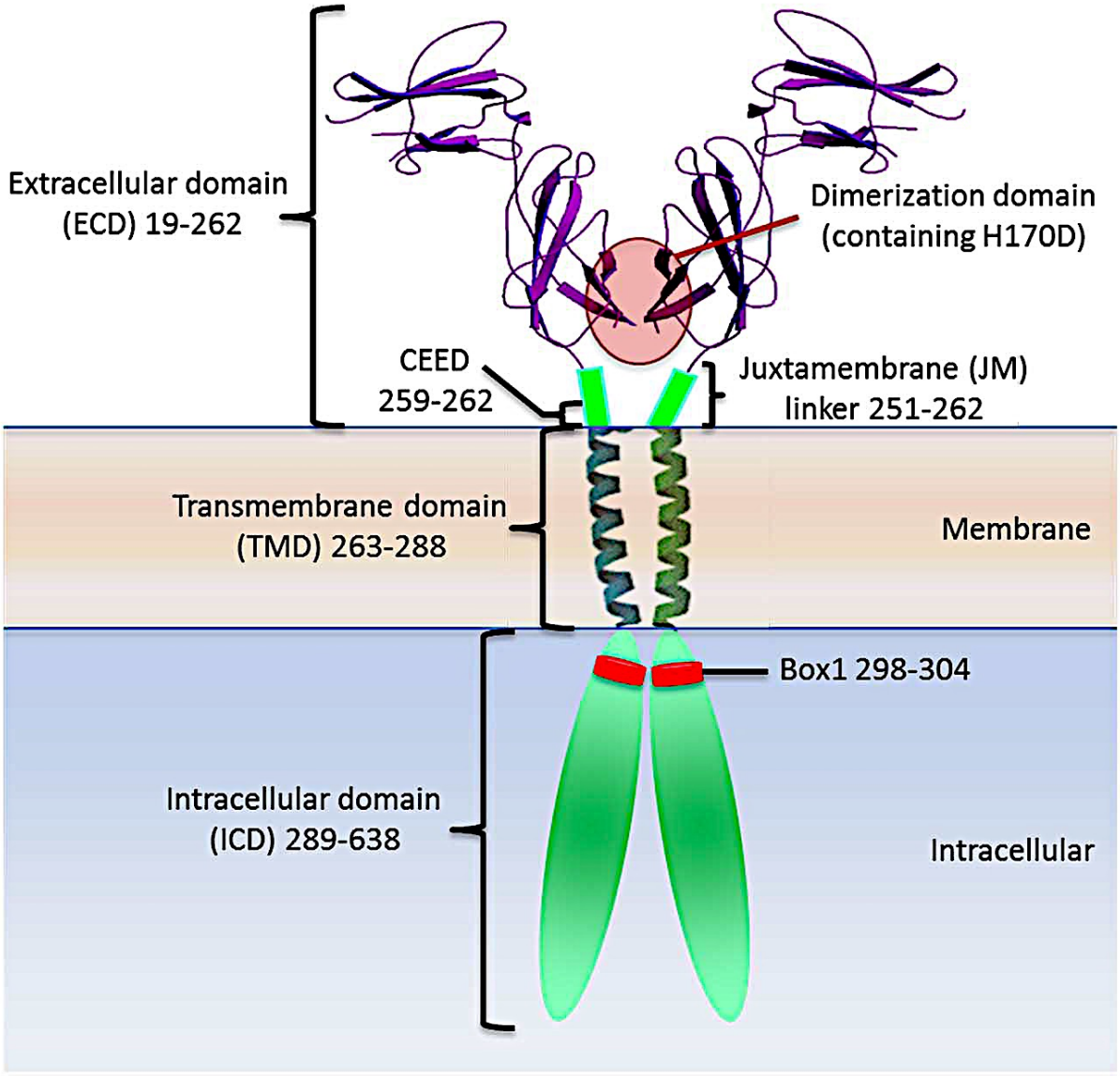

Fig. 1.3. Illustration of the GHR and its segments including residue numbers for the respective domains (modified from Lichanska and Waters, 2016).

The schematic representation demonstrates the segments of the GHR as well as other key components contributing to its activity such as the juxtamembrane linker sequence (JM; residues 251-262), which provides flexibility in the absence of a ligand (Kubatzky *et al.,* 2005).

The extracellular domain of the GHR can occur naturally in the circulation in the form of a GH binding protein (GHBP; residues 19-246), which binds GH with the same affinity as the GHR (Fuh *et al.,* 1990), and functions as regulator of GH bioavailability (Barnard and Waters, 1997). Binding of the GH to the GHR occurs in a stoichiometry of 1:2. Basically, one molecule of GH will bind to two molecules of the GHR (Cunningham *et al.,* 1991), and therefore initiate activation of the GHR and its downstream signaling pathway.

1.3. The Growth Hormone

The growth hormone (GH), also known as somatotropin or somatropin, is a polypeptide hormone produced and secreted by somatotropic cells of the anterior pituitary gland in mammals. It has a molecular weight of 22,124 daltons and is comprised of 191 amino acids. Its three-dimensional structure is arranged in four α-helices and two disulfide bridges, which was initially characterized for the porcine growth hormone (Abdel-Meguid *et al.,* 1987; Chantalat *et al.,* 1995) (Fig. 1.4).

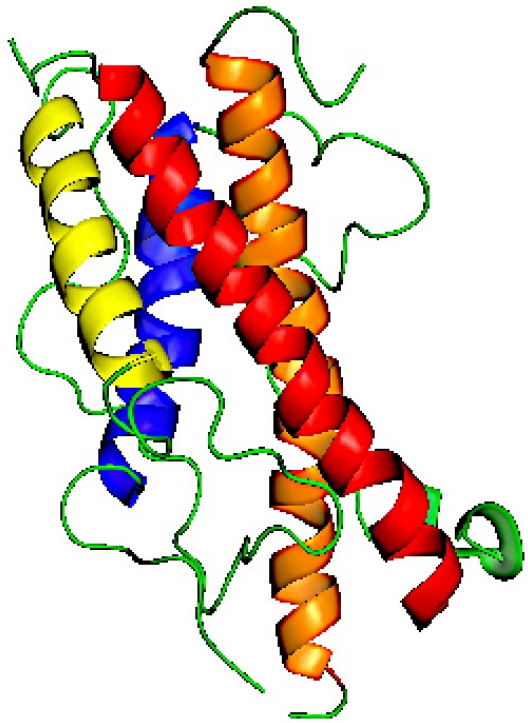

Fig. 1.4. Crystal structure of the human GH (hGH) determined by X-ray crystallography at 2.5 Angstrom (modified from Chantalat *et al.,* 1995).

Amino acid residues of the corresponding helices are labeled as follows: helix 1 = residues 9-34 (red); helix 2 = residues 72-92 (blue); helix 3 = residues 106-128 (yellow); helix 4 = residues 155-184 (orange) (de Vos *et al.,* 1992).

Release of the GH follows a pulsatile mode, which is controlled by an endocrine system involving the hypothalamic GH-releasing hormone (GHRH; also known as somatocrinin) and the GH-inhibiting hormone (GHIH; also known as somatostatin, or somatotropin release-inhibiting factor (SRIF)) (Farhy *et al.,* 2001; Plotsky and Vale, 1985; Tannenbaum, 1991; Tannenbaum and Ling, 1984; Terry and Martin, 1981; Wehrenberg *et al.,* 1982). Both hormones are produced by neuroendocrine neurons of the hypothalamus and circulate through the hypophysial

portal axis to reach the pituitary somatotrope cells, where the GHRH stimulates GH release and the GHIH, respectively, suppresses GH release (Hartman *et al.,* 1993). Furthermore, excessive levels of GH cause inhibition of secretion through stimulation of GHIH, and repression of GHRH in a negative feedback loop to restore homeostasis (Davis *et al.,* 1977; Frohman *et al.,* 1992; Giustina and Veldhuis, 1998; Jansson *et al.,* 1985; Plotsky and Vale, 1985; Steiner *et al.,* 1978; Veldhuis *et al.,* 2000). Additionally, the pulsatile release of GH exhibits a sexually dimorphic divergence in rodents and humans, which are characterized by rapid oscillations differing in amplitude, duration and frequency (Giustina and Veldhuis, 1998; Painson *et al.,* 2000; Pincus *et al.,* 1996; Carlsson *et al.,* 1990; Chen *et al.,* 1995; Clark *et al.,* 1987; Clark *et al.,* 1988; Gevers *et al.,* 1998; Hartman *et al.,* 1991; Jansson *et al.,* 1985; Maiter *et al.,* 1990; Mueller *et al.,* 1999; Ono *et al.,* 1991; Ono *et al.,* 1995; Painson *et al.,* 1992; Robinson, 1991; Tannenbaum, 1991; Farhy *et al.,* 2001) (Fig. 1.5.).

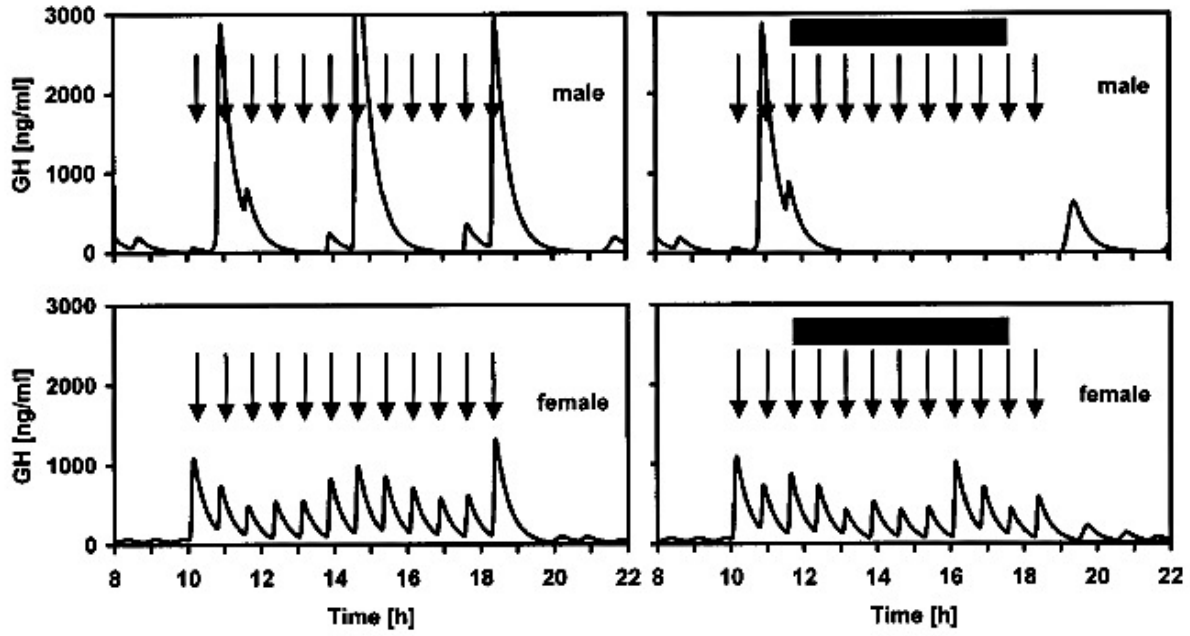

Fig. 1.5. Sexually dimorphistic GH pulsatile secretion patterns in male and female rats (modified from Farhy *et al.,* 2002).

The gender-specific GH secretion models controlled by GHRH and GHIH have especially been extensively studied in rats. The gender-specific characteristics are due to differences in responses to external stimuli of GHRH (Clark and Robinson, 1985; Wehrenberg *et al.,* 1985), endogenous hypothalamic protein concentrations of GHRH and GHIH (Ganzetti *et al.,* 1986), hypothalamic mRNA concentrations of GHRH and GHIH (Choween-Breed *et al.,* 1989, Uchiyama *et al.,* 1990; Argente *et al.,* 1991; Maiter et al., 1991), GHRH receptor expression on somatotropic cells of the anterior pituitary gland (Ono *et al.,* 1995), and GH auto feedback regulation (Carlsson *et al.,* 1990).

1.4. Functional Implications of the Growth Hormone

After the release of GH into the bloodstream from the anterior pituitary gland, it exerts a wide variety of physiological effects, which can generally be defined as anabolic. GH can mediate anabolic effects either directly through binding to the GHR on target cells, or indirectly through inducing the expression of insulin-like growth factor I (IGF-1), which is primarily secreted from the liver in response to activation of the GH signaling pathway. Indirect effects mediated through IGF-1 involve the stimulation of proliferation and regulation of differentiation of chondrocytes during development (Tsukazaki *et al.,* 1994). Moreover, GH exerts a wide variety of actions on substrate metabolism, involving lipid, glucose and protein metabolism. Changes in the corresponding metabolic pathways and their interplay has been shown to be of evolutionary advantage: During periods of substantial energy excess in form of food, GH is mediating retention of nitrogen sources, while during periods of prolonged deprivation of energy sources and scarcity of food, GH acts as a molecular switch substituting carbohydrate and protein metabolism to consumption of lipids as energy source to enable preservation of essential protein sources and survival during periods of energy source deprivation (Møller and Jørgensen, 2009).

1.4.1. Effects of GH on Lipid Metabolism

Nocturnal bursts of GH secretion have been correlated with an increased circulating concentration of free fatty acids and ketone bodies, indicative of ketogenesis as well as β-oxidation of triglycerides and their breakdown into free fatty acids (FFA) and glycerol (Møller *et al.,* 1990). Supportive evidence of this phenomenon has been experimentally demonstrated in a study performed in healthy participants, where GH has been administered in a pulsatile fashion or continuously in a dose-dependent manner ranging from 70 µg to 500 µg, leading to increased circulating concentrations of FFA and glycerol, as well as higher rates of lipid oxidation (Krag *et al.,* 2007; Møller *et al.,* 1990; Møller *et al.,* 1992; Hansen *et al.,* 2002). Additional studies have shown that elevated FFA levels are mainly derived from femoral and abdominal adipose tissue (Gravhølt *et al.,* 1999; Hansen *et al.,* 2002). Visceral adipose tissue has not been directly attributed to contribute to the phenomena described above, but experimental evidence based on long-term GH administration has been shown to decrease visceral fat content, indicating

participation (Atallah *et al.,* 2007). Breakdown of triglycerides into FFA and glycerol is to some extent attributed to the hormone-sensitive-lipase (HSL), as experimental evidence based on the application of the nicotinic derivative acipimox, an HSL inhibitor, indicates induction of downregulated lipolytic activity of GH in humans (Beauville *et al.,* 1992; Nielsen *et al.,* 2001; Nørrelund *et al.,* 2004; Segerlantz *et al.,* 2001; Piatti *et al.,* 1999).

1.4.2. Effects of GH on Glucose Metabolism

Infusion of GH (100 µg/h) over a timeframe of 4 hours into healthy participants leads to an initial 40% rapid decline of glucose uptake in the forearm muscles, and simultaneously to a postponed 50% decline of glucose oxidation and equal decline in non-oxidative glucose usage (Møller *et al.,* 1990). In contrast to this, total turnover rates of glucose appear to be constant (Møller *et al.,* 1990). This aspect of GH effect is supported by initial studies reporting an accelerated > 50% decline of glucose uptake in the forearm after GH administration (Rabinowitz *et al.,* 1965; Zierler and Rabinowitz, 1963). It has been described that the initial rapid decline might primarily be due to a direct effect mediated by GH or secondarily attributed to an increased lipid oxidation, potentially inhibiting glucose uptake (Dagenais *et al.,* 1976; Rabinowitz *et al.,* 1965). Furthermore, *in vitro* studies based on GH treatment revealed increased gluconeogenesis originating from alanine or lactate in canine kidney cortex (Rogers *et al.,* 1990).

1.4.3. Effects of GH on Protein Metabolism

Effects of GH related to protein metabolism can generally be described as being anabolic, associated with the promotion of protein synthesis and reduced degradation and oxidation of amino acid residues within the whole body and the muscle (Møller *et al.,* 2009). Evidence supporting the phenomena described above was experimentally delivered through the administration of GH in the brachial artery of the forearm contributing to elevated rates of amino acid assembly and decreased levels of proteolysis in the muscle (Fryburg *et al.,* 1991; Fryburg *et al.,* 1992). Moreover, studies performed by Copeland and Nair delivered experimental proof of a 20% reduction in leucine oxidation and an increase in the non-oxidative assembly of

leucine residues within the whole body, as well as decreased proteolysis rates for phenylalanine and leucine in the muscle (Copeland and Nair, 1994). Studies assessing the long-term effect GH on protein metabolism were performed through the delivery of high doses of GH (0.1 mg/kg/d) over a period of seven days showing increased rates for leucine protein biosynthesis and leucine oxidation within the whole body (Horber and Haymond, 1990). Investigations supporting these reports were concluded by Yarasheski *et al.,* effectively demonstrating no changes in muscle protein biosynthesis after continuous administration of GH over 14 weeks (Yarasheski *et al.,* 1992).

1.5. GH-GHR Interaction and GH Receptor Subunit Rotation

The physiological and metabolic effects mediated through GH occur as a result of its binding to the GHR leading to subsequent subunit rotation of the receptor and activation of downstream signaling. Interactions of GH, a ligand, with its corresponding receptor, the GHR, are described as examples of molecular recognition (de Vos *et al.,* 1992). Crystal structure analysis of the extracellular domain of the human GHR (hGHR) bound to human GH (hGH), indicates that binding and molecular recognition appears in a stochiometry of 1:2 (de Vos *et al.,* 1992). A ternary complex is formed consisting of one molecule of GH, which is asymmetrically bound to two extracellular molecules of the GHR stabilized by interactions of C-terminal subdomains of both extracellular domains, forming a homodimer (de Vos *et al.,* 1992; Chen *et al.,* 1997; Bernat *et al.,* 2003) (Fig. 1.6.).

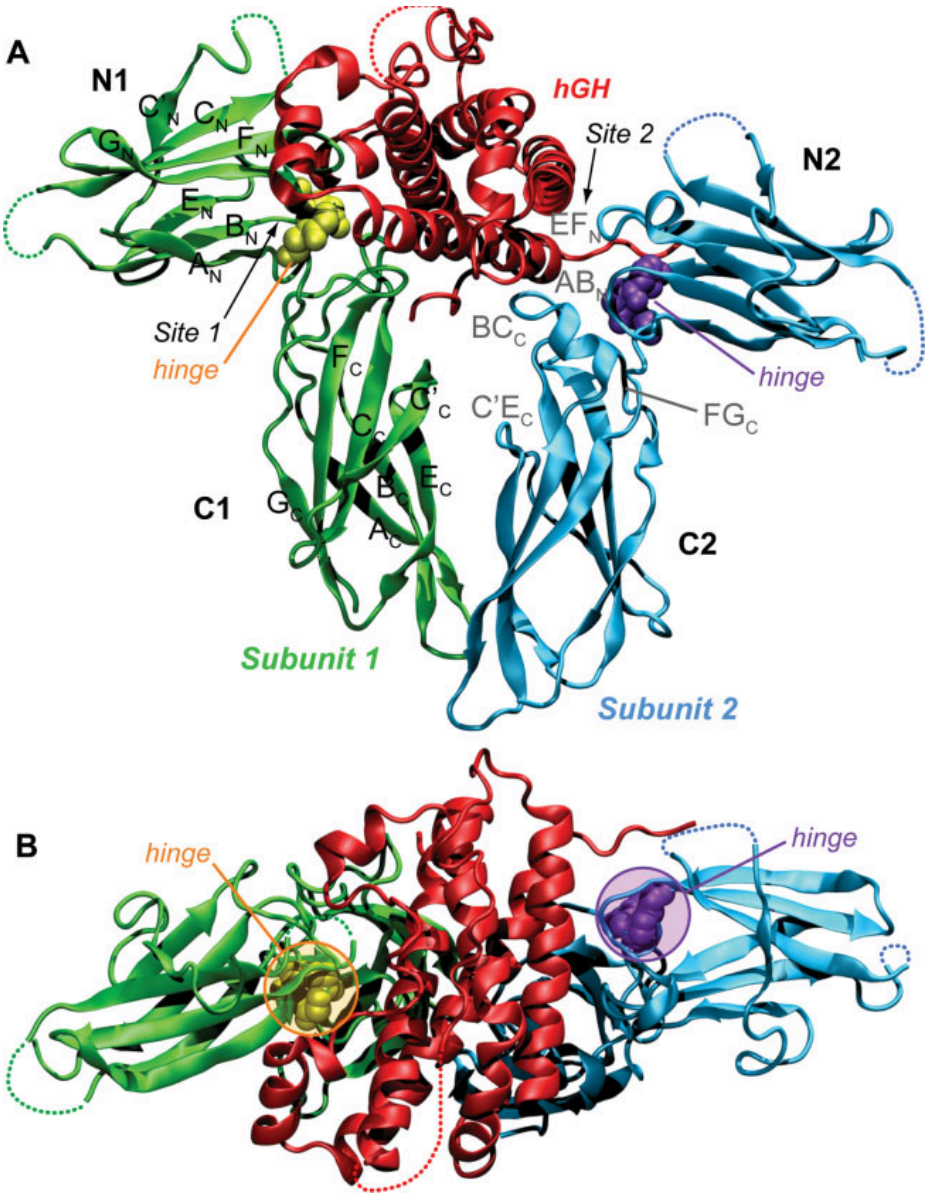

Fig. 1.6. Ribbon presentation of the hGH-hGHR ternary complex (modified from Poger and Mark, 2009).

Side view (A) and top view (B) of the hGh-hGHR ternary complex (GH: red; GHR subunit 1: green; GHR subunit 2: blue). Both subunits consist of an N-terminal subdomain (N1 and N2) and a C-terminal subdomain (C1 and C2). The respective subdomains are associated through a tetrapeptide hinge region (amino acid residues 124-127: yellow and violet balls). Loops absent in the crystal structure are depicted as dotted lines. Loops involved in key interactions are highlighted in gray.

Within the ternary complex, both GHR subunits contribute the same amino acid residues to the binding process while both binding sites (binding site I and binding site II) on the hGH display no structural similarity (de Vos *et al.,* 1992; Lee and Richards, 1971) (Fig. 1.7.).

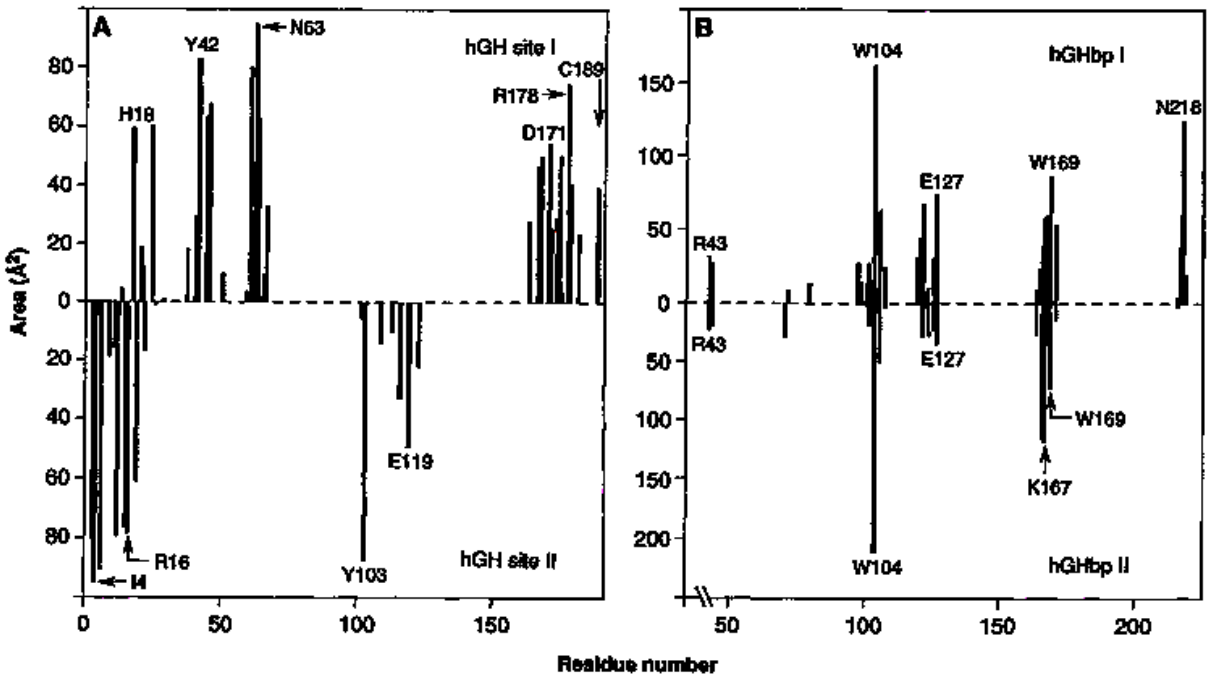

Fig. 1.7. Solvent accessibility upon ternary complex formation (modified from de Vos *et al.,* 1992; Lee and Richards, 1971).

Amino acid residues of GH on binding site I (panel A, top) and on binding site II (panel A, bottom) contributing to binding (A). Amino acid residues of the GHR contributing to binding on the extracellular domain of molecule I (panel B, top) and of molecule II (panel B, bottom) (B).

Although structural data regarding the arrangement of the ternary complex has been available over two decades, the mechanism of hGHR activation remains highly disputed. In a preliminary model, it has been assumed that binding of GH to the GHR induces receptor homodimerization leading to subsequent activation of the receptor itself and downstream signaling since dimerization has been attributed as an essential process contributing to intracellular signaling (Chen *et al.,* 1997; Poger and Mark, 2009) (Fig. 1.8. A). According to this model, receptor dimerization leads to the interaction of the Box 1 and Box 2 motifs of the intracellular domains of the GHR, leading to subsequent recruitment and activation JAK2, which in turn phosphorylates and therefore activates the hGHR and STAT5 to initiate downstream signaling (Argetsinger *et al.,* 1993; Carter-Su *et al.,* 2000; Herrington and Carter, 2001). However, although there are *in vitro* and *in vivo* indications seemingly supporting this assumption (de Vos *et al.,* 1992; Fuh *et al.,* 1992; Cunningham *et al.,* 1991; Clackson *et al.,* 1998), this assumption has been challenged due to the fact that even in the absence of GH, the GHR already exists as a preformed homodimer (Gent *et al.,* 2003; Frank, 2002; Brown *et al.,* 2005; Gent *et al.,* 2002).

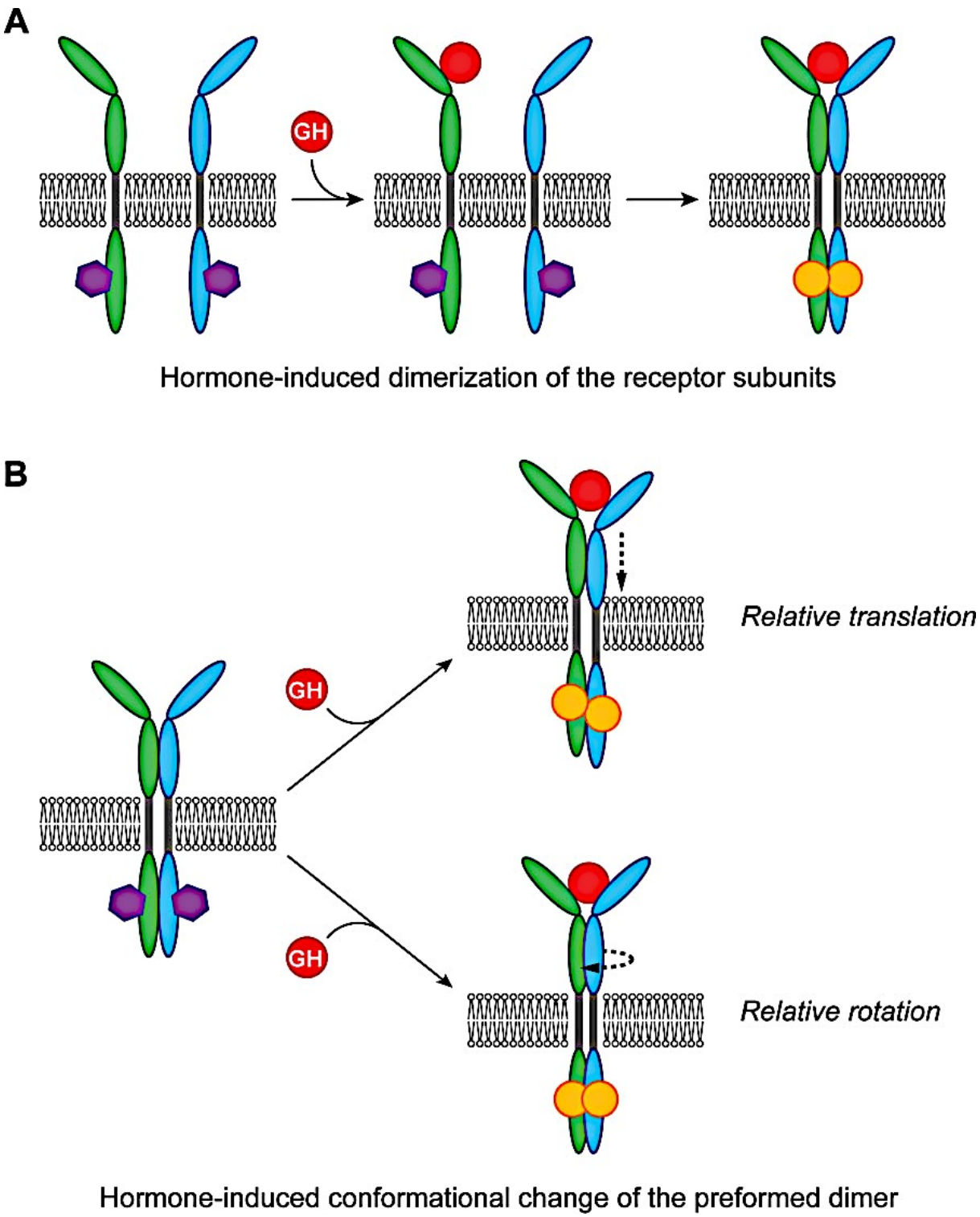

Fig. 1.8. Models of hGHR activation (modified from Poger and Mark, 2009).
In the original model, binding of hGH induces dimerization of the hGHR subunits (subunit 1 and subunit 2) (panel A). In a new model challenging the existing dogma, hGHR already exists as a preformed dimer (panel B). Binding of hGH to the hGHR induces conformational changes within the receptor in order to activate the hGHR, either through a relative transition of the corresponding receptor subunits (panel B, upper right panel) or through a relative rotation of the receptor subunits.

Considering the fact that a preexisting homodimer on the cell surface of target cells is already given in a physiological state, activation of the hGHR must be

accomplished through induced conformational rearrangements within the receptor subunits. Additional evidence supporting this assumption comes from detailed analysis and comparison of three essential states of hGHR: (1) the hGH bound to both receptor subunits, (2) the hGH bound to a receptor monomer, and (3) the unbound hGHR monomer (Brown *et al.,* 2005). Comparative studies show insignificant structural differences of the receptor subunits and within the dimerization domain (Brown *et al.,* 2005). Given the comparative studies and the evidence of a preexisting homodimer, the activation of the hGHR must be mediated through a structural rearrangement. There are three scenarios outlining the activation of a dimer: (1) the activation involves a relative translation of the receptor subunits (Fig. 1.8. B, upper right panel), (2) the receptor subunits are engaged in a relative rotation to induce receptor activation (Fig. 1.8. B, lower right panel), or (3) a juxtaposition of the receptor subunits inducing a shifted angle or dissociation of the receptor subunits (Poger and Mark, 2009). Activation of the hGHR leads to subsequent downstream activation of GH signaling.

1.6. GH Signaling

Physiological effects of GH are mediated through its binding to the GHR on the cell surface of target cells. Activation of the GHR initiates a cascade of intracellular signaling events, which contribute to the physiological manifestations of GH action (Okada and Kopchick, 2001) (Fig. 1.9.).

Signal transduction of GH-GHR interaction initiates activation of JAK2 (Carter-Su and Smith, 1998). Activation of JAK2 subsequently promotes phosphorylation of the GHR, establishing docking sites for intracellular proteins, such as the STATs (Carter-Su and Smith, 1998). Although STAT5 has been predominantly associated with GH signaling, STAT1, STAT3, and STAT4 are also proven to be engaged in signaling events (Smit *et al.,* 1996). After association with the docking sites on the GHR, STAT molecules become phosphorylated at tyrosine residues, dissociate from the receptor to form dimers in the cytosol and translocate into the nucleus to regulate the transcription of genes, involving IGF-1, serum protease inhibitor 2.1 (spi2.1) and interferon-α-sequence (GAS)-like response element (GLE) (Kopchick *et al.,* 1999).

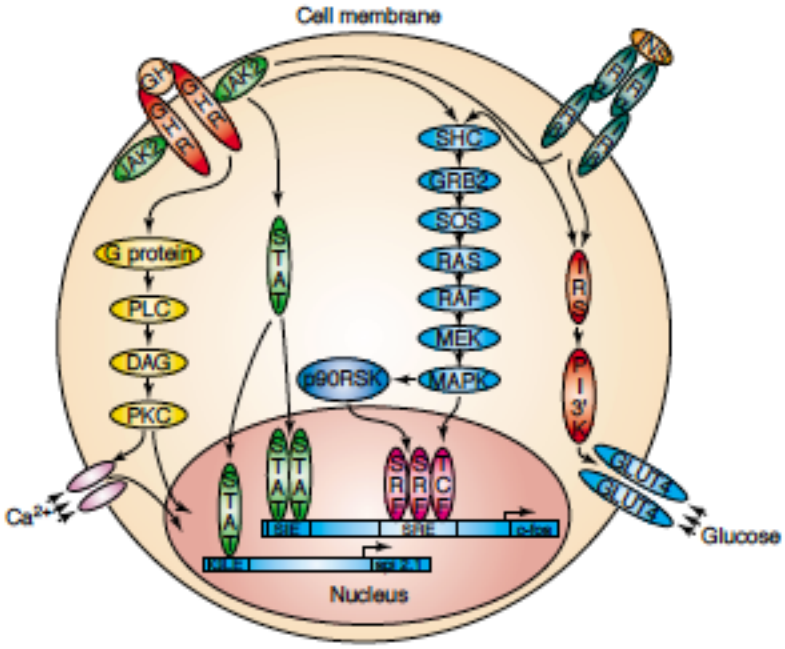

Fig. 1.9. Intracellular signal transduction of GH (modified from Okada and Kopchick, 2001; Kopchick *et al.,* 1999).

Following activation of the GHR, JAK2 becomes phosphorylated and therefore activated. Phosphorylated JAK2 phosphorylates GHR to create docking sites for the STATs. Once bound to the docking sites, the STATs become phosphorylated, dissociated from the receptor, dimerize and translocate into the nucleus to regulate the expression of genes. STAT5 regulates the expression of the serum protease inhibitor 2.1 (spi2.1) gene through biding to the interferon-α-sequence (GAS)-like response element (GLE). STAT5 and STAT1 are also engaged in the regulation of the sis-inducible element (SIE) of the C-fos promoter. Activation of the MAPK (mitogen-activated protein kinase; also attributed as ERK, extracellular signal-regulated kinase) pathway involves a cascade of intracellular proteins including SHC (Src homology 2 domain-containing), GRB2 (growth factor receptor bound protein 2), SOS (son of sevenless), RAS (proto-oncogene protein p21), RAF (rapidly accelerated fibrosarcoma), and MEK (MAP-ERK kinase). PLC (phospholipase C) activation causes an increase in DAG (diacylglycerol), leading to the initiation of the PKC (protein kinase C) pathway. Activation of the insulin-signaling pathway is mediated through interaction of insulin (INS) with the insulin receptor (IR), where each monomer is comprised of a monomer consisting of the two subunits IRα and IRβ. The pathway involves IRS (insulin receptor substrate), PI3K (phosphatidylinositol 3-kinase), and GLUT-4 (Glucose transporter type 4).

The MAPK and the insulin-signaling pathway are also implied to be involved in GH signaling (Vanderkuur *et al.,* 1997). A plethora of intracellular proteins mediate activation of the MAPK pathway involving SHC, GRB2, SOS, RAS, RAF, and MEK (Yamauchi *et al.,* 1998). The insulin-signaling pathway involves IRS1, IRS2, and IRS3 (Yamauchi *et al.,* 1998; Souza *et al.,* 1994). IRS phosphorylates PI3K, which in turn phosphorylates GLUT4 to induce its translocation to the cell membrane to promote glucose uptake (Le Marchand-Brustel *et al.,* 1999).

1.7. IGF-1 Signaling

The GH-GHR signaling pathway is controlling the expression of the *igf-1* gene, which encodes for its corresponding protein, IGF-1. Effects of IGF-1 are indirectly mediated through GH, as it is produced in response to GH signaling predominantly by the liver (Fürstenberger and Senn, 2002). Once released into circulation, it mediates physiological effects such as the promotion of cell growth and differentiation, transformation, and inhibition of apoptotic signaling pathways through activation of survival signaling pathways (Zha and Lackner, 2010). IGF-1 signaling compromises the engagement of two receptors, IGF-1R (IGF-1 receptor) and IGF-2R (IGF-2 receptor), their corresponding ligands IGF-1 and IGF-2, as well as a set of intracellular proteins transmitting the extracellular signal into an intracellular event (Zha and Lackner, 2010) (Fig. 1.10.).

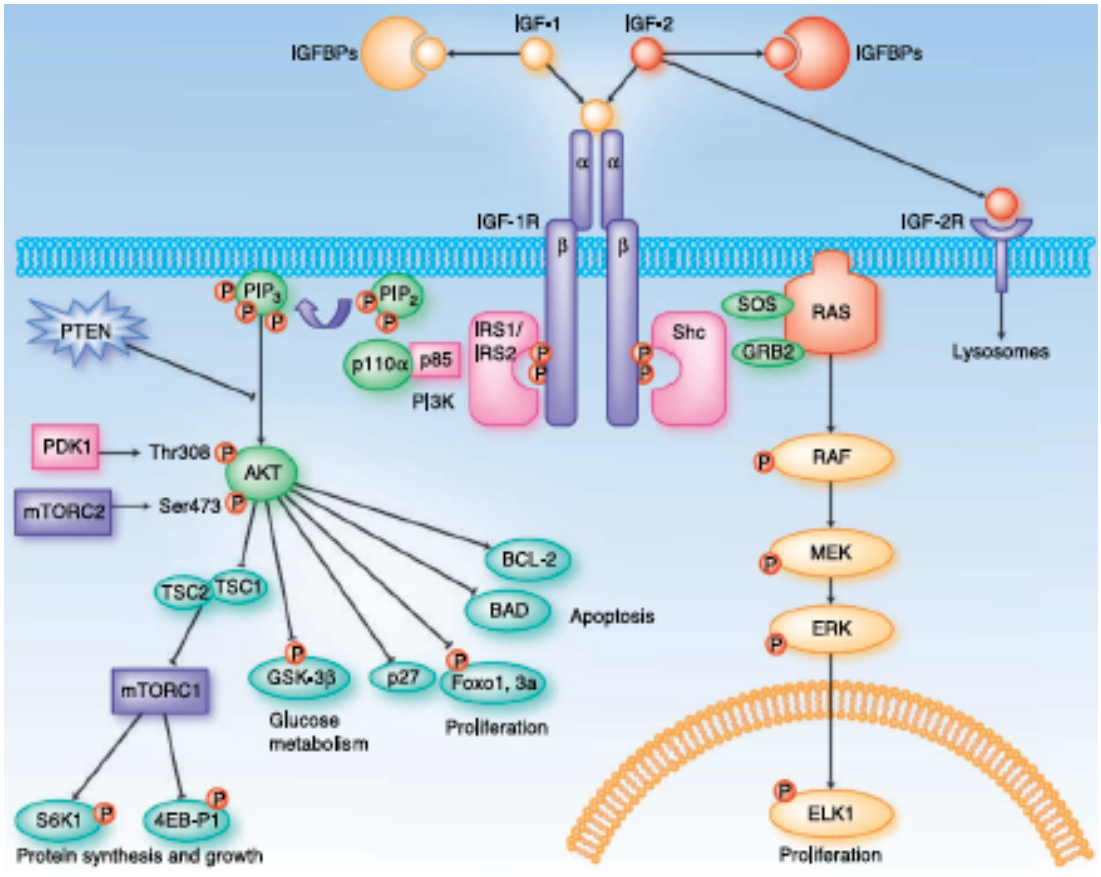

Fig. 1.10. Intracellular signal transduction of IGF-1 (modified from Zha and Lackner, 2010).
Binding of IGF-1 to the IGF1-R and subsequent receptor activation leads to the recruitment of intracellular adaptor proteins, such as IRS1 and IRS2, as well as Shc. The adaptor proteins transmit the signal through the PI3K-AKT (protein kinase B; PKB)-mTOR (mammalian target of rapamycin) pathway, and through the MAPK pathway. Both pathways promote survival signals, such as proliferation and resistance to apoptosis.

Binding of IGF-1 or IGF-2 to the IGF-1R stimulate catalytic activity of the corresponding receptor leading to cross-linking and autophosphorylation of the receptor (Zha and Lackner, 2010). Bioavailability of IGF-1 is meditated through insulin-like growth factor binding proteins (IGFBPs), a family of six carrier proteins, with IGFBP-3 being the most abundant protein (Shimizu and Dickhoff, 2017). In contrast to this, the bioavailability of IGF-2 is mediated through IGFBPs and IGF-2R, where receptor binding leads to the internalization and degradation of IGF-2 in lysosomes (Zha and Lackner, 2010) (Fig. 1.10.). Autophosphorylation of the IGF-1R creates docking sites for the adaptor proteins IRS1, IRS2, and Shc. IRS1 and IRS2 transmit the signal through the PI3K-AKT-mTOR pathway, in which the conversion of PIP2 (phosphatidylinositol 3,4-bisphosphate) to PIP3 (phosphatidylinositol 3,4,5-trisphosphate) through PI3K leads to the recruitment of kinases of the AKT family, in order to be phosphorylated by PDK1 (phosphoinositide-dependent kinase 1) and mTORC2 (mTOR Complex 2) (Zha and Lackner, 2010) (Fig. 1.10.). Phosphorylated AKT is then promoting a myriad of cellular effects, including protein synthesis and growth through the activation of mTORC1 (mTOR Complex 1), increased gluconeogenesis through the conversion of glucose into glycogen mediated by inhibition of GSK-3β (glycogen synthase kinase 3 beta), and most importantly resistance to apoptosis and increased cellular proliferation through the inhibition of FOXO (Forkhead box proteins), p27 (cyclin-dependent kinase inhibitor 1B), BAD (Bcl-2-associated death promoter), and Bcl-2 (B-cell lymphoma 2) (Zha and Lackner, 2010) (Fig. 1.10.).

1.8. Pathophysiological Effects of GH

Understanding the molecular basis of GH and its physiological effects allows the interpretation of clinical conditions associated with pathophysiological conditions of GH, which are attributed to its dysregulation. Acromegaly, a disorder that is characterized by excessive production of GH through the anterior pituitary gland leading to the enlargement of extremities, resembles one pathophysiological condition attributed to the dysregulation of GH. 25% of patients affected by acromegaly also develop diabetes (Sönksen *et al.,* 1993). Furthermore, considering its role in cellular proliferation and growth, experimental evidence supports the assumption that GH might impact neoplastic tissue growth (Jenkins *et al.,* 2006).

1.8.1. Acromegaly

Acromegaly represents a disorder characterized by a benign tumor of the anterior pituitary gland, which causes excessive GH production (Newman, 1999). As a consequence, this leads to an increase in circulating IGF-1 serum levels contributing to the development of pathophysiological manifestations characteristic for the disorder. Such characteristics include the enlargement of extremities, thyroid enlargement, thickening of the skin, sleep apnea, vascular endothelial dysfunction and hypertension contributing to cardiac complications, development of type two diabetes mellitus, dyslipidemia and glucose intolerance (Newman, 1999; Clayton, 2003) (Fig. 1.11.).

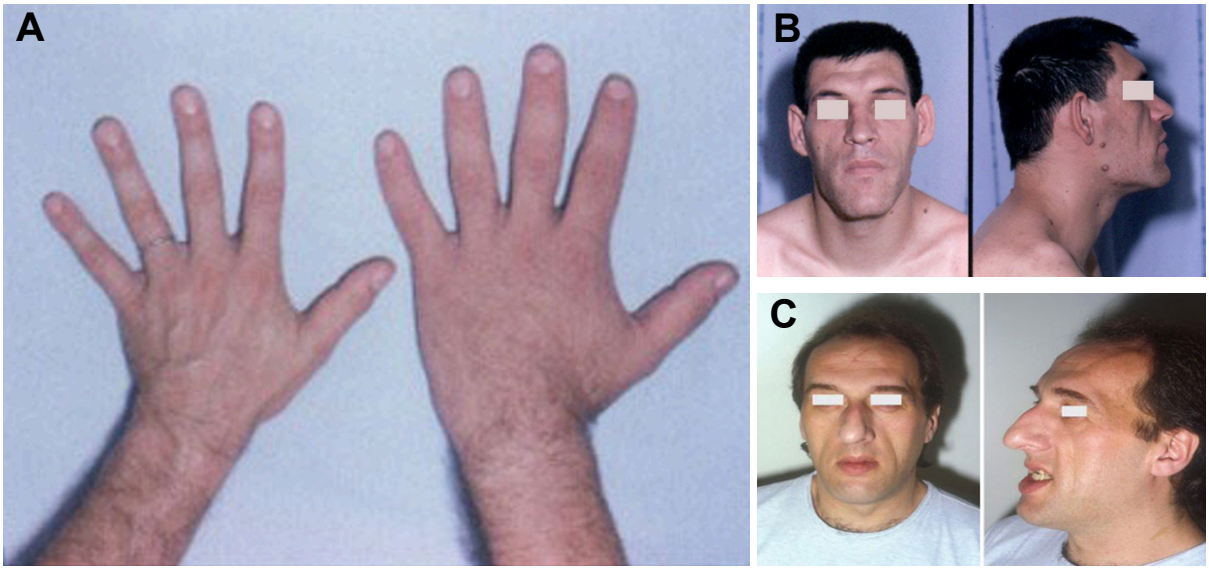

Fig. 1.11. Clinical manifestations of acromegaly (modified from Chanson and Salenave, 2008). The enlarged hand of an acromegalic patient (A, right) indicating characteristics such as soft tissue thickening, widened and stubby fingers in contrast to the hand of a physiologically healthy person (A, left). Facial features of an acromegalic patient indicate a widening of the nose, protruding eye brows and jaw, thick lips and a bulged forehead (B), as well as prognathism and dental malocclusion (C).

Treatment for this condition constitutes the surgical removal of the benign tumor (Freda *et al.,* 1998). However, a more promising approach entails treatment of acromegalic patients with a mutated form of GH termed pegvisomant. Pegvisomant represents a GHR antagonist, which possesses three modifications compared to native GH: (1) an amino acid substitution at the third α-helix at site 2 (Gly120Lys), (2) covalently bound PEG (polyethylene glycol) residues to increase the half-life of the antagonist (Olsen *et al.,* 1997; Clark *et al.,* 1996), and (3) amino acid substitutions at

site 1 to increase the binding affinity to the GHR (Clark *et al.,* 1996; Okada and Kopchick, 2001). Efficacy of pegvisomant has been proven in a double-blinded, randomized clinical study of 12 weeks, showing a decrease of circulating IGF-1 levels in 54%, 81%, and 89% of acromegalic patients after injection with 10mg, 15mg, and 20mg of pegvisomant, respectively (Trainer *et al.,* 2000). Furthermore, pathophysiological manifestations were also decreased after exposure to pegvisomant (Trainer *et al.,* 2000), indicating a successful and promising treatment for acromegalic patients (Fig. 1.12.).

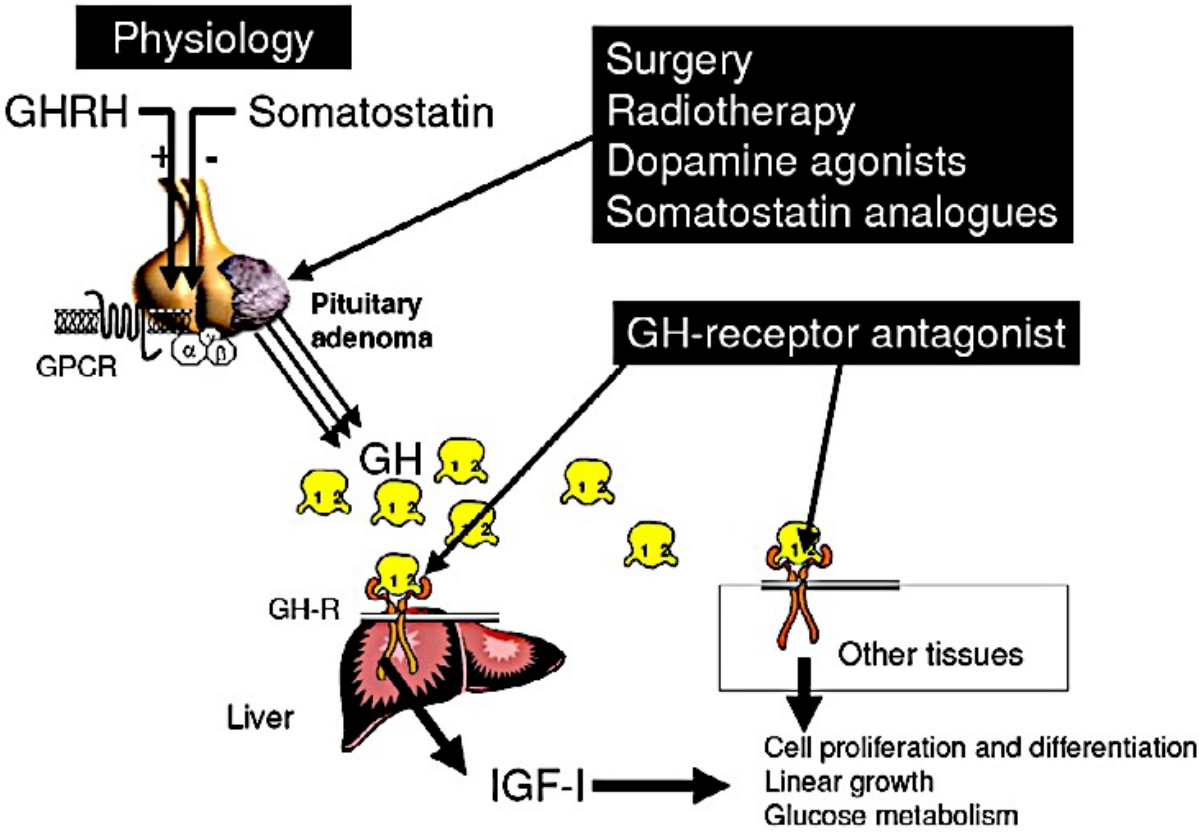

Fig. 1.12. Therapeutic approaches in acromegaly (modified from Chanson and Salenave, 2008). Adenectomy, radiotherapy, dopamine agonists and somatostatin analogues target the anterior pituitary adenoma, while GHR antagonists compete with native GH for binding to the GHR on the cell surface of target cells.

Irradiation of the pituitary adenoma with a dose of 50 Gray (Gy) represents an alternative approach. However, the efficacy of this treatment has been challenged due to data showing an increased likelihood of suffering from stroke many years after radiotherapy (Brada *et al.,* 1999). Dopamine agonists, such as bromocriptine, reduce IGF-1 levels only in 10% of patients affected by the condition (Newman, 1999; Abs *et al.,* 1998). Somatostatin analogs, such as octreotide and lanreotide, are able to

reduce IGF-1 levels in 50% to 80% of patients and are also able to reduce the volume of the pituitary adenoma in 70% of the patients (Sassolas *et al.,* 1990; Chanson *et al.,* 1993; Newman *et al.,* 1998; Gillis *et al.,* 1997; Freda, 2002; Colao *et al.,* 2001; Chanson *et al.,* 2000; Caron *et al.,* 2002; Bevan *et al.,* 2002). However, the treatments have to be administered indefinitely, indicating again that pegvisomant is the most effective treatment.

1.8.2. Diabetes Mellitus

Diabetic damage of the eye and the kidney are causes that are directly associated with diabetes (Flyvbjerg, 1990). Evidence indicating the involvement of the GH-IGF-1 axis in diabetes comes from studies, where adenectomy in diabetic patients led to a discontinuation or delay of diabetic retinopathy (Flyvbjerg, 1990). Increased circulating GH levels are implicated to be involved in the development of insulin resistance (Sönksen *et al.,* 1993). Additionally, patients suffering from acromegaly have been shown to develop insulin resistance contributing to the emergence of diabetes (Press, 1988). Direct evidence substantiating the involvement of the GH-IGF-1 axis comes from experimental documentation in GH transgenic mice (Yang *et al.,* 1993). It could be shown that these mice develop glomerulosclerosis over time (Doi *et al.,* 1988). Moreover, additional validation experiments demonstrated that IGF-1 transgenic mice did not develop glomerulosclerosis, but transgenic mice expressing the GH antagonist were documented to not have any type of kidney damage (Doi *et al.,* 1988; Chen *et al.,* 1995). The role of transgenic mice expressing the GH antagonist has additionally been studied to deliver further validation of GH involvement in retinal neovascularization (Smith *et al.,* 1997). Neovascularization of the retina could be arrested in GH antagonist mice, but the arrest could be reversed through exogenous administration of IGF-1 (Smith *et al.,* 1997). Taken together, these data validate a potential role of the GH-IGF-1 axis in the diabetic damage of the eye and kidney.

1.8.3. Cancer

The GH-IGF-1 axis has also been implicated in carcinogenesis. High IGF-1 serum concentrations are associated with an increased risk for several types of cancer (Chan *et al.,* 1998; Shaneyfelt *et al.,* 2000). Furthermore, high IGF-1 serum

concentrations in premenopausal women have been associated with an increased risk for breast cancer (Bohlke *et al.,* 1998). Xenografted breast cancer cells in immunocompromised mice, treated with pegvisomant at 202.2mg/kg/week, displayed decreased growth rates (Roshan *et al.,* 1999). Furthermore, transgenic mice expressing the GH antagonist were shown to be resistant to carcinogenesis in a DMBA (dimethylbenz[a]anthracene) breast cancer model (Pollak *et al.,* 1999). The breast cancer was not detectable in 68.2% of these mice after 39 weeks of treatment, whereas a mere 31.6% in the control group were shown to be cancer-free, implicating a major role of GH in carcinogenesis.

1.9. The Laron Syndrome

In contrast to being a pathophysiological condition characterized by continuous pro-growth signaling, specifically GH and IGF-1 signaling, the Laron syndrome or GHI (GH insensitivity) represents an autosomal recessive disorder based on a deficiency to produce IGF-1 in response to GH due to mutations of the GHR rendering it dysfunctional (Laron, 2004; Shevah and Laron, 2011). 70 mutations have been attributed to cause the condition (David *et al.,* 2011). However, the E180 splice mutation has been found to be the most prevalent type of mutation (Gonçalves *et al.,* 2014). The splice mutation encoded by codon 198 (180 in the fully mature protein) is based on a single nucleotide exchange (c.594A>G, rs121909360) in exon 6, which leads to the activation of a cryptic 5' donor splice site (Fang *et al.,* 2008). The activation of the cryptic splice site generates an in-frame deletion of eight amino acid residues (p.V199_M208 del) within the extracellular domain of the GHR, rendering membrane trafficking of the GHR to the cell surface dysfunctional (Fang *et al.,* 2008). A cohort of 100 individuals in Southern Ecuador of Spanish descent constitutes the biggest population documented (Berg *et al.,* 1992; Guevara-Aguirre *et al.,* 2011) (Fig. 1.13.).

Fig. 1.13. Members of the Ecuadorian cohort (modified from Guevara-Aguirre *et al.,* 2011).
The image depicts Jaime Guevara-Aguirre with members of the Ecuadorian cohort in 2009. Jaime Guevara-Aguirre is monitoring the population since 1988, which has been identified based on the distinct short stature of the Laron patients (Guevara-Aguirre *et al.,* 1993; Rosenbloom *et al.,* 1990; Bachrach *et al.,* 1998).

Analysis of mortality data comparing 30 death incidences of Laron patients to their normal relatives, reports 9 age-related deaths (8 resulting from cardiac disorders, 1 stroke incident) and 21 non-age-related deaths amongst the Laron subjects (Guevara-Aguirre *et al.,* 2011) (Fig. 1.14).

Cancer was responsible for 20% of the deaths in the relatives, while only a single incident of cancer has been reported for a subject of the Laron cohort since 1988 (Guevara-Aguirre *et al.,* 2011). The affected person was suffering from an epithelial tumor of the ovary, but has been cancer-free since treatment (Guevara-Aguirre *et al.,* 2011). Diabetes mellitus accounts for 5% of the deaths in the relatives, while no mortality as a result of diabetes has been reported for Laron subjects (Guevara-Aguirre *et al.,* 2011). Mortality based on cardiac diseases seems to be elevated in Laron subjects (Guevara-Aguirre *et al.,* 2011). However, deaths as a result of vascular disease differ insignificantly compared to normal relatives, as supported by studies in human populations with GH deficiency (Aguiar-Oliveira *et al.,* 2010).

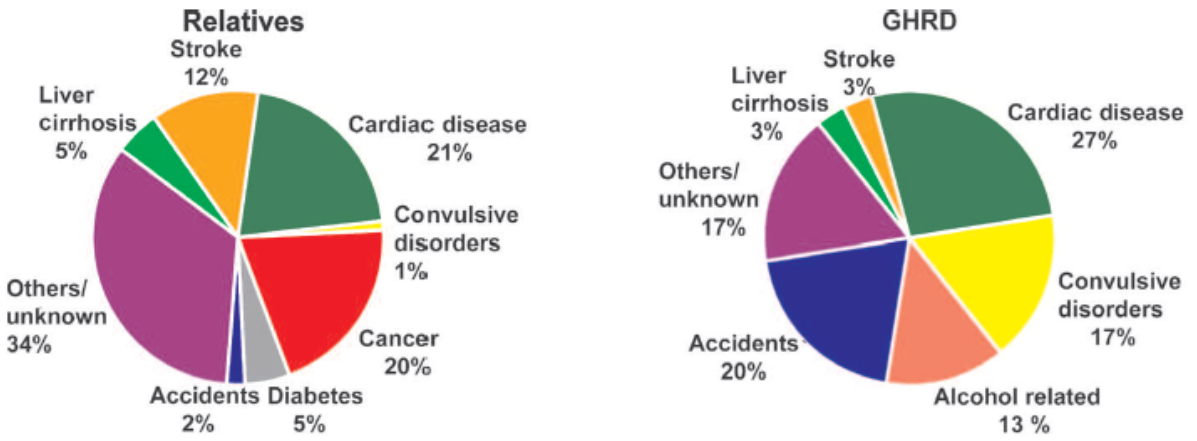

Fig. 1.14. Mortality and causes of death in Laron subjects and their normal relatives (modified from Guevara-Aguirre *et al.,* 2011).

The charts compare age-related and non-age-related causes of mortality in Laron subjects and their normal relatives.

1.10. The Laron Mouse

The Laron mouse has been developed to unravel the molecular mechanisms and basis of GHR dysfunctions in human subjects (Zhou *et al.,* 1997). These mice display a dwarf phenotype due to their insensitivity to GH, just as the human Laron subjects (Okada and Kopchick, 2001). They have normal body weights at birth, but their growth delays just a few days after birth (Zhou *et al.,* 1997). At three months of age, their size only corresponds to half of their normal littermates (Okada and Kopchick, 2001) (Barclay *et al.,* 2010) (Fig. 1.15.). Remarkably, longevity studies show that the dwarf mice have a significantly longer lifespan compared to their normal littermates, indicating a potential involvement of GH in the control and regulation of longevity and senescence/aging (Coschigano *et al.,* 2000). Studies resembling this assumption comes from experiments that have shown an extension in longevity due to a decrease in circulating GH levels, implicating a genetic control of aging and longevity (Bartke, 2000).

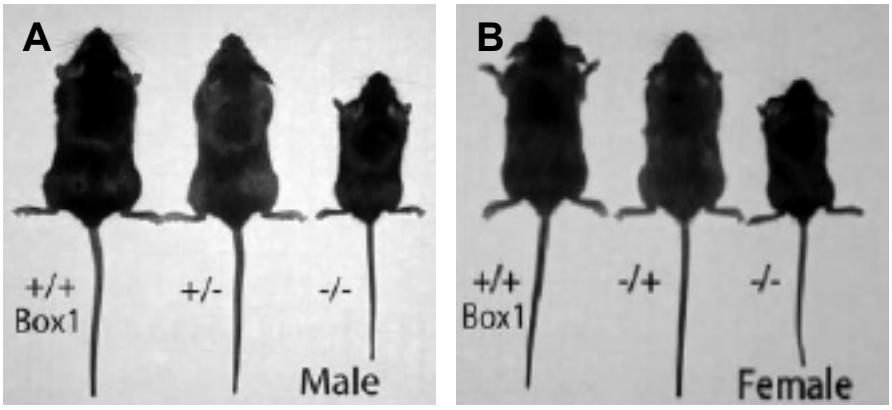

Fig. 1.15. Physiological comparison of GHR disrupted mice and their normal littermates (modified from Barclay *et al.,* 2010).

Male (A) and female (B) C57BL/6 mice at 60 days of age. From left to right, normal WT (wild type) mouse, compared to heterozygous $GHR^{Box1\ +/-}$ and homozygous $GHR^{Box1\ -/-}$ mice.

1.11. Interventions to Delay Aging and the Onset of Age-Related Diseases

The observations made in Laron subjects and the Laron mice led to the question whether the identification and development of dietary interventions or pharmacological interventions targeted at GH-IGF-1 signaling could interfere in the aging process and therefore delay the onset of age-related diseases. Dietary interventions represent nutritionally dense, calorically restricted diets and cycles of fasting and fasting-mimicking diets. Pharmacological interventions involve exposure to molecular drug compounds aimed at reducing the activity of specific signaling pathways, such as the GH-IGF-1 axis as discussed below.

1.11.1. Calorie Restriction

Calorie restriction (CR) is a dietary strategy proven to delay aging, increase average and maximum lifespan, and prevent or delay the onset of age-related disease in several model organisms including rodents (Weindruch and Walford, 1988). The first study in humans was performed in an enclosed ecological space in Arizona, termed Biosphere 2, under the supervision of Roy Walford, the pioneer of calorie restriction (Walford *et al.,* 2002). The study group consisted of four women and four men, entering Biosphere in 1991 for a period of two years. The set up of Biosphere 2 was designed to be a self-sustaining system, maintained by the study group (Walford *et al.,* 1996; Walford, 2002). The daily caloric intake consisted of

1784 kcal over an initial period of six months but was increased to 2000 kcal/day for the remaining 18 months (Walford *et al.,* 2002). However, all study subjects displayed severe weight loss in the first six to eight months, with the new adapted and reduced body weight being maintained until the end of the study (Walford *et al.,* 2002) (Fig. 1.16.).

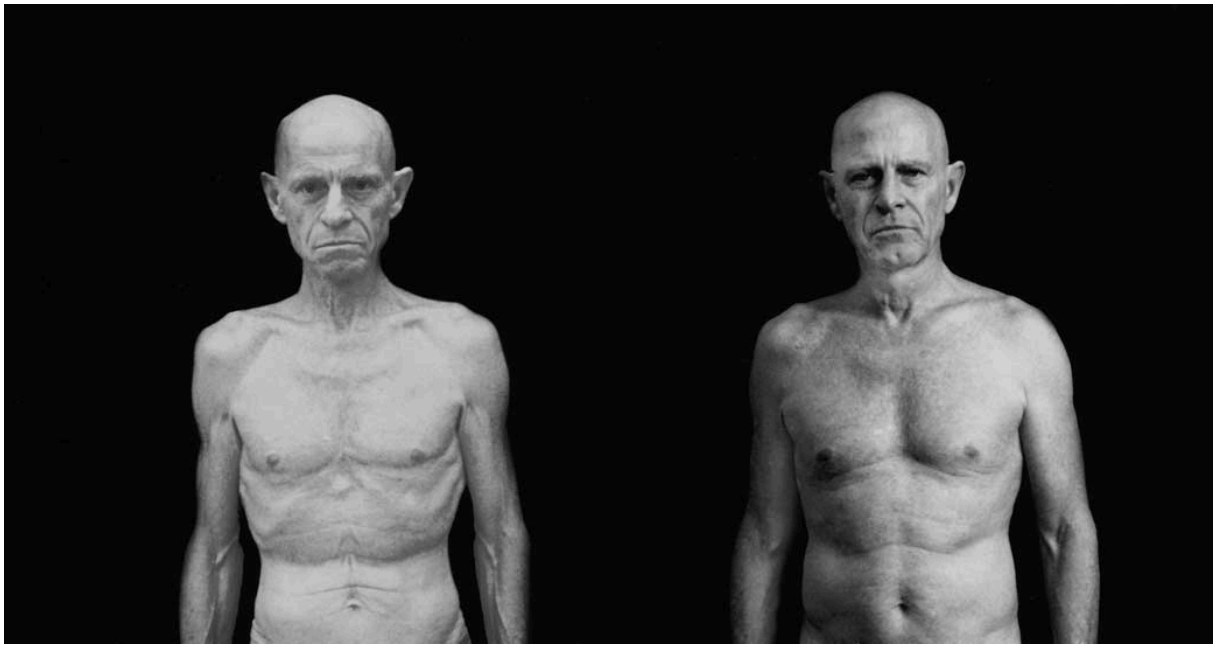

Fig. 1.16. Body weight loss in Biosphere 2 (modified from Walford *et al.,* 2002).
The image depicts Roy Walford before and after entering Biosphere 2. On the left, severe body weight loss after 15 months of entering Biosphere 2 is seen, while the image on the right side depicts Roy Walford 18 months after the end of the study and adapting a normal diet.

A follow-up period of 30 months after completing study posed serious questions as to the benefit of caloric restriction regarding the physiological response and health of the subjects (Walford *et al.,* 2002). Evaluation of the subjects demonstrated no signs of lethargy, mental confusion, weakness or any other signs related to malnutrition, although individuals were subjected to intensive mental and physical labor throughout the study (Walford *et al.,* 1996; Walford, 2002). Assessment of serum biomarkers showed a decline in LDL (low-density lipoprotein) and HDL (high-density lipoprotein) levels (Verdery, Walford, 1998). However, no significant changes in circulating GH or IGF-1 levels could be observed, in contrast to reductions of both parameters in calorically restricted rodents and monkeys (Lane *et al.,* 1998; Hursting *et al.,* 1993; Meites, 1990; Parr 1996; Sonntag *et al.,* 1995; Sonntag *et al.,* 1999; Breese *et al.,* 1991; Cocchi *et al.,* 1991; Dunn *et al.,* 1997; Bodkin *et al.,* 1995; Quigley *et al.,* 1990). However, the dataset presented is only

limited, and life-long studies in human cohorts are necessary for the interpretation of solid conclusions.

1.11.2. Fasting and Fasting-Mimicking Diets

Prolonged fasting has been attributed to reduced pro-growth signaling pathways and the stimulation of cellular protection mechanism in a variety of model organisms raging from unicellular eukaryotes to mammals (Longo and Mattson, 2014). The beneficial effects arise from reduction of glucose, but more importantly from the decrease in serum IGF-1 levels (Cheng *et al.,* 2014; Sonntag *et al.,* 1999; Ikeno *et al.,* 2003; Flurkey *et al.,* 2001; Dunn *et al.,* 1997; Bonkowski *et al.,* 2009). Prolonged fasting reconstitutes a regimen of water only intake over a minimum of two days. In addition to this regimen, the intake of a very low calorie fasting-mimicking diet (FMD), both have been shown to improve the prevalence of age-related diseases such as cancer and multiple sclerosis (Choi *et al.,* 2016; Brandhorst *et al.,* 2015; Longo and Panda, 2016). A recent clinical study in a cohort of 100 healthy human participants assessed the efficacy of periodic FMD cycles regarding risk factors for aging, cancer, the metabolic syndrome and cardiovascular disease (Wei *et al.,* 2017). An improved incidence for the corresponding diseases based on the evaluation of biological and metabolic markers as well as age-related risk factors served as a basis for the interpretation and conclusion of the efficacy of FMD (Wei *et al.,* 2017).

1.11.3. Pharmacological Interventions

Reduced signaling of the GH-IGF-1 somatotropic axis has been associated with the intervention in the aging process and the delayed onset of age-related diseases. Evidence comes from studies where, for instance, low serum IGF-1 concentrations are associated with survival in long-lived individuals, or gene polymorphisms are implicated in lifespan extension (Milman *et al.,* 2014; Suh *et al.,* 2008). Furthermore, Laron patients seem to be protected from diabetes mellitus and neoplasms (Guevara-Aguirre *et al.,* 2011), implicating an essential role of GH-IGF-1 signaling in the control of healthspan and lifespan. Thus, pharmacological interventions aimed at reducing signaling of the GH-IGF-1 somatotropic axis might represent a promising target to intervene in the aging process and therefore prevent

or delay the onset of age-related diseases. Monoclonal antibodies (mAbs) targeting the IGF-1R have been tested in clinical studies of neoplasia but were not approved for clinical use (Warshamana-Greene *et al.,* 2005; Carboni *et al.,* 2009). Peptides, such as somatostatin analogs for the treatment of acromegaly, suppress GH secretion contributing to lower IGF-1 circulating levels. Furthermore, pegvisomant, a GH receptor antagonist, works directly on the cell surface of target cells by suppressing GH signaling (Kopchick *et al.,* 2002). However, the development of mAbs targeting the GH-IGF-1 axis seem to represent a more promising approach on a long-term basis.

1.12. Anatomy of an Antibody

Antibodies, also termed as immunoglobulins (Igs), are components of the humoral immune system, which are responsible for the elimination of pathogenic bacteria and viruses. They are produced by plasma cells, a differentiated population of immune cells of the adaptive immune response. Antibodies produced from different plasma cell clones are described as polyclonal antibodies (pAbs), whereas antibodies produced from a single clone are termed as monoclonal antibodies (mAbs). The latter represents a promising clinical tool for the treatment of a variety of diseases, as well as an important biochemical tool in biotechnological, immunological and diagnostics settings.

Structurally, mAbs are organized in a distinct Y shape anatomy, which is composed of two heavy and two light chains (Fig. 1.17). There are five isotypes, which are determined based on the composition of amino acid residues and size of the heavy chains: IgM, IgD, IgA, IgE, and IgG (Kolar and Capra, 2003). Furthermore, each heavy chain is comprised of three successive constant regions (C_H1, C_H2, C_H3), and a variable region (V_H). The constant region is indistinguishable in all Igs belonging to the same isotype group, whereas the variable region differs for all antibodies produced by different clones but is identical in antibodies produced by the same clone. Moreover, the light chains are composed of a constant region (C_L) and a successive variable region (V_L), which are identical within the same antibody. There are two types of light chains described in the literature, which are λ and κ.

Igs are also functionally divided into sections, namely the F(ab) (antigen-binding fragment) region and the Fc (fragment crystallizable region) region. The F(ab) fragment is composed of a variable and constant domain of one heavy chain

(C_H1 and V_H) and one light chain (C_L and V_L). The variable domains harbor the paratope, a region responsible for the recognition and binding of the antigenic determinant/epitope on the antigen. The Fc portion of an antibody is composed of the C_H2, C_H3 regions each heavy chain. It is in charge of binding to the Fc receptors on the cell surface of target cells to stimulate specific immune cell populations or activate the complement system.

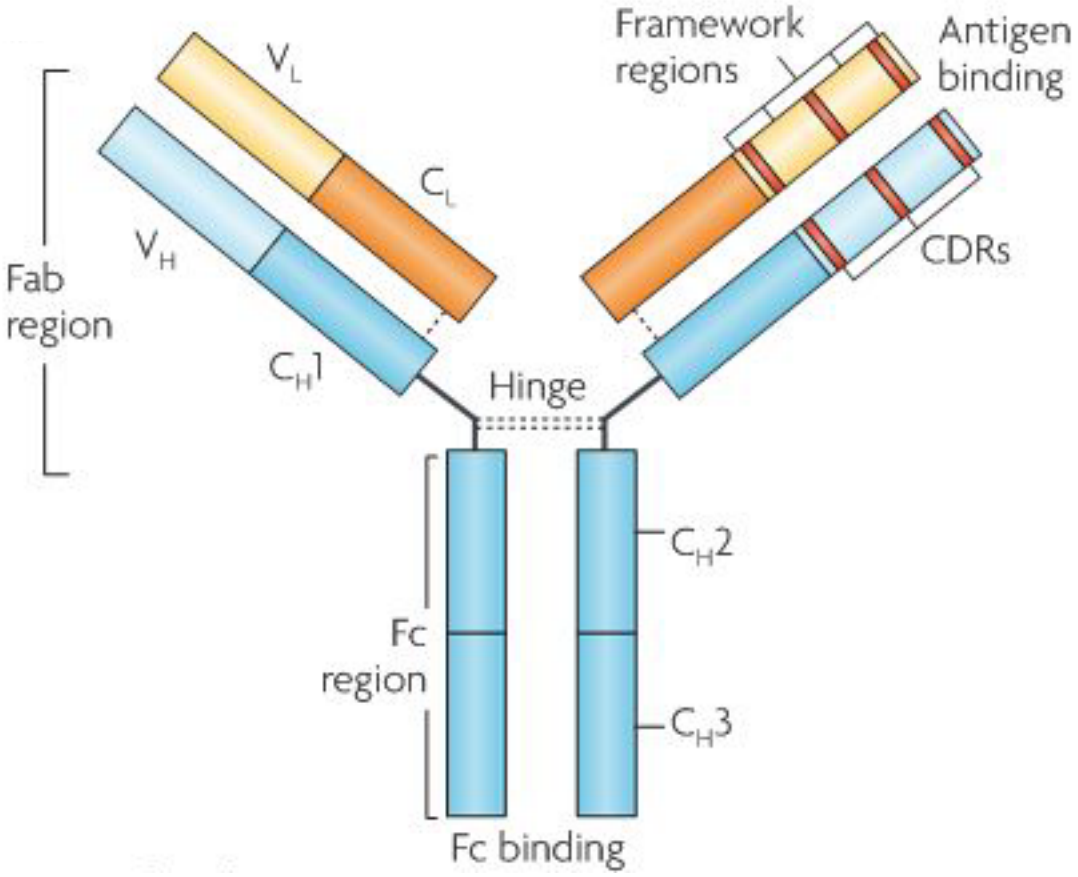

Fig. 1.17. Structure of an antibody (modified from Hansel *et al.,* 2010).
The scheme represents the structural organization of an antibody into its domains. The hinge region in the center links the heavy and light chain by covalent disulfide bonds and allows flexibility.

There are two enzymes capable of cleaving the antibody into different fragments: papain and pepsin. Enzymatic cleavage by papain occurs N-terminally and results in the generation of three fragments: Two F(ab) fragments and one Fc fragment. The F(ab) fragment harbors domains V_L, C_L, V_H and C_H1, whereas the Fc fragment harbors domains C_H2 and C_H3. Pepsin digests the antibody C-terminally, producing an F(ab')2 fragment composed of two F(ab) fragments joined through disulfide bonds, and multiple dysfunctional peptides of the Fc fragment.

1.13. Hybridoma Technology

Köhler and Milstein have originally described the technology for the production of mAbs in 1975, for which discovery they were awarded with the Nobel Prize in 1984 (Köhler and Milstein, 1975). It allowed the biotechnological generation of murine antibodies. However, given the significance in the clinical application of antibodies, the murine nature of mAbs represented a barrier given the immune response in humans (Keizer *et al.,* 2010) (Fig. 1.18.). Recombinant DNA technologies helped to overcome immunogenicity by assisting in the development of chimeric antibodies, in which the resulting antibody was designed to be human, except for the murine variable region (Weiner, 2006; Yang *et al.,* 2001). The following stage in the development process was characterized by the substitution of murine amino acid residues with human amino acid residues resulting in a humanized antibody, merely containing murine amino acid residues within the antigen-binding complementarity determining region (Weiner, 2006). The generation of fully human monoclonal antibodies was enabled by phage-display platforms and usage of transgenic mouse models, such as the XenoMouse or UltiMAb (Longberg, 2005; Longberg, 2008; Hochholzer and Giugliano, 2010; Michnick and Sidhu, 2008).

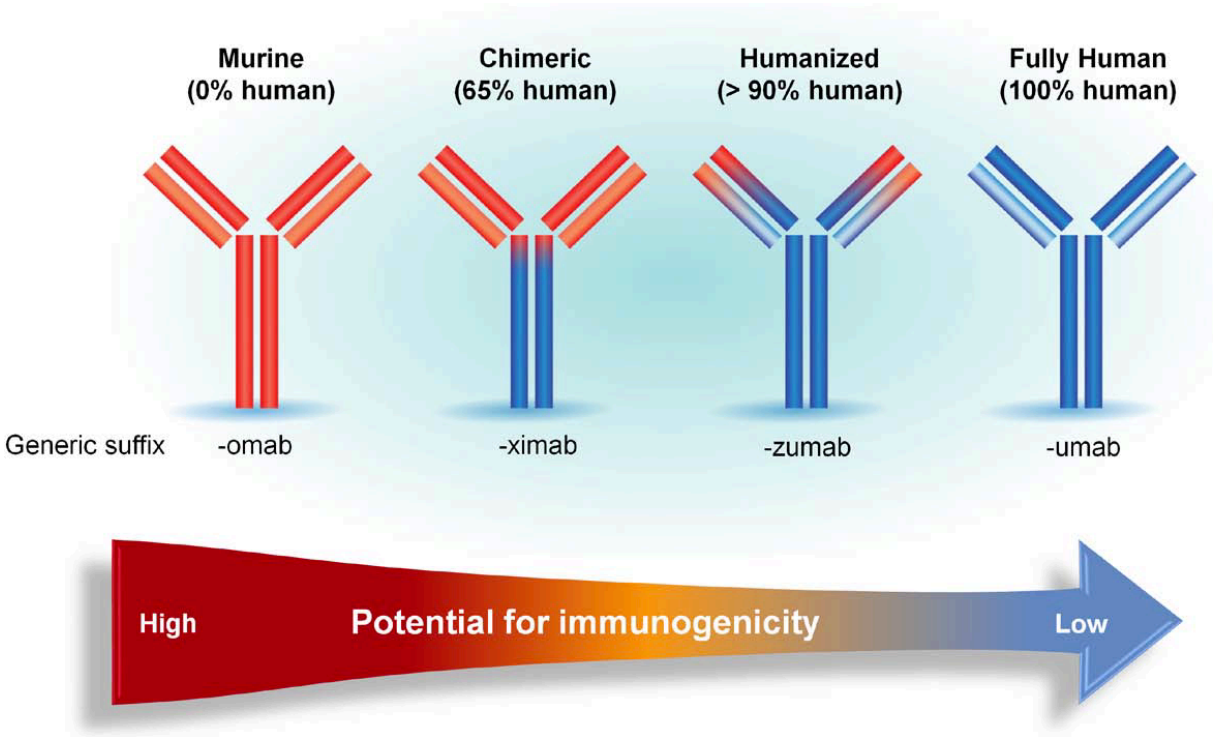

Fig. 1.18. Immunogenicity of antibodies of different origin (modified from Foltz *et al.,* 2013).
The illustration shows a reduction of immunogenicity with successive substitution of the murine amino acid residues with human amino acid residues.

Although there are complications associated with murine antibodies, the hybridoma technology still represents the classical platform for the generation of mAbs (Glukhova *et al.,* 2016). The procedure starts with the immunization of mice with an antigen of interest (Fig. 1.19.). Subsequently, serum antibody titer is measured via enzyme-linked immunosorbent assay (ELISA). The spleen of the immunized mouse is aseptically removed, and B cells are harvested and fused with myeloma cells *ex vivo*. The fusion results in the generation of hybridoma cells, in which the antibody-secretion feature of the B cells is combined with the immortality of the myeloma cells. The hybridoma clones are then cultured in 96-well plates and screened in selective hypoxanthine-aminopterin-thymidine (HAT) medium to eliminate unfused hypoxanthine-guanine phosphoribosyltransferase (HGPRT) negative myeloma cells. Successful clones are then selected and expanded for maintenance purpose.

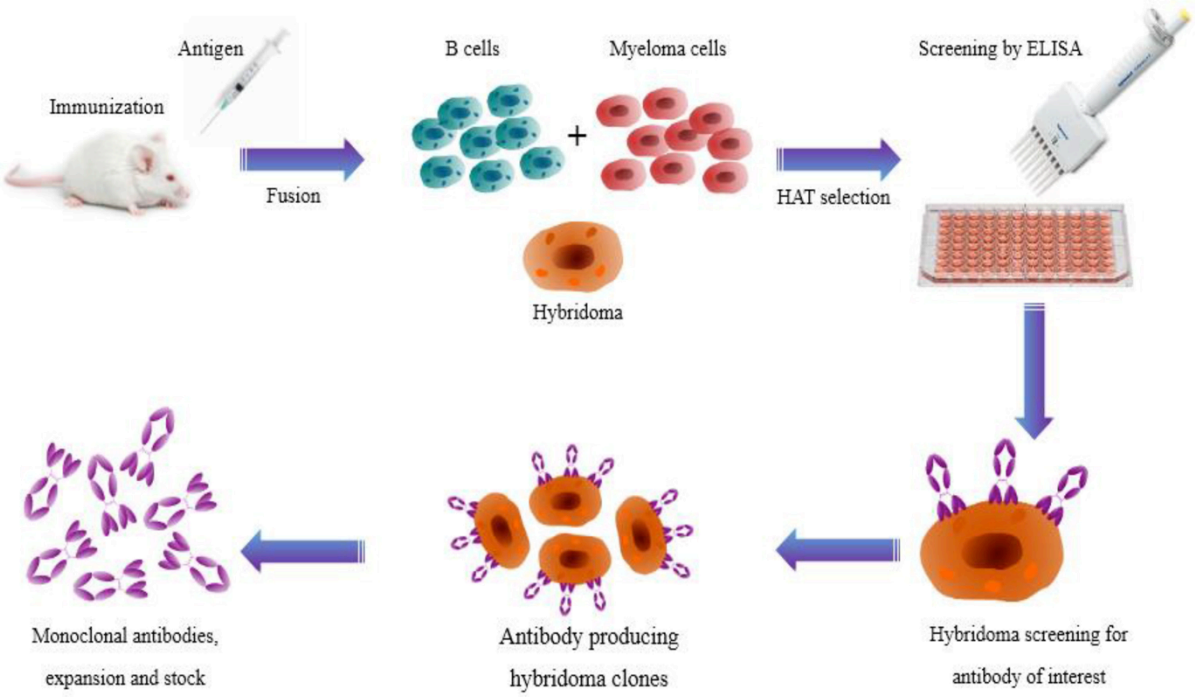

Fig. 1.19. Schematic presentation of hybridoma technology (modified from Saeed *et al.,* 2017). Generation and production of mAbs begins with the immunization of a mouse with an antigen of interest. B cells and myeloma cells are then fused, and the resulting hybridoma cells are screened for their ability to produce the mAb of interest.

The produced antibodies are subjected to purification and subsequent characterization in a variety of *in vitro* and *in vivo* experiments to determine essential characteristics such as binding affinity, avidity, immunoreactivity, and specificity.

1.14. Aim of the Study

IGF-1 represents a major risk factor for aging-associated pathological conditions (Sonntag *et al.,* 1999). Hence, lowering circulating IGF-1 levels to a protective level is of interest for the prevention of age-related diseases and to augment the treatment of age-related diseases. Several interventions such as caloric restriction, fasting, and fasting-mimicking diets have been proven to be beneficial. However, a pharmaceutical intervention aimed at reducing circulating IGF-1 levels has yet to be established. Pharmaceutical agents are of certain advantage for patients where caloric restriction, fasting or a fasting-mimicking diet is not feasible. Therefore, a pharmaceutical intervention has the potential to serve as a significant second-line treatment for patients not being capable of fasting or adhering to a calorically reduced regimen. In this dissertation, the development and characterization of monoclonal antibodies targeting the GHR is in the focus. The α-GHR mAb candidates will be subjected to various *in vitro* and *in vivo* experiments. The mammalian cell culture system will be used for *in vitro* studies. For this purpose, GHR-overexpressing fibroblasts, namely L cells, will be used to examine the ability of the α-GHR mAbs to downregulate STAT5 phosphorylation induced by GH, and to reduce IGF-1 promoter reporter activity after transfection of the respective cell line and treatment with GH. For the *in vivo* studies, the α-GHR mAbs will be injected intravenously into C57BL/6 mice and serum will be collected to evaluate in vivo efficacy of the drugs to reduce serum IGF-1 levels.

2. Methods

2.1. Bioinformatical Analysis of Sequences and Structures

Quantitative and qualitative *in silico* analysis of sequential and structural information of a protein target of interest enables the researcher to draw conclusions regarding the identification and prediction of functionally important domains by using computational algorithms. For *in silico* analysis, all sequential information of the proteins of interest was downloaded from the protein database UniProt in the FASTA format.

2.1.1. Sequence Alignment of GHR Protein Sequences

Multiple sequence alignments were generated using Clustal Omega alignment tool (Clustal O 1.2.4.). FASTA formats of the protein sequence identifiers were downloaded from UniProt sequence database and submitted for processing. Local and pairwise sequence alignments were obtained using the BLAST (Basic Local Alignment Search Tool) algorithm.

2.1.2. Quantitative Assessment of Sequence Homology

Quantitative *in silico* assessment of protein sequence homology between species was generated using Clustal Omega (Clustal O 1.2.4.). Alignment scores were calculated by applying the hidden Markov model (HMM) algorithm after Söding (Söding, 2005). Scored values are visualized in a percentage identity matrix.

2.1.3. Building of a Phylogenetic Tree

Representation of evolutionary relationships among species and the evolution from a common ancestor were illustrated in a phylogenetic tree. Origins were computed using the Neighbor-Joining method with Poisson correction in MEGA7 (molecular evolutionary genetics analysis 7) software.

2.1.4. Identification of Antigens on the GHR

A company specialized in the development of monoclonal antibodies (Abmart Inc., Shanghai, China) was commissioned with the generation of mouse monoclonal antibodies targeting the GHR. For the development, the mouse GHR protein sequence was submitted in the FASTA format and subjected to computational epitope analysis using a proprietary algorithm named SEAL^{TM}. After careful examination of sequential and structural information, several antigens were designed. Each antigen consisted of a hydrophobic stretch of 12 amino acid residues. These peptide antigens were optimized for immunization and mouse monoclonal antibodies were generated using the hybridoma technology. Out of the generated hybridoma clones, five candidates were selected for further investigation and the establishment of a functional and effective mouse α-mouse GHR mAb.

2.1.5. Structural Analysis of Functionally Relevant Domains of the GHR

Structural analysis was performed using the PyMOL visualization tool. The crystalized human GHR protein (from de Vos *et al.,* 1992) was accessed through NCBI (National Center for Biotechnology Information) and downloaded from the PDB (Protein Data Bank). After opening the structure in PyMOL, the selected five mouse antigens were highlighted within the structure to enable differential derivation of functionally important information of GHR domains.

2.2. Cellular and Biochemical Methods

Mammalian cell culture experiments were performed under a sterile laminar flow hood. Materials were autoclaved and sterilized using 70% ethanol. Experiments were performed using the hybridoma clones and the murine fibroblast cell line L cell. However, this fibroblast cell line was genetically modified to overexpress the mouse GHR on its cell surface.

2.2.1. Cultivation of Mammalian Cells

Cell lines were seeded in T-75 tissue culture flasks (BD, Cat.: BD353136) and incubated under stable conditions at 37°C, 5% CO_2, and a relative humidity of 95%. DMEM (Dulbecco's Modified Eagle's Medium, Thermo Fisher Scientific, Cat.: 11995-065) supplemented with 10% FBS (Fetal Bovine Serum, Corning, Cat.: 35- 010-CV) and 1x HAT (hypoxanthine, aminopterin, and thymidine, Corning, Cat.: 25-046-CI) were used for the cultivation of L cells. For the cultivation of the hybridoma clones, RPMI (Roswell Park Memorial Institute, Corning, Cat.: 10-041-CV) supplemented with 15% FBS was used.

2.2.2. Subcultivation of Mammalian Cells

After reaching confluency, cells culture supernatant was transferred into conical tubes. Adherent cells were detached using 3ml of trypsin (Invitrogen, Cat.: 12605-028) per T-75 flask. To optimize the enzymatic reaction of trypsin, cells were incubated at 37°C for 5 minutes. After incubation, the enzymatic reaction was terminated using the cell culture supernatant and the mixture was centrifuged for 5 minutes at 1000 rpm. The cell culture supernatant was aspired and the resulting cell pellet was resuspended in the corresponding culture medium of each cell line.

2.2.3. Cell Counting

Quantification of cell numbers was assessed manually using the trypan blue exclusion test (Sigma-Aldrich, Cat.: T8154-20ml). The dye is not capable to diffuse through an intact cell membrane. Therefore, the test enables the selective differentiation of viable from dead cells. For quantification purpose, an aliquot of the

cell suspension was diluted in a ratio of 1:10 with the dye. A small amount of the dilution was added to the hemacytometer. Cells in the four gridded squares were counted and the average was calculated. The average was then multiplied by 10^4 and the dilution factor to obtain the amount of cells per milliliter.

2.2.4. Cryopreservation of Cells

For cryopreservation, the cell lines were subcultured as described above (see 2.2.2.). After centrifugation, cells were resuspended in freezing medium consisting of 50% DMEM or RPMI, 40% FBS, and 10% DMSO (dimethyl sulfoxide, Sigma-Aldrich, Cat.: D2650-5x10ml). Cells were placed in a freezing box and incubated at -80°C overnight. The next day, cells were transferred to liquid nitrogen.

2.2.5. Immunofluorescent Staining of L Cells

To study binding interaction between the α-GHR mAbs and the GHR, L cells were initially seeded at 100.000 cells/well in a 24-well plate (Corning, Cat.: 353047) and grown for 24 hours. After 24 hours, a mixture of each individual purified mAb was incubated with its antigenic determinant it was designed against for one hour at room temperature (RT). The mixture was then given on the cells and incubated for 1.5 hours at RT on a rocker to allow binding of the mAbs to the GHR expressed on the cell surface. Following incubation, cells were fixed in 4% paraformaldehyde (Alfa Aesar, Cat.: AAJ61899-AP) for 10 minutes in the cold room, and then blocked in 2%NGS (normal goat serum, Jackson Immuno Research, Cat.: 005-000-001) solution for one hour at RT. The secondary antibody labeled with Alexa Fluor 488 (Thermo Fisher Scientific, Cat.: A-11001) was given on the cells for one hour and incubated at RT. The cells were then washed with DPBS (Dulbecco's Phosphate-Buffered Saline, Corning, Cat.: 21-031-CV) followed by incubation with Hoechst 33342 (Thermo Fisher Scientific, Cat.: H3570) according to manufacturer's instructions. Cells were washed again in PBS and mounted using mounting medium (Sigma-Aldrich, Cat.: 10981-100ml). The slides were stored for at least 24 hours before images were taken at the confocal microscope at 63x magnification.

2.2.6. The Biacore Platform to Study Binding Kinetics

The Biacore platform (GE Healthcare Life Sciences) is a specialized label-free system allowing the detection of biomolecular interactions, such as peptide-protein interactions, protein-protein interactions, nucleic acid-protein interactions, and low molecular weight/small molecule-protein interactions. The technology is popularly used in the drug discovery and development process, where it serves as a tool to screen, confirm and rank potential hits based on results obtained for selectivity and affinity kinetics. The identified hits can then be subjected to a detailed kinetic analysis to differentiate promising leads. Therefore, the Biacore platform greatly enhances the understanding of the underlying molecular mechanisms of biomolecular interactions and contributes to the acceleration of the drug discovery process by allowing the selection and optimization of potential lead compounds (hit-to-lead generation). The virtual screening is based on surface plasmon resonance spectroscopy (SPR), which describes a phenomenon where electron oscillations (namely plasmons) are generated at the interface of two media by polarized light. The resonant excitation of the plasmons is then measured at a specific angle in proportion to the mass on the surface of the sensor. This event is expressed in response units (RU), which is defined as 1 RU = 1pg/mm^2 and is used to evaluate surface coverage of the chip.

Studying biomolecular interactions between the α-GHR mAbs and their corresponding peptides were carried out at 25°C on a Biacore T100 system. Ligands were diluted in acetate immobilization buffer and covalently coupled to the surface of a CM5 sensor chip (GE Healthcare Life Sciences, BR100530) using the amine coupling kit according to manufacturer's instructions (GE Healthcare Life Sciences, BR10050). A serial dilution series of the analyte was prepared in running buffer (0.01M HEPES, 0.15M NaCl, 0.3M EDTA, 0.05% Tween-20, pH 7.4) and equivalent volumes were injected over the surface. Regeneration of the surface was achieved by injecting glycine (GE Healthcare Life Sciences, BR100356). Due to differences in the isolelectric points of the α-GHR mAbs, two differential approaches were carried out. A conventional approach was used for α-GHR565. Using this approach, the peptide served as ligand to be immobilized at 20µg/ml (in acetate 5.0 immobilization buffer, GE Healthcare Life Sciences, BR100351) on the surface of the chip at a flow rate of 20µl/min. The mAb served as an analyte and was injected for 30s at each individual injection at a flow rate of 50µl/min. An unconventional approach was used for mAbs α-GHR562 and α-GHR592. In this case, the mAb served as ligand at 10

µg/ml (in acetate 4.5 immobilization buffer, GE Healthcare Life Sciences, BR100350) injected at a flow rate of 10µl/min. The peptide served as analyte and each injection lasted 30s at a flow rate of 50µl/min.

2.2.7. Transfection of L Cells

L cells were seeded at 10.000cells/well in a 96-well plate (VWR, Cat., 10062-900) in the corresponding culture medium and grown for 24 hours. The next day, cells were transfected with an IGF-1 promoter reporter construct (Switch Gear Genomics, Cat.: S721634) using X-tremeGENE HP DNA transfection reagent using the 3:1 ratio (µl of X-tremeGENE HP DNA transfection reagent : µg DNA) according to manufacturer's instructions (Sigma-Aldrich, Cat.: 6366236001). The construct expresses an optimized Renilla luminescent reporter gene (RenSP) with enhanced Renilla enzymatic activity and is optimized to decrease the half-life of the RenSP protein. Three hours after transfection, cells were transferred to serum-free medium and incubated overnight. After incubation, cells were pre-treated with the respective α-GHR mAbs for an hour before GH (obtained from Cohen lab) was added at 500ng/ml for four and eight hours to the mixture at a ratio of 1:10 (GH: α-GHR mAb). Renilla luciferase reporter signal was measured using Light Switch^{TM} Assay Reagent (Switch Gear Genomics, Cat.: LS010) according to manufacturer's instructions.

2.3. Proteinbiochemical Methods

2.3.1. Phosphorylation of STAT5 and ERK1/2

The ability of the α-GHR mAbs to induce any changes in the phosphorylation of STAT5 and ERK1/2 was assessed using the L cells. For this purpose, cells were seeded at $5x10^5$ cells/well/3ml in 6 well plates and grown for 24 hours. After expansion, cells were transferred to serum-free medium and incubated overnight. The next day cells were pre-treated with the corresponding α-GHR mAbs for an hour. GH was added at 500ng/ml and the mixture was cultured at ratios 1:0, 1:1, 1:10, and 1:20 (GH:α-GHR mAb) for 10 minutes. Subsequently, cells were subjected to lysis (see 2.3.2.).

2.3.2. Cell Lysis

Cells were washed with ice cold DPBS and then lysed in 1x RIPA (Radioimmunoprecipitation assay buffer, Merck Millipore, Cat.: 20-188) supplemented with 1x of a protease and phosphatase inhibitor cocktail (Thermo Fisher Scientific, Cat.: 78443). The resulting lysate was centrifuged for 10 minutes at 800 rpm and then transferred to new microtubes for the subsequent determination of the protein concentration (see 2.3.3.).

2.3.3. Determination of the Protein Concentration

Quantification of the protein concentration is based on the BCA (bicinchoninic acid) protein assay kit (Thermo Fischer Scientific, Cat.: 23227). Samples were diluted at 1:10 and prepared in triplicates according to manufacturer's instructions. After measuring the absorbance at 562nm, protein samples were prepared using Laemmli sample buffer (BioRad, Cat.: 1610747) and boiled at 90°C for 10 minutes for subsequent analysis by SDS-PAGE (see 2.3.4.) and Western blot (see 3.2.5.).

2.3.4. SDS-Polyacrylamide Gel Electrophoresis (SDS-PAGE)

After preparation of the protein samples, 30 µg was loaded onto a precast 4-20% gradient gel system (Thermo Fisher Scientific, Cat.: XP04200BOX) and separated at 130 volts. Protein detection was performed using the Western blot method (see 2.3.5.).

2.3.5. Western Blot Analysis

Following SDS-PAGE, the gel was equilibrated for 15 minutes in transfer buffer (BioRad, Cat.: 1610771). Simultaneously, a PVDF membrane (polyvinylidene fluoride, Merck Millipore, Cat.:IPVH00010) was activated in 100% methanol for 5 minutes. The Western blot sandwich was assembled and protein samples were transferred at 300 mA (milliampere) for an hour on ice. After the transfer, unspecific binding sites on the membrane were blocked in 3%BSA/PBS-T for one hour at RT. Subsequently, the membrane was incubated with the corresponding primary antibodies [Cell Signaling, Cat.: 9363 (STAT5); 9351 (p-STAT5); 4659 (ERK1/2); 4370 (p-ERK1/2); 2148 (α/β-Tubulin)] at 1:1000 dilution for one hour at RT, followed by a 15 minute wash in PBS-T. The wash buffer was exchanged every 5 minutes. Incubation with the secondary antibody (Jackson Immuno Research, Cat.: 111-035-003) was performed for one hour at RT, followed by washing steps. Protein bands were visualized using chemiluminescence (Thermo Fisher Scientific, Cat.: 32106) and subjected to densitometric analysis using ImageJ software.

2.3.6. Isotyping of Ascitic Fluid

Produced ascitic fluid of each corresponding hybridoma clone (see 2.4.1.) was subjected to a rapid isotyping assay for the determination of class and subclass identity of each mAb contained in the ascitic fluid. The assay performed following manufacturer's instructions (Thermo Fisher Scientific, Cat.: 26178). Briefly, diluted ascites samples were loaded onto the well of the cassette for the formation of a complex with conjugates embedded in the membrane. The complexes are then separated along the class- and subclass-specific impregnation on the membrane, usually indicated as a red band.

2.3.7. Titer Determination

Quantitative titer determination of the ascitic fluid was realized using the Easy-Titer IgG Assay kit (Thermo Fisher Scientific, Cat.: 23300). The assay is based on the aggregation of α-IgG sensitized monodispersed polystrene beads with sample IgGs. Samples were prepared accordingly and the assay was performed following manufacturer's instructions.

2.3.8. Purification of Ascitic Fluid

Ascites samples were purified using the Melon^{TM} Gel IgG Spin Purification kit (Thermo Fisher Scientific, Cat.: 45206). The assay is making use of a proprietary ligand for the binding of non-antibody proteins contained in the sample. Purified samples are obtained in the flow-through fraction. The assay was performed according to manufacturer's instructions. Aliquots of samples were then separated by SDS-PAGE (see 2.3.4.) and stained with GelCode Blue Stain Reagent (Thermo Fisher Scientific, Cat.: 24590) following manufacturer's instructions for the verification of the purification procedure.

2.4. *In vivo* Studies

2.4.1. Production of Ascites

All experimental procedures were approved and performed according to Institutional Animal Care and Use Committee (IACUC) of USC.

BALB/c mice (n=2/group) were intraperitoneally (i.p.) primed with pristane (TCI America, T0149-5ML) prior to inoculation with the respective hybridoma cell clones. Five days after priming, mice were inoculated with $1x10^6$ cells per mouse. Inoculated mice were checked daily for signs of distress and abdominal tension. Body weight measurements were taken, as well as body fluid, and lean mass measurements on a MiniSpec whole body composition analyzer. Ascitic fluid was collected 19 days after injection, cleared by centrifugation for 10 minutes at 500 xg, and subjected to isotyping (2.3.6.), titer determination (2.3.7.), and purification (2.3.8.).

2.4.2. In vivo Testing of the α-GHR mAbs

C57BL/6 mice (n=4-6/group) were intravenously (i.v.) injected with 10mg/kg of body weight with the respective mAbs for three consecutive days. 24 hours after the last injection, blood was sampled from the tail vein and centrifuged for 15 minutes at 14.000 rpm to obtain serum. Serum samples were tested for ALT, SAP, and IGF-1 following manufacturer's instructions (alanine transaminase, Cayman, Cat.: 700260; amyloid p component, serum, Boster Biological Technology, Cat.: EK1208; R&D Systems, Cat.: MG100). Small aliquots of whole blood were subjected to a complete blood count (CBC).

3. Results

3.1. Bioinformatical Assessment of the GHR

Sequential and structural *in silico* analysis of a protein of interest allows a better understanding of its mechanism of action, identification of functionally important domains, or association of evolutionarily conserved sequences through alignment and profile comparison of the corresponding target protein within different species. Hence, gathered relevant information contributes to a better interpretation enabling the researcher to target specific sequences and structures of the protein of interest, in order to manipulate and modify its function. Here, high-throughput methods were used to analyze the GHR for significant regions and domains designed to target sensitive structures to facilitate understanding of its function and its modification thereof.

In an initial screening, GHR protein sequences of different species were subjected to a multiple sequence alignment using computational algorithms to construct evolutionary relationships by homology, and assess sequences that are descendant from a common ancestor (Fig. 3.1.). The species that were considered for GHR protein sequence analysis were from human, the rhesus macaque, rat, mouse, bovine, dog, and chicken. Furthermore, sequence homology results of the multiple sequence alignment have been used to calculate sequence homology and create a phylogenetic tree to depict evolutionary relationships visually (Table 3.1. and Fig. 3.2.). A full version of the multiple sequence alignment and the phylogenetic tree including an expanded list of species can be found in the supplementary section (Fig. 11.1., Table 11.1 and Fig. 11.2.).

```
GHR_HUMAN      MDLWQLLLTLALAGSSDAFSGSEATAAILSRAPWSLQSVNPGLKTNSSKEPKFTKCRSPE    60
GHR_MACMU      ------------------------------------------------------------    0
GHR_RAT        MDLWRVFLTLALAVSSDMFPGSGATPATLGKASPVLQRINPSLRESSSGKPRFTKCRSPE    60
GHR_MOUSE      MDLCQVFLTLALAVTSSTFSGSEATPATLGKASPVLQRINPSLGTSSSGKPRFTKCRSPE    60
GHR_BOVIN      MDLWQLLLTLAVAGSSDAFSGSEATPAFLVRASQSLQILYPVLETNSSGNPKFTKCRSPE    60
GHR_CNLF       MDLWQLLLTLAVAGSGSAFSGSEATPTILGSASQSLQRVNPGLGTNSSEKPKFTKCRSPE    60
GHR_CHICK      MDLRHLLFTLALVCANDSLSASDD----------------------LLQWPQISKCRSPE    38


GHR_HUMAN      RETFSCHWTDEVHHGTKNLGPIQLFYTRRN--------TQEWTQEWKECPDYVSAGENSC    112
GHR_MACMU      ----------AVHHGSKSLGPIQLFYTRRN--------IQGQTQEWKECPDYVSAGENSC    42
GHR_RAT        LETFSCYWTEGDDHNLKVPGSIQLYYAR--------RIAHEWTPEWKECPDYVSAGANSC    112
GHR_MOUSE      LETFSCYWTEGDNPDLKTPGSIQLYYAKRESQRQAARIAHEWTQEWKECPDYVSAGKNSC    120
GHR_BOVIN      LETFSCHWTDGANHSLQSPGSVQMFYIRRD--------IQ----EWKECPDYVSAGENSC    108
GHR_CNLF       LETFSCHWTDGVRHGLKNAGSVQLFYIRRS--------TQEWTQEWKECPDYVSAGENSC    112
GHR_CHICK      LETFSCYWTDGKV---TTSGTIQLLYMKRS------------DEDWKECPDYITAGENSC    83
                                * :*: * :               :*******::** ***


GHR_HUMAN      YFNSSFTSIWIPYCIKLTSNGGTVDEKCFSVDEIVQPDPPIALNWTLLNVSLTGIHADIQ    172
GHR_MACMU      YFNSSFTSVWIPYCIKLTSNGDTVDGKCFSVDEIVQPDPPIALNWTLLNVSLTGIHADIL    102
GHR_RAT        YFNSSYTSIWIPYCIKLTTNGDLLDEKCFTVDEIVQPDPPIGLNWTLLNISLPGIRGDIQ    172
GHR_MOUSE      YFNSSYTSIWIPYCIKLTTNGDLLDQKCFTVDEIVQPDPPIGLNWTLLNISLTGIRGDIQ    180
GHR_BOVIN      YFNSSYTSVWTPYCIKLTSNGGIVDHKCFSVEDIVQPDPPVGLNWTLLNISLTEIHADIL    168
GHR_CNLF       YFNSSYTSIWIPYCIKLTSNGGTVDQKCFSVEEIVQPDPPIGLNWTLLNISLTGIHADIQ    172
GHR_CHICK      YFNTSYTSIWIPYCVKLANKDEVFDEKCFSVDEIVLPDPPVHLNWTLLNTSQTGIHGDIQ    143
               ***:*:**:* ***:**:.:.  .* ***:*::** **** : ******* *   *:.**


GHR_HUMAN      VRWEAPRNADIQKGWMVLEYELQYKEVNETKWKMMDPILTTSVPVYSLKVDKEYEVRVRS    232
GHR_MACMU      VRWEAPPNADIQKGWMVLEYELQYKEVNETKWKMMDPILSTSVPVYSLKVDKEYEVLVRS    162
GHR_RAT        VSWQPPPSADVLKGWIILEYEIQYKEVNETKWKTMSPIWSTSVPLYSLRLDKEHEVRVRS    232
GHR_MOUSE      VSWQPPPNADVLKGWIILEYEIQYKEVNESKWKVMGPIWLTYCPVYSLRMDKEHEVRVRS    240
GHR_BOVIN      VKWEPPPNTDVKMGWIILEYELHYKELNETQWKMMDPLMVTSVPMYSLRLDKEYEVRVRT    228
GHR_CNLF       VRWEPPPNADVQKGWIVLKYELQYKEVNESQWKMMDPVSATSVPVYSLRLDKEYEVRVRS    232
GHR_CHICK      VRWDPPPTADVQKGWITLEYELQYKEVNETKWKELEPRLSTVVPLYSLKMGRDYEIRVRS    203
               * *: * .:*:  **: *:**::***:**::** : *   *  *:***::.:::*: **:


GHR_HUMAN      KQRNSGNYGEFSEVLYVTLPQMS-QF-TCEEDFYFPWLLIIIFGIFGLTVMLFVFLFSKQ    290
GHR_MACMU      KRRNSRNYGEFSEVLYVTLPQMN-QF-TCEEDFYFPWLLIIIFGIFGLTVMLFVFLFSKQ    220
GHR_RAT        RQRSFEKYSEFSEVLRVTFPQMD-TLAACEEDFRFPWFLIIIFGIFGVAVMLFVVIFSKQ    291
GHR_MOUSE      RQRSFEKYSEFSEVLRVIFPQTN-ILEACEEDIQFPWFLIIIFGIFGVAVMLFVVIFSKQ    299
GHR_BOVIN      RQRNTEKYGKFSEVLLITFPQMN-PS-ACEEDFQFPWFLIIIFGILGLAVTLYLLIFSKQ    286
GHR_CNLF       RQRNSEKYGEFSEALYVTLPQMS-PF-ACEEDFQFPWFLIIIFGIFGLTMILFLFIFSKQ    290
GHR_CHICK      RQRTSEKFGEFSEILYVSFTQAGIEFVHCAEEIEFPWFLVVVFGVCGLAVTAILILLSKQ    263
               ::*.  ::.:*** * : : * .     * *:: ***:*:::**: *:::   :.::***


GHR_HUMAN      QRIKMLILPPVPVPKIKGIDPDLLKEGKLEEVNTILAIHDSYKPEFHSDDSWVEFIELDI    350
GHR_MACMU      QRIKMLILPPVPVPKIKGINPDLLKEGKLEEVNAILAIHDSYKPEFHSDDSWVEFIELDI    280
GHR_RAT        QRIKMLILPPVPVPKIKGIDPDLLKEGKLEEVNTILGIHDNYKPDFYNDDSWVEFIELDI    351
GHR_MOUSE      QRIKMLILPPVPVPKIKGIDPDLLKEGKLEEVNTILGIHDNYKPDFYNDDSWVEFIELDI    359
GHR_BOVIN      QRIKMLILPPVPVPKIKGIDPDLLKEGKLEEVNTILAIHDNYKHEFYNDDSWVEFIELDI    346
GHR_CNLF       QRIKMLILPPVPVPKIKGIDPDLLKEGKLEEVNTILAIHDNYKPEFYNDDSWVEFIELDI    350
GHR_CHICK      PRLKMLIFPPVPVPKIKGIDPDLLKKGKLDEVNSILASHDNYKTQLYNDDLWVEFIELDI    323
                *:****:***********:*****:***:***:**. **.** :::.** *********


GHR_HUMAN      DEP--DEKTEESDTDRLLSSDHEKSHSNLGVKDGDSGRTSCCEPDILETDFNANDIHEGT    408
GHR_MACMU      DEP--DEKNEGSDTDRLLSSDHQKSHSNLGVKDGDSGRTSCYEPDILETDFNANNIHEGT    338
GHR_RAT        DDA--DEKTEESDTDRLLSDDQEKSAGILGAKDDDSGRTSCYDPDILDTDFHTSDMCDGT    409
GHR_MOUSE      DEADVDEKTEGSDTDRLLSNDHEKSAGILGAKDDDSGRTSCYDPDILDTDFHTSDMCDGT    419
GHR_BOVIN      DDP--DEKTEGSDTDRLLSNDHEKSLNIFGAKDDDSGRTSCYEPDILEADFHVSDMCDGT    404
GHR_CNLF       DDL--DEKTEGSDTDRLLSNDHEKSLNILGAKDDDSGRTSCYEPDILETDFNASDVCDGT    408
GHR_CHICK      DDS--DEKNRVSDTDRLLSDDHLKSHSCLGAKDDDSGRASCYEPDIPETDFSASDTCDAI    381
               *:   ***.. ********.*: ** . :*.**.****:** :*** ::** ..:  :.


GHR_HUMAN      SEVAQPQRLK-GEADLLCLDQKNQNNSPYHDACPATQQPS-VIQAEKNKPQPLPTEGAES    466
GHR_MACMU      SEVAQPQRLK-GEADLLCLDQKNQNKSPYHDACPATQQPS-VIQAEKNKPQPLPTDGAES    396
GHR_RAT        SEFAQPQKLK-AEADLLCLDQKNLKNSPYDASLGSLHPSI-TLTM-EDKPQPLLGSETES    466
GHR_MOUSE      LKFRQSQKLN-MEADLLCLDQKNLKNLPYDASLGSLHPSI-TQTVEENKPQPLLSSETEA    477
GHR_BOVIN      SEVAQPQRLK-GEADISCLDQKNQNNSPSNDAAPASQQPS-VILVEENKPRPLLIGGTES    462
GHR_CNLF       SEVAQPQRLK-GEVDLLCLDQKNQNNSPSTDTTPTTQQPS-IILAKENKPRPLLISGTES    466
GHR_CHICK      SDIDQFKKVTEKEEDLLCLHRKDDVEALQSLANTDTQQPHTSTQSESRESWPPFADSTDS    441
                .. * :::.  * *: **.:*:  :     :    :          . :  *     :::
```

```
GHR_HUMAN      THQAAHIQLSNPSSLSNIDFYAQVSDITPAGSVVLSPGQKNKAGMSQCDMHPEMVSLCQE    526
GHR_MACMU      THQAAHIQLSNPSSLANIDFYAQVSDITPAGSVVLSPGQKNKAGMSQCDMHLEMVSLCQE    456
GHR_RAT        THQLPSTPMSSPVSLANIDFYAQVSDITPAGGVVLSPGQKIKAGLAQGNTQLEVAAPCQE    526
GHR_MOUSE      THQLASTPMSNPTSLANIDFYAQVSDITPAGGDVLSPGQKIKAGIAQGNTQREVATPCQE    537
GHR_BOVIN      THQAVHTQLSNPSSLANIDFYAQVSDITPAGNVVLSPGQKNKTGNPQCDTHPEVVTPCQA    522
GHR_CNLF       TQQAAHTQLSNPSSLANIDFYAQVSDITLAGSVVLSPGQKNKAGISPCDMPPEVASLCQA    526
GHR_CHICK      ANPSVQTQLSNQNSLTNTDFYAQVSDITPAGSVVLSPGQKSKVGRAQCESC------TEQ    495
               ::      :*.  **:* ********** **. ******* *.*    :         :

GHR_HUMAN      NFLMDNAYFCEADAKKCIPVAPHIKVESHIQPSLNQEDIYITTESLTTAAGRPG-TGEHV    585
GHR_MACMU      DFIMDNAYFCEADAKKCIPVAPHIKVESHIEPSFNQEDIYITTESLTTTAGRPG-TTEHI    515
GHR_RAT        NYSMNSAYFCESDAKKCIAAAPHMEATTCVKPSFNQEDIYITTESLTTTARMSE-TADTA    585
GHR_MOUSE      NYSMNSAYFCESDAKKCIAVARRMEATSCIKPSFNQEDIYITTESLTTTAQMSE-TADIA    596
GHR_BOVIN      NFIVDNAYFCEVDAKKYIALAPHVEAESHVEPSFNQEDIYITTESLTTTAGRSG-TAEHV    581
GHR_CNLF       NFIMDNAYFCEADAKKCITVAPHVEAESRVEPSFNQEDIYITTESLTTTAGQSG-TTERA    585
GHR_CHICK      NFTMDNAYFCEADVKKCIAVISQEEDEPRVQEQSCNEDTYFTTESLTTTGINLGASMAET    555
               :: ::.***** *.** *    : :    :: .  :** *:*******:.     :

GHR_HUMAN      PGSEMPVPDYTSIHIVQSPQGLILNATALPLPDK-EFLSSCGYVSTDQLNKIMP   638
GHR_MACMU      PGSEMPVPDYTSIHIVQSPQGLILNATALPLPGK-EFLSSCGYVSTDQLNKIMP   568
GHR_RAT        PDAE-PVPDYTTVHTVKSPRGLILNATALPLPDKKKFLSSCGYVSTDQLNKIMQ   638
GHR_MOUSE      PDAEMSVPDYTTVHTVQSPRGLILNATALPLPDKKNFPSSCGYVSTDQLNKIMQ   650
GHR_BOVIN      PSSEIPVPDYTSIHIVQSPQGLVLNATALPLPDK-EFLSSCGYVSTDQLNKIMP   634
GHR_CNLF       VSSEMPVPDYTSIHIIQSPRGLVLNATALPLPDK-EFLSSCGYVSTDQLNKIMP   638
GHR_CHICK      PSMEMPVPDYTSIHIVHSPQGLVLNATALPVPEK-EFNMSCGYVSTDQLNKIMP   608
                . *  *****::* ::**:**:*******:* * :*  **************
```

Fig. 3.1. Multiple sequence alignment of the GHR.

Protein sequences of the GHR of multiple species were aligned using the Clustal Omega tool to assess for homology and evolutionary correlation. An asterisk (*) symbolizes fully conserved amino acid residues. A colon (:) stands for conserved amino acid groups sharing strongly similar features, while a period (.) stands for conserved amino acid groups sharing weakly similar features. (GHR_HUMAN: Homo sapiens [Human], UniProt ID: P10912; GHR_MACMU: Macaca mulatta [Rhesus macaque], UniProt ID: P79194; GHR_RAT: Rattus norvegicus [Rat], UniProt ID: P16310; GHR_MOUSE: Mus musculus [Mouse], UniProt ID: P16882; GHR_BOVIN: Bos taurus [Bovine], UniProt ID: O46600; GHR_CNLF: Canis lupus familiaris [Dog], UniProt: Q9TU69; GHR_CHICK: Gallus gallus [Chicken], UniProt ID: Q02092).

Interpretation of the multiple sequence alignment shows a pattern of identical or similar features of the amino acid residues, which in turn implies homology of the GHR protein between the various species unequivocally and is potentially indicative of structural homology. Moreover, the alignment has been utilized to conduct quantitative and phylogenetic *in silico* analysis, represented by an identity matrix indicating calculated percentages of homology and a phylogenetic tree indicating shared ancestry (Table 3.1 and Fig. 3.2.).

Table 3.1. Percentage identity matrix of the GHR between species.

Homologous relationships of the GHR protein between different species were calculated by applying the hidden Markov model (HMM) algorithm described by Söding (Söding, 2005). The scored values are presented in a percentage identity matrix.

(%)	GHR_HUMAN	GHR_MACMU	GHR_RAT	GHR_MOUSE	GHR_BOVIN	GHR_CNLF	GHR_CHICK
GHR_HUMAN	100.00	93.84	69.56	68.34	77.13	82.29	61.19
GHR_MACMU	93.84	100.00	68.97	67.78	76.77	80.81	61.08
GHR_RAT	69.56	68.97	100.00	89.34	72.06	73.50	58.33
GHR_MOUSE	68.34	67.78	89.34	100.00	70.66	73.20	57.78
GHR_BOVIN	77.13	76.77	72.06	70.66	100.00	83.60	60.23
GHR_CNLF	82.29	80.81	73.50	73.20	83.60	100.00	62.52
GHR_CHICK	61.19	61.08	58.33	57.78	60.23	62.52	100.00

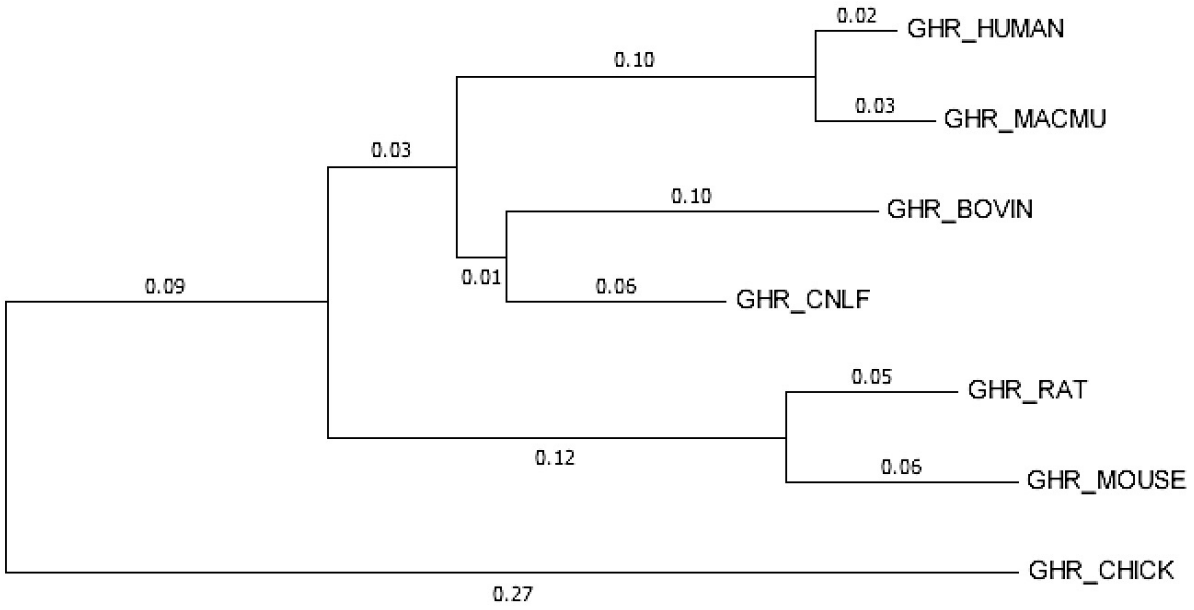

Fig. 3.2. Phylogenetic tree of the GHR between species.

Evolutionary origins of the GHR were calculated in MEGA7 (molecular evolutionary genetics analysis 7) software using the Neighbor-Joining method with Poisson correction. (GHR_HUMAN: Homo sapiens [Human], UniProt ID: P10912; GHR_MACMU: Macaca mulatta [Rhesus macaque], UniProt ID: P79194; GHR_RAT: Rattus norvegicus [Rat], UniProt ID: P16310; GHR_MOUSE: Mus musculus [Mouse], UniProt ID: P16882; GHR_BOVIN: Bos taurus [Bovine], UniProt ID: O46600; GHR_CNLF: Canis lupus familiaris [Dog], UniProt: Q9TU69; GHR_CHICK: Gallus gallus [Chicken], UniProt ID: Q02092).

Computational assessment of homologies between sequences in the given data set was generated by scoring the alignments using the hidden Markov model (HMM) algorithm by Söding (Söding, 2005). The results are implicated in a percentage identity matrix (Table 3.1.). Percentage identity comparisons of the

human GHR protein reveal a 93.84% match with the Rhesus macaque GHR protein, a match of 69.56% with the rat GHR protein, a similarity of 68.34% with the mouse GHR protein, an identity of 77.13% with the bovine form, 82.29% identity with the dog GHR protein, and 61.19% similarity with the chicken GHR protein (Table 3.1.). Furthermore, phylogenetic analysis using the Neighbor-Joining method was performed to determine evolutionary distances of the respective species (Fig. 3.2.). Horizontal dimensions are representative of evolutionary changes over time. Branches illustrate these changes. Their lengths are reflective of the dimensional changes and serve as units of evolutionary distances. For instance, the human GHR protein and the Rhesus macaque GHR protein share common ancestry. However, evolutionary distance of the human GHR protein to their common ancestor has a value of 0.02, while the distance of the Rhesus macaque GHR protein to the common ancestor has in comparison an extended evolutionary distance of 0.03 (Fig. 3.2.). The units of branch lengths are representative of amino acid residues substitutions per site, exemplifying amino acid residue substitutions divided by the entire amino acid sequence.

3.2. Identification of Potential Epitopes on the GHR

The design of the here presented drug development project is focused on the generation and characterization of mouse anti-mouse monoclonal antibodies targeting the GHR regarding their potency to modify GH signaling. Therefore, sequential and structural analysis of the mouse GHR protein will be in the center of interest. The presented framework will also elaborate homology to the human GHR protein, to further enable conclusions regarding the identification of important functional domains and investigate drug-protein interactions. For this purpose, an antibody development company has been commissioned to produce hybridoma clones, which secrete mouse anti-mouse mAbs targeting the GHR, accomplished by the hybridoma technology (see 1.13.). The mouse GHR protein sequence has been submitted and was subjected to a rigorous analysis using a proprietary algorithm (SEAL^{TM}) aimed at identifying potential epitopes/antigens that would most likely yield mAbs. Five hybridoma clones producing five different mouse anti-mouse GHR mAbs were selected for further investigation (Fig. 3.3. and Table 3.2.).

>sp|P16882|GHR_MOUSE Growth hormone receptor OS=Mus musculus GN=Ghr PE=1 SV=1
MDLCQVFLTLALAVTSSTFSGSEATPATLGKASPVLQRINPSLGTSSSGKPRFTKCRSPELE
TFSCYW**TEGDNPDLKTP**GSIQLYYAKRESQRQAARIAHEWTQEWKECPDYVSAGKNSCYFNS
SYTSIWIPYCI**KLTTNGDLLDQK**CF**TVDEIVQPDPPI**GLNWTLLNISLTGIRGDIQVSWQPP
PNADVLKGWIILEYEIQYKEVN**ESKWKVMGPIWL**TYCPVYSLRMDKEHEVRVRSRQ**RSFEKY**
SEFSEVLRVIFPQTNILEACEEDIQFPWFLIIIFGIFGVAVMLFVVIFSKQQRIKMLILPPV
PVPKIKGIDPDLLKEGKLEEVNTILGIHDNYKPDFYNDDSWVEFIELDIDEADVDEKTEGSD
TDRLLSNDHEKSAGILGAKDDDSGRTSCYDPDILDTDFHTSDMCDGTLKFRQSQKLNMEADL
LCLDQKNLKNLPYDASLGSLHPSITQTVEENKPQPLLSSETEATHQLASTPMSNPTSLANID
FYAQVSDITPAGGDVLSPGQKIKAGIAQGNTQREVATPCQENYSMNSAYFCESDAKKCIAVA
RRMEATSCIKPSFNQEDIYITTESLTTTAQMSETADIAPDAEMSVPDYTTVHTVQSPRGLIL
NATALPLPDKKNFPSSCGYVSTDQLNKIMQ

Fig. 3.3. FASTA format of the mouse GHR protein.
The mouse GHR protein sequential information illustrated by the FASTA format reveals the location of the identified targets (yellow: signal peptide [amino acid residues 1 - 24]; green: extracellular domain [amino acid residues 25 - 273]; blue: transmembrane domain [amino acid residues 274 – 297]; burgundy: intracellular/cytoplasmic domain [amino acid residues 298 – 650]).

Table 3.2. Location of the five identified targets within the GHR protein sequence.
Hybridoma clones (C562, C565, C570, C576, and C592) and each produced α-GHR monoclonal antibody (α-GHR562, α-GHR565, α-GHR570, α-GHR576, α-GHR592) by the respective clone as well as their exact location within the GHR amino acid sequence are depicted.

Product Name	The Epitope Identification/Peptide Sequence	Start	End
C562 (α-GHR562)	TEGDNPDLKTPG	69	80
C565 (α-GHR565)	ESKWKVMGPIWL	209	220
C570 (α-GHR570)	KLTTNGDLLDQK	136	147
C576 (α-GHR576)	RSFEKYSEFSEV	243	254
C592 (α-GHR592)	TVDEIVQPDPPI	150	161

Topological analysis reveals that all of the five identified antigens are located within the extracellular domain of the GHR (Fig. 3.3.). Moreover, all antigens represent small peptide fragments composed of a hydrophobic stretch of 12 amino acid residues (Fig. 3.3. and Table 3.2.). Structural analysis was performed to further determine if the identified antigen targets were located within a specific region of the extracellular domain of functional relevance and implication. For this purpose, the mouse antigens were highlighted within the crystalized structure of the human GHR extracellular domain (Fig. 3.4.).

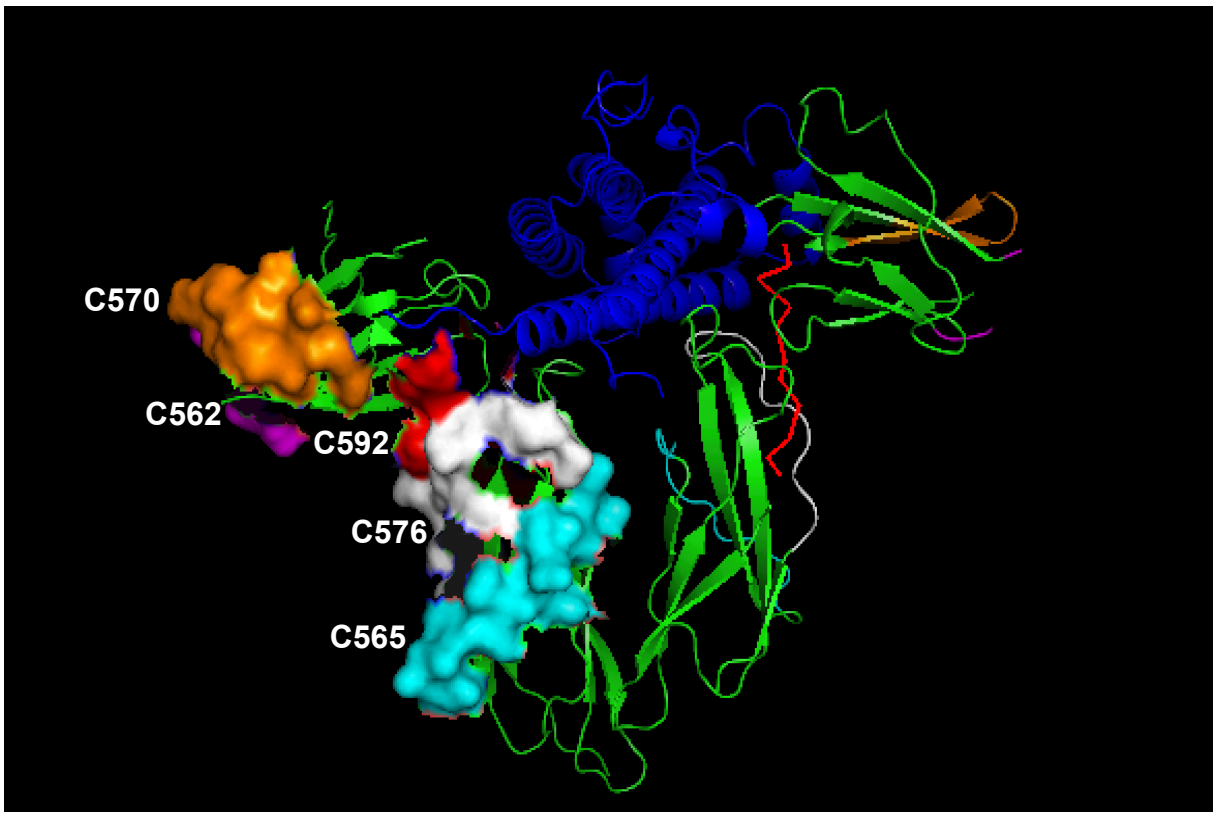

Family and Domains (Mouse):

Feature Key	Position(s)	Length	Description
Domain	159 - 262	104	Fibronectin type-III
Region	303 - 390	88	Required for JAK2 binding
Motif	248 - 252	5	WSXWS motif
Motif	306 - 314	9	Box 1 motif
Motif	349 - 358	10	UbE motif

Family and Domains (Human):

Feature Key	Position(s)	Length	Description
Domain	151 - 254	104	Fibronectin type-III
Region	260 - 262	3	Required for proteolysis
Motif	240 - 244	5	WSXWS motif
Motif	297 - 305	9	Box 1 motif
Motif	340 - 349	10	UbE motif

Fig. 3.4. Illustration of the target sequences within the extracellular domain of the GHR.
The five mouse antigens were highlighted within the crystalized human GHR protein (from de Vos *et al.,* 1992) to derive functional information. Furthermore, functional important domains of the mouse and human GHR protein are summarized (blue: GH; green: extracellular domain/dimer [mouse amino acid residues 25 – 273; human amino acid residues 19 - 264]).

Association of the sequential and structural information shows that monoclonal antibodies α-GHR565 and α-GHR592, respectively produced by hybridoma clones C565 and C592, are theoretically targeting the Fibronectin type-III of the human and the mouse GHR protein (Fig. 3.4.). Moreover, monoclonal antibody α-GHR576, produced by hybridoma clone C576, is targeting the Fibronectin type-III domain as well as the WSXWS motif of the human and mouse GHR protein (Fig. 3.4.). Implications of structurally functional relevance for α-GHR562 and α-GHR570 could

not be made. However, it is important to emphasize the functional role of the respective domains. Fibronectin type-III domain is mediating non-covalent interactions with other proteins, while the WSXWS motif is required for protein folding efficiency, ligand binding, and receptor signaling. Unaffected domains of the GHR by the mAbs are the box 1 motif and the UbE (ubiquitination-dependent endocytosis) motif (Fig. 3.4.). The box 1 motif effectuates interaction of the GHR with JAK2, while the UbE motif is required for the recruitment of ubiquitin system components for the internalization and degradation of the receptor.

To further evaluate cross-reactivity of the mouse anti-mouse GHR mAbs between the human and mouse GHR protein, the target antigens were locally aligned (Table 3.3.). It could be shown, that the target antigen for α-GHR592 has the most significant sequence homology of 100% between the human and mouse version (Table 3.3.). In comparison, the antigen of α-GHR576 has the second most significant sequence similarity of 86%, while target antigens for α-GHR562, GHR565, and GHR570 have a sequence identity of 83%, 70%, and 58%, respectively (Table 3.3.).

Table 3.3. Local and pairwise alignment between the human and mouse GHR antigen targets.
The Basic Local Alignment Search Tool (BLAST) algorithm was used for comparison and pairwise sequence alignment to determine sequence homology.

Hit		Identity	mAb
GHR_MOUSE GHR_HUMAN	NPDLKT NP LKT NPGLKT	83%	C562 (α-GHR562)
GHR_MOUSE GHR_HUMAN	ESKWKVMGPI E KWK M PI ETKWKMMDPI	70%	C565 (α-GHR565)
GHR_MOUSE GHR_HUMAN	KLTTNGDLLDQK KLT NG D+K KLTSNGGTVDEK	58%	C570 (α-GHR570)
GHR_MOUSE GHR_HUMAN	YSEFSEV Y EFSEV YGEFSEV	86%	C576 (α-GHR576)
GHR_MOUSE GHR_HUMAN	VDEIVQPDPPI VDEIVQPDPPI VDEIVQPDPPI	100%	C592 (α-GHR592)

3.3. Ascites Production in Balb/c Mice

Production of mAbs in ascites fluid is a cost-effective method, designed to generate high titer antibody within a relatively short timeframe. Depending on the capacity of each hybridoma clone, the concentration of produced mAbs can reach milligram quantities per milliliter of ascites fluid. Hybridoma clones, which exhibit self-limiting growth characteristics or yield low mAb concentrations in the cell culture system, will qualify for this approach. Here, the production of our five candidates in pristane-primed Balb/c mice is reported. This approach has been chosen due to the inadaptability of the five corresponding hybridoma clones with the *in vitro* system.

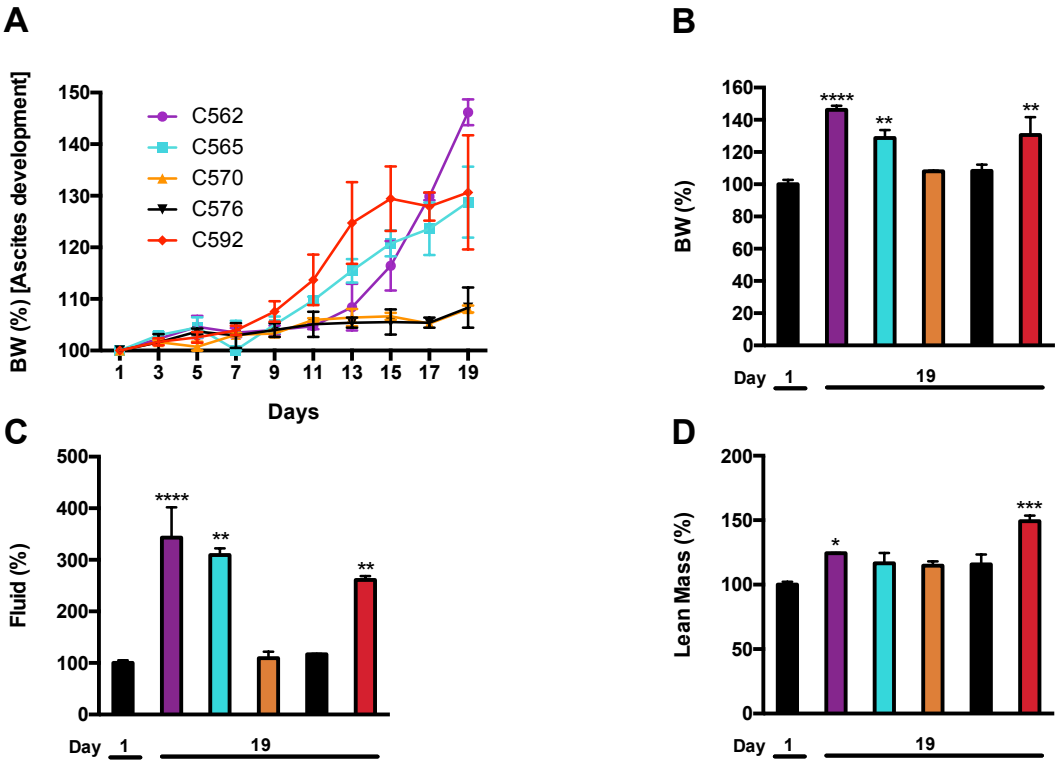

Fig. 3.5. Production of ascites fluid after inoculation of Balb/c mice with the ascites tumor.
The development of ascites fluid after inoculation with the respective hybridoma clones over 19 days is shown (A), as well as changes in the total body weight (B), the percentage of body fluid (C), and increases in lean body mass (D) between the first and last day of development. A one-way ANOVA analysis with post-hoc Tukey test was applied to the dataset to assess significance (purple: C562; turquoise: C565; orange: C570; black: C576; red: C592).

The dataset shows a progressive incline in the total body weight percentage for pristane-primed Balb/c mice inoculated with the hybridoma clones C562, C565, and C592 (Fig. 3.5. A). Balb/c mice intraperitoneally injected with C570 and C576

exhibit no changes in the total body weight percentage over 19 days (Fig. 3.5. A). Further comparison of body weight changes between the first and the last day of the study (day 19), displays a significant increase for mice inoculated with C562 (~ 43% - 48%), C565 (~ 23% - 33%), and C592 (~ 20% - 40%) (Fig. 3.5. B). However, no significant changes for mice injected with C570 and C576 could be observed (Fig. 3.5. B). Breakdown of the dataset into components derived from total body weight, namely body fluid and lean body mass, demonstrates significant increases in body fluid for mice injected with C562 (~ 248% - 400%), C565 (~ 296% - 322%), and C592 (~ 253% - 268%) (Fig. 3.5. C and D). This incline in body fluid percentage is proportional to the increase in total body weight and is representative of ascites production. Due to the deficiency of clone C570 and C576 to adapt to the applied method for production purpose, these candidates were excluded from the study and were not subjected to any further investigations. The lack of C570 and C576 ascites fluid makes it inevitable to exclude them at this point since their corresponding mAbs cannot be subjected to any further application. Instead, ascites fluid produced by clones C562, C565, and C592, and their corresponding mAbs were the subject of any extensive characterization reported in this study.

3.3.1. Isotyping and Determination of Antibody Titer

Typical mAb concentrations and volumes generated by the inoculation of mice with hybridoma clones range from 1-10mg/ml. Individual production rates are highly dependent upon the potency of each hybridoma clone. Therefore, it is necessary to select clones that were qualitatively screened during the hybridoma development procedure for their ability to grant high yield to avoid systematic errors. Once the production of the ascites fluid is completed, it can be harvested from the peritoneal cavity of the mouse to enable further processing for functional applications. In a first step, the ascites fluid was used to determine class and subclass of the harvested mAbs. This initial step is a necessity and represents a pre-experimental design due to the commercial availability of immunoglobulin-specific titer kit assays for the accurate determination of mAb concentrations. Results of the isotyping screening are displayed as red bands on an antibody-impregnated membrane, which indicate class and subclass specificity of the mAbs (Fig. 3.6.).

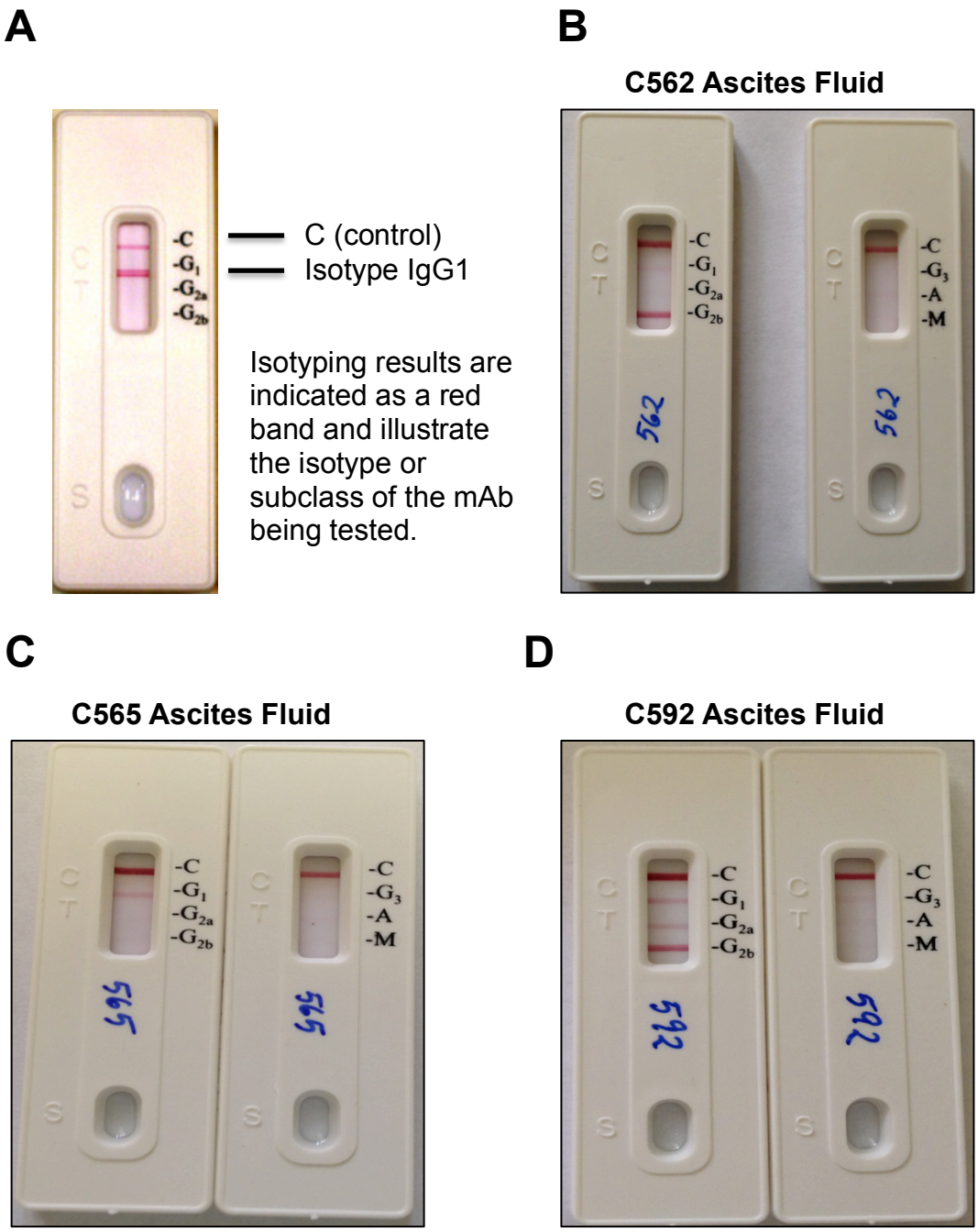

Fig. 3.6. Isotyping of C562, C565, and C592 ascites fluid.

The image indicates immunoglobulin class and subclass specificity. For their determination, diluted ascites samples were loaded onto the antibody-impregnated membrane and incubated [A: Thermo Scientific Pierce Rapid Mouse Isotyping Kit figure with legends. B – D: C562 (B), C565 (C), and C592 (D) ascites fluid tested on cassettes after samples were applied and loaded into the sample wells (C: control; mouse monoclonal antibody class and subclass identity: G_1 (IgG_1), G_{2a} (IgG_{2a}), G_{2b} (IgG_{2b}), G_3 (IgG_3), A (IgA), and M (IgM)].

Determination of mAb class and subclasses reveals isotype IgG2b for ascites produced by C562 and C592 (Fig. 3.6. B and D), and isotype class IgG1 for ascites

generated by clone C565 (Fig. 3.6. B). This knowledge facilitated the implementation of an IgG-specific titer kit for the accurate measurement of mAb concentrations. The detection of mAbs in the ascites fluid is based on the microagglutination of microspheres coated with anti-IgG polyclonal antibodies. Total protein concentration of the ascites fluid was measured before quantification of the mAb titer, as well as the mAb concentration after subsequent ascites purification was determined to evaluate the efficiency of the system being used. Three independent batches per clone are shown for each independent approach (Fig. 3.7.).

Total protein concentration of the ascites fluid indicates approximately 150µg/µl of total protein contained in ascites fluid generated by clones C562 and C565, while for C592 total protein concentration is about 250µg/µl (Fig. 3.7. A). Subsequent titer determination shows a mAb concentration of 6-8µg/µl contained in the ascites fluid for each clone (Fig. 3.7. B). In contrast, subjecting the ascites fluid to purification and extraction of the mAbs of interest reduces their concentration to about 2µg/µl (Fig. 3.7. C). However, SDS-PAGE analysis followed by colorimetric staining is indicative of the recovery of pure mAbs (Fig. 3.7. D).

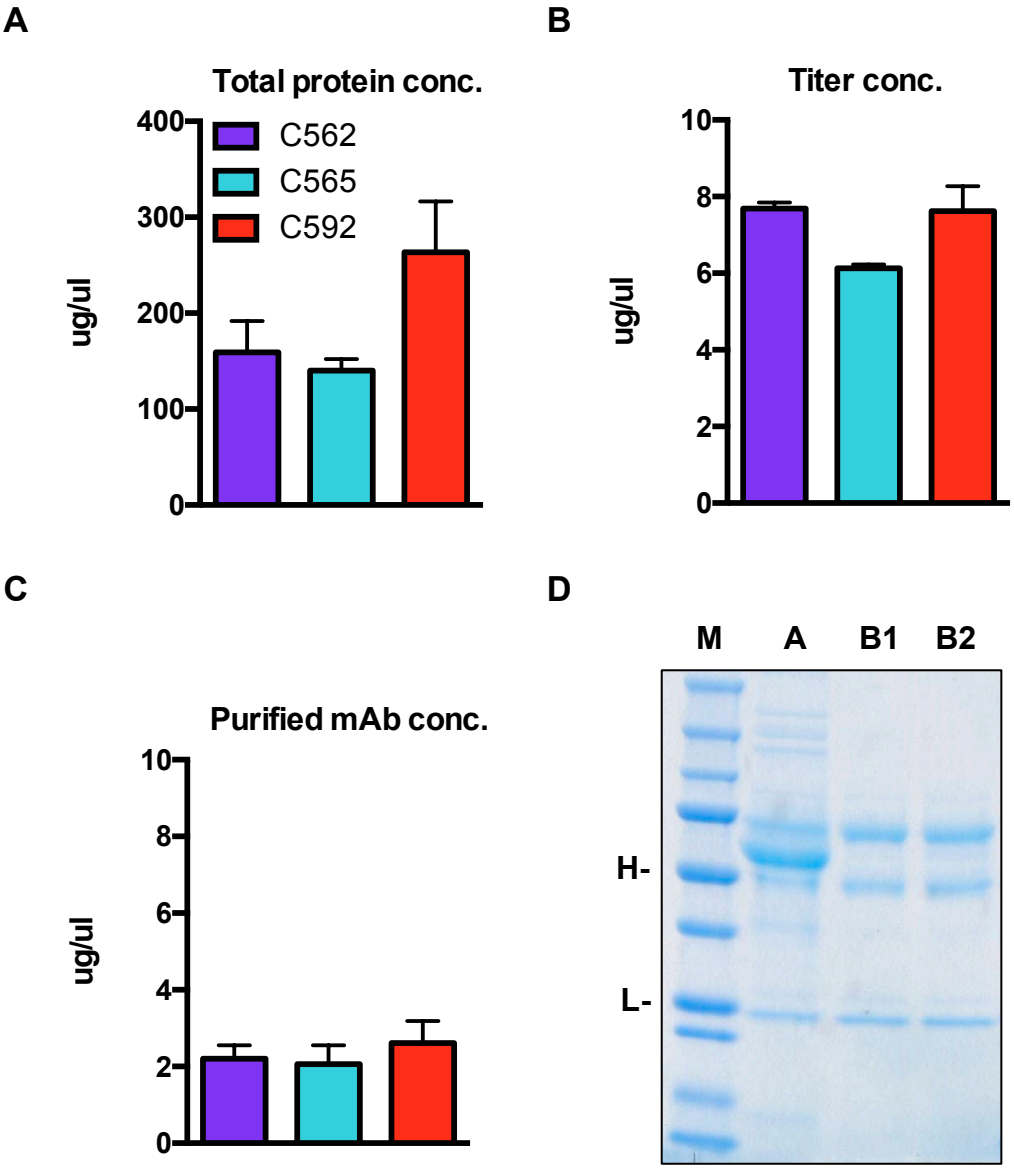

Fig. 3.7. Determination of total protein and mAb concentration.

The graphs represent total protein concentration in ascites fluid (A), mAb titer contained in ascites fluid (B), and mAb concentration after their extraction from the ascites fluid (C) (purple: C562; turquoise: C565; red: C592). The gel implies purity of the purified mAb batches (D). Three independent batches per individual clone were subjected to the procedures. Each batch was purified in two successive batches [**H** (Heavy chain = 50kDa); **L** (Light chain = 25kDa); **M** (Marker); **A** (Starting ascites sample); **B1** (Purified batch 1); **B2** (Purified batch 2)].

3.4. Binding of the mAbs to their GHR Target Antigen

Evaluation of the ability of the mAbs to bind to their corresponding antigen target on the GHR allows a better prediction of their potential relevance to assess alternative effects induced to modify GHR function. Furthermore, corresponding studies provide the capability and enhance the understanding of molecular

interactions as well as structure-function relationships. Moreover, the gathered knowledge provides the basis to derive complex functional relationships between the drug to be developed and the target antigen. Here, two independent approaches were used to study binding interactions. In a first attempt, immunofluorescent staining and analysis was performed followed by surface plasmon resonance (SPR) analysis to examine binding and kinetics (3.4.1. and 3.4.2.).

3.4.1. Immunofluorescent Staining of L Cells to Determine Binding

The capability of the α-GHR mAbs to bind specifically to the particular antigenic determinant they were designed against, can be qualitatively and quantitatively assessed. Here, a competitive approach was used to identify and measure the qualities mentioned above (Fig. 3.8. A and B). Briefly, α-GHR mAbs were incubated with their antigenic determinant/peptide they were designed against to allow the binding process to occur. Afterwards, the mixture was given to L cells, which overexpress the murine GHR followed by immunofluorescent staining and examination using confocal microscopy (Fig. 3.8. A and B).

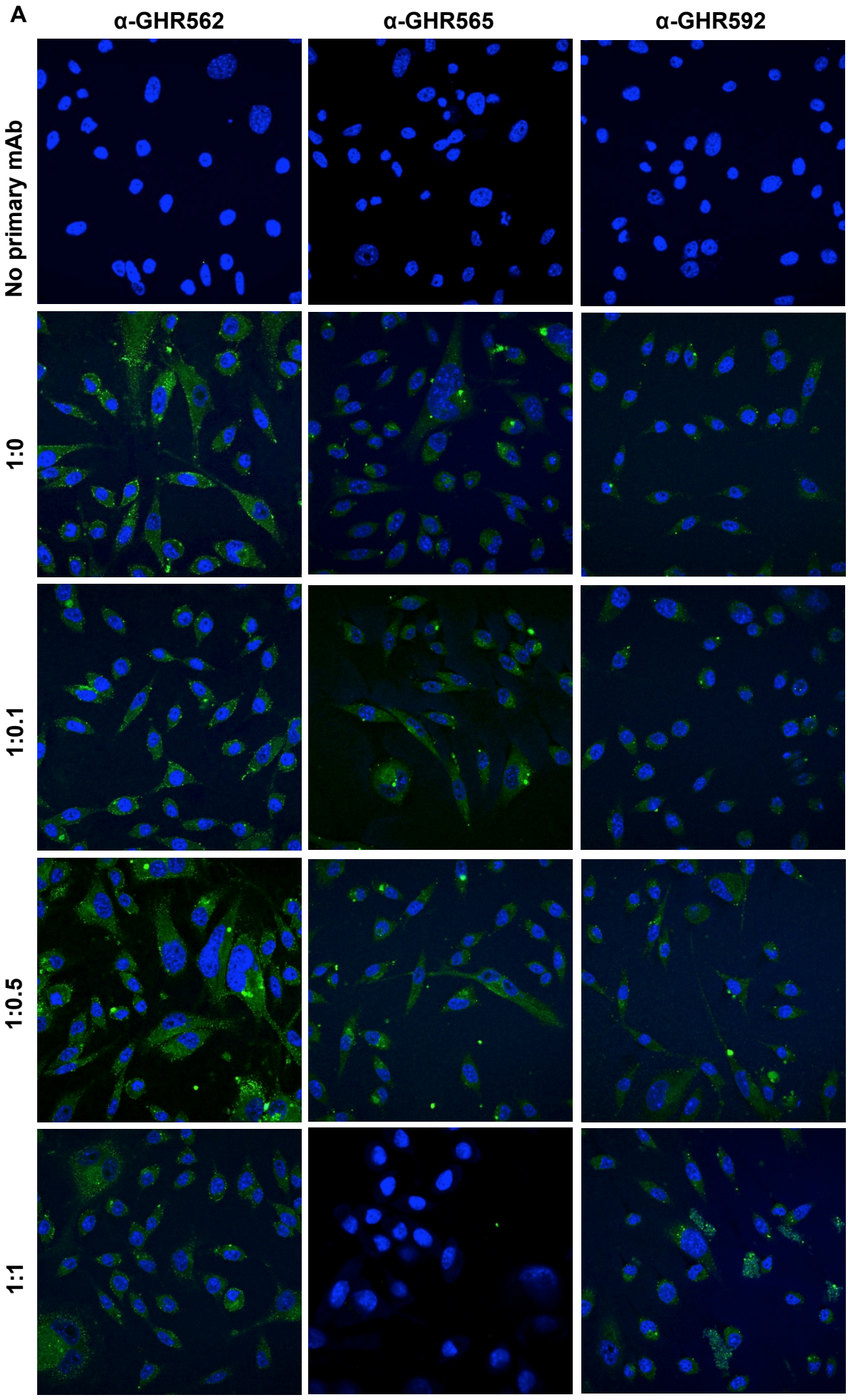
A
α-GHR562
α-GHR565
α-GHR592
No primary mAb
1:0
1:0.1
1:0.5
1:1

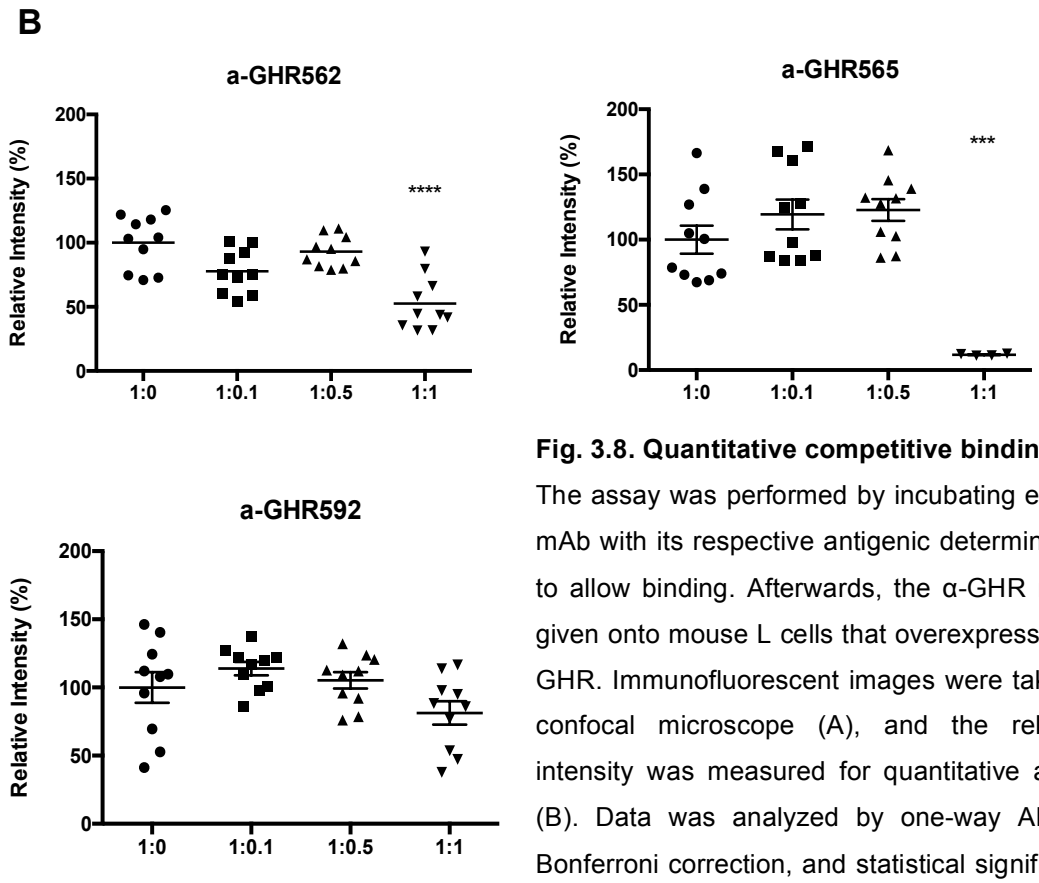

Fig. 3.8. Quantitative competitive binding assay. The assay was performed by incubating each α-GHR mAb with its respective antigenic determinant/peptide to allow binding. Afterwards, the α-GHR mAbs were given onto mouse L cells that overexpress the murine GHR. Immunofluorescent images were taken using a confocal microscope (A), and the relative pixel intensity was measured for quantitative assessment (B). Data was analyzed by one-way ANOVA with Bonferroni correction, and statistical significance ($P < 0.0001$) is expressed compared to the control (1:0).

Incubation of a constant molar concentration of each α-GHR mAb (α-GHR562, α-GHR565, and α-GHR592) with increasing molar ratios (mAb:peptide = 1:0; 1:0.1; 1:0.5; 1:1) of the peptide/antigenic determinant they were designed against, shows overall a serial decline of the quantified relative pixel intensity for the captured confocal fluorescent images corresponding with each condition (Fig. 3.8. A and B). Analysis of the images revealed that this decline is most significant for α-GHR565 (1:1) ratio, but no significant differences were observed for α-GHR592 (Fig. 3.8. B). However, incubation of α-GHR562 with increasing molar ratios of its complementary peptide followed by incubation of this mixture with mGHR overexpressing L cells is indicative of a successive decline in the relative pixel intensity, with the 1:1 (mAb:peptide) molar ratio being the most significant data point (Fig. 3.8. B).

3.4.2. Examination of Biomolecular Interactions using the Biacore Platform

The Biacore platform enables the investigation of biomolecular interactions between a target and its antigen. It delivers sensitive thermodynamic data regarding several parameters, including specificity, affinity, and concentration of the analyte

and ligand being investigated. In this case, the biomolecular interaction of the α-GHR mAbs and their peptides were analyzed. In an initial step, the isoelectric points (pI) of the peptides were calculated using the Expasy calculation tool. This step is necessary to avoid technical difficulties during the experiment and to determine optimal buffer compositions and concentrations. This step also determines whether the peptide of its complementary α-GHR mAb will be used as analyte or ligand. The calculated pIs for the peptides are listed below (Table 3.4.).

Table 3.4. Isoelectric point (pI) of the peptides.

The table depicts the pI for the respective peptides. The pI was calculated using the Expasy calculation tool.

Product Name	The Epitope Identification/Peptide Sequence	Isoelectric Point (pI)
C562 (α-GHR562)	TEGDNPDLKTPG	4.03
C565 (α-GHR565)	ESKWKVMGPIWL	8.69
C592 (α-GHR592)	TVDEIVQPDPPI	3.49

The table illustrates that the pI for the peptide of mAb α-GHR565 has a value of 8.69 and is located within the basic spectrum (Table 3.4.). In contrast to this, the pIs for the peptides of α-GHR562 and α-GHR592 have calculated values of 4.03 and 3.49 and are therefore inhabited within the acidic spectrum (Table 3.4.). Therefore, two different approaches were used to perform the SPR experiment. A conventional approach for α-GHR565 and its peptide was used, where the peptide was immobilized on the surface of the CM5 chip and served therefore as a ligand, whereas α-GHR565 was used as the analyte that was injected at different concentrations over the surface. For α-GHR562 and α-GHR592 mAbs, the reversed design was used, where the mAbs served as ligand and the peptides as analyte. The obtained results are shown in the sensorgrams below (Fig. 3.9.).

A) α-GHR562

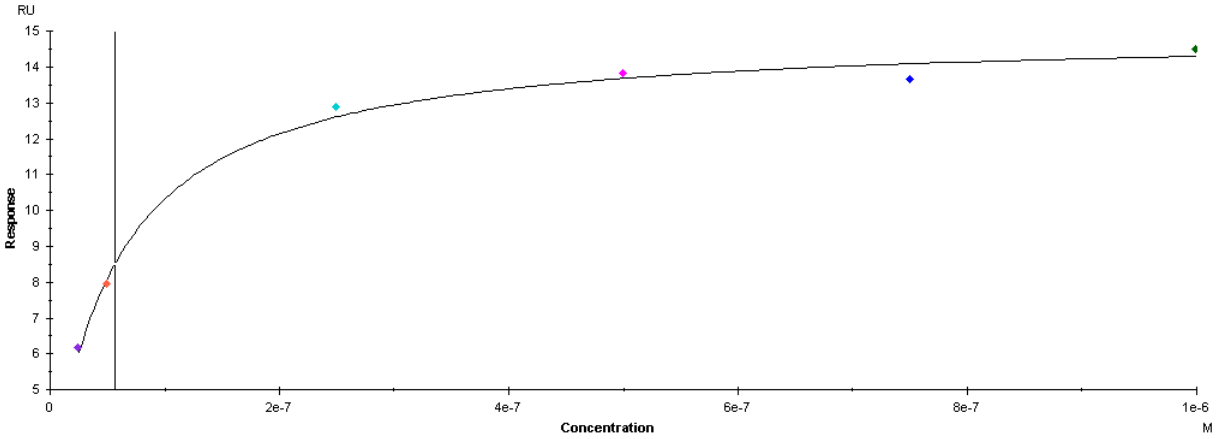

KD (M): 5.659E-8; Rmax (RU): 12.92; offset (RU): 2.075; Chi≤ (RU≤): 0.127.

B) α-GHR565

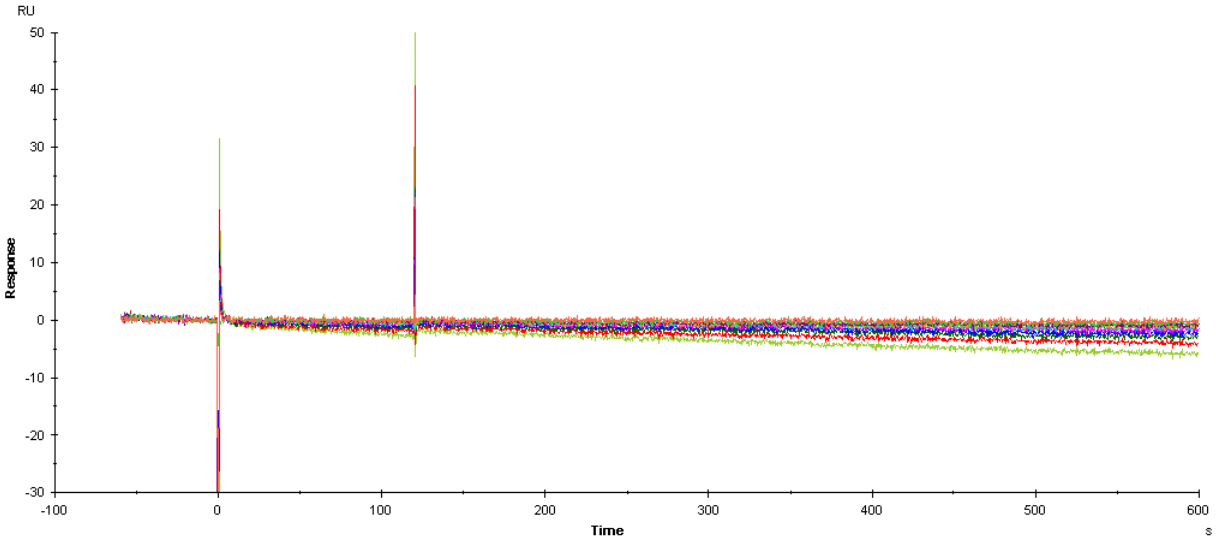

C) α-GHR592

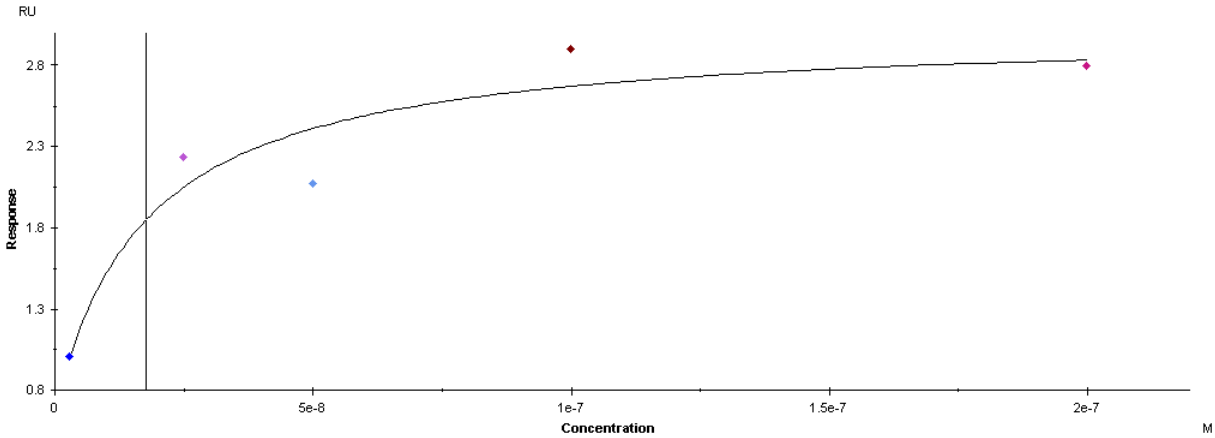

KD (M): 1.771E-8; Rmax (RU): 2.340; offset (RU): 0.6816; Chi≤ (RU≤): 0.101.

Fig. 3.9. Assessment of binding kinetics using the Biocore T100 platform.

Binding affinity and specificity was determined through concentration series injections of the analyte after immobilization of the ligand on the surface of the CM5 chip.

Interpretation of the data shows that no valuable data could be obtained in case of α-GHR565 (Fig. 3.9.). Binding affinity could not be determined. The sensorgram does not indicate any oscillations although a series of α-GHR565 mAb concentrations was injected (Fig. 3.9.). However, data could be obtained using the unconventional approach for mAbs α-GHR562 and α-GHR592, where the mAbs were immobilized across the surface of the chip and a series of peptide concentrations was injected (Fig. 3.9.). The equilibrium dissociation constant (KD) in case of α-GHR562 is 5.659E-8 M and the response unit (RU) is 12.92, whereas in the instance of α-GHR592 this binding affinity is in a range of 1.771E-8 M and the RU is 2.340 (Fig. 3.9.).

3.5. Testing of Intracellular Markers

GH is known to activate signal transduction pathways including intracellular markers such as STAT5 (signal transducer and activator of transcription 5) and ERK1/2 (extracellular signal-regulated kinases 1/2) (see 1.6.). Since the aim of this drug development project involves the establishment of α-GHR mAbs to potentially modify GHR function and/or manipulate the GH signaling pathway, the ability of the three α-GHR mAb candidates regarding their potential to activate or inhibit STAT5 and ERK1/2 phosphorylation was tested using an *in vitro* system. The intention of this experiment is to characterize the mAbs regarding their agonistic, antagonistic or neutral behavior in regards to the GH signaling pathway. In an initial screening, a concentration of 500ng/ml of GH was used to induce STAT5 phosphorylation in murine L cells using differential time scan points to determine the optimal condition for this assay (Fig. 3.10.).

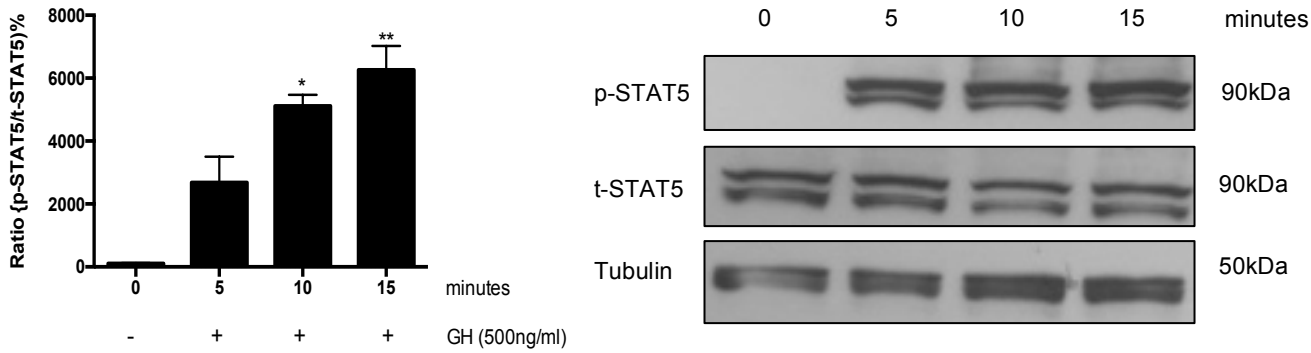

Fig. 3.10. GH screening in murine L cells.
L cells were serum starved and then treated with GH for the indicated time points to induce STAT5 phosphorylation. Cell lysates were analyzed by Western blot and data were statistically analyzed by one-way ANOVA ($P < 0.05$).

As indicated above, GH is inducing a significant induction of STAT5 phosphorylation after 10 and 15 minutes of treatment (Fig. 3.10.). However, there is no statistically significant difference comparing 10 to 15 minutes of treatment. Therefore, the 10 minutes time screen point was chosen for further experiments, where L cells were pre-treated with the α-GHR mAbs to allow binding to the GHR expressed on the cell surface and the treated with GH for 10 minutes to trigger STAT5 phosphorylation. In addition to STAT5, ERK1/2 was included as an additional complementary marker for validation purpose. The compiled data is shown below (Fig. 3.11.).

A

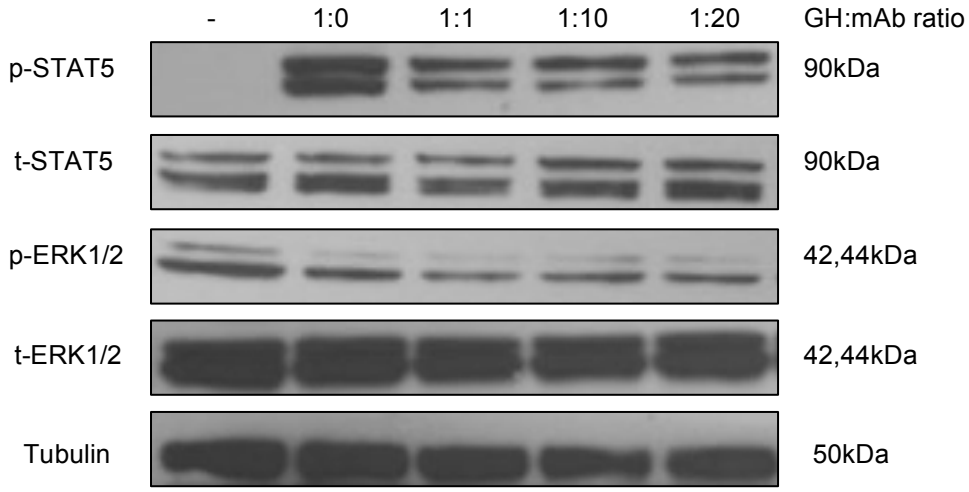

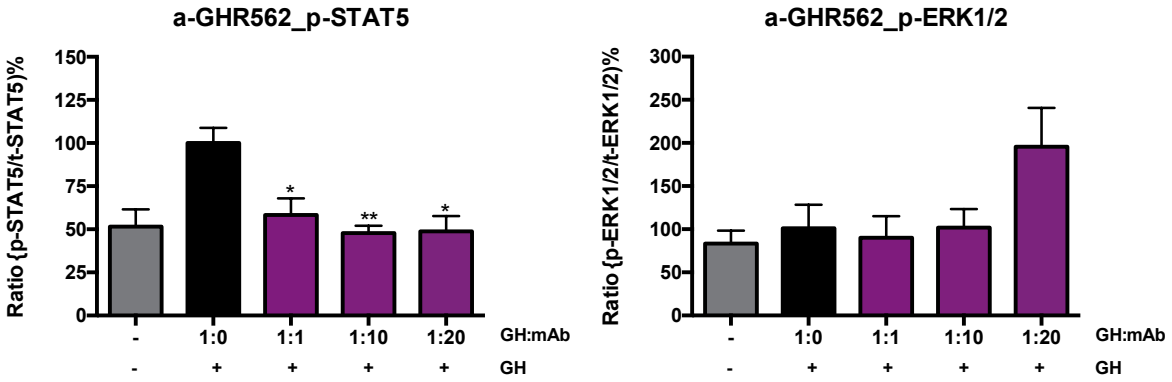

B

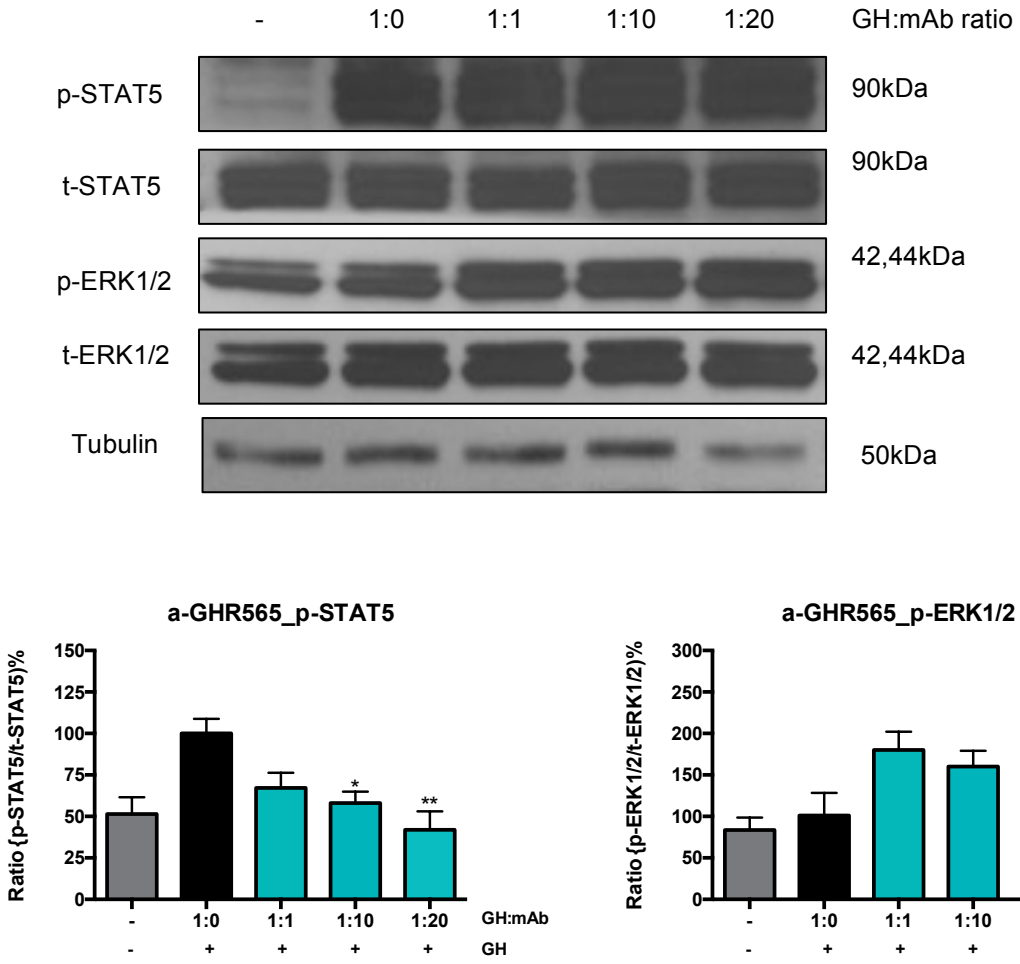
- 1:0 1:1 1:10 1:20 GH:mAb ratio
p-STAT5
90kDa
t-STAT5
90kDa
p-ERK1/2
42,44kDa
t-ERK1/2
42,44kDa
Tubulin
50kDa
a-GHR565_p-STAT5
Ratio {p-STAT5/t-STAT5}%
150
125
100
75
50
25
0
*
**
- 1:0 1:1 1:10 1:20 GH:mAb
- + + + + GH
a-GHR565_p-ERK1/2
Ratio {p-ERK1/2/t-ERK1/2}%
300
250
200
150
100
50
0
- 1:0 1:1 1:10 1:20 GH:mAb
- + + + + GH

C

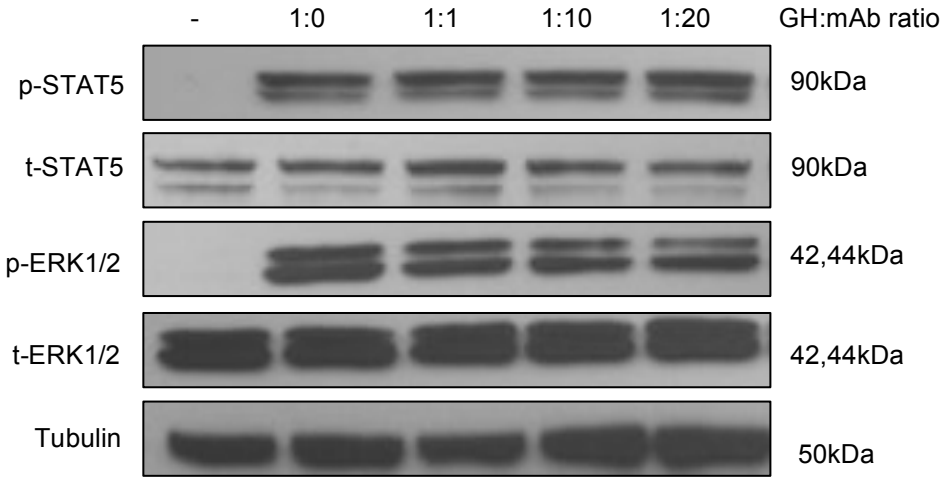
- 1:0 1:1 1:10 1:20 GH:mAb ratio
p-STAT5
90kDa
t-STAT5
90kDa
p-ERK1/2
42,44kDa
t-ERK1/2
42,44kDa
Tubulin
50kDa

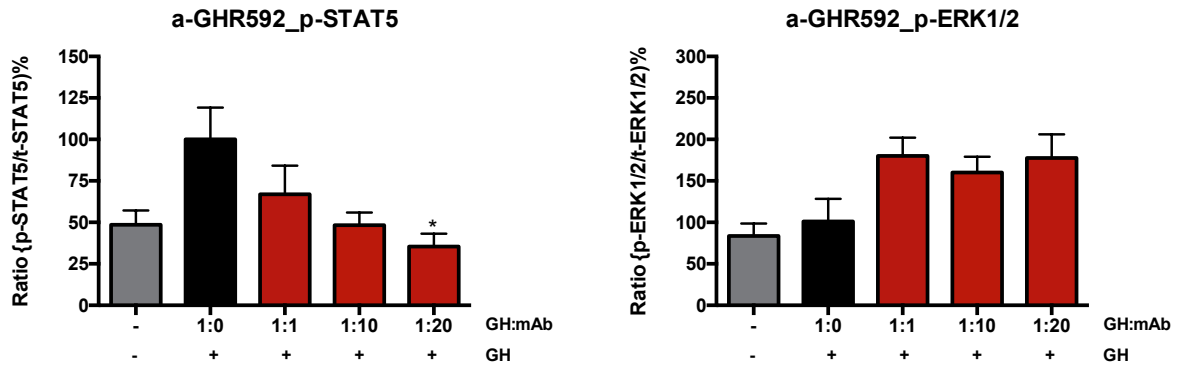

Fig. 3.11. p-STAT5 and p-ERK1/2 as intracellular markers for α-GHR mAb characterization.
Serum starved L cells were pre-treated with the corresponding α-GHR mAbs and then with GH to trigger induction of the GH signaling pathway. Cells were lysed and subjected to western blot analysis. The dataset was analyzed by one-way ANOVA and represents the average of three to four independent experiments ($P < 0.05$).

Western blot analysis reveals that a significant downregulation of p-STAT5 could be achieved with each of the mAbs α-GHR562, α-GHR565, and α-GHR592 (Fig. 3.11. A, B, and C). However, α-GHR562 mAb seems to be the most potent mAb since the phosphorylation of STAT5 is significantly downregulated using all three concentration ratios of 1:1, 1:10, and 1:20 (Fig. 3.11. A). For α-GHR565 mAb the decrease in p-STAT is only significant using the concentration ratios of 1:10 and 1:20, and for α-GHR592 mAb only the highest concentration of 1:20 was able to significantly decrease phosphorylation of STAT5 (Fig. 3.11. B and C). However, no significant changes could be observed in the phosphorylation of ERK1/2 for any of the respective α-GHR mAbs (Fig. 3.11. A, B, and C).

3.6. IGF-1 Luciferase Reporter Assay

Using an IGF-1 luciferase promoter reporter assay, the ability of the α-GHR mAb candidates to downregulate the reporter activity and therefore suppress IGF-1 expression was measured (Fig. 3.12.). Changes in IGF-1 expression represent a key element in assessing the ability of the respective mAbs to be characterized as either agonistic or antagonistic candidates for successful characterization. The compiled data is shown below (Fig. 3.12.).

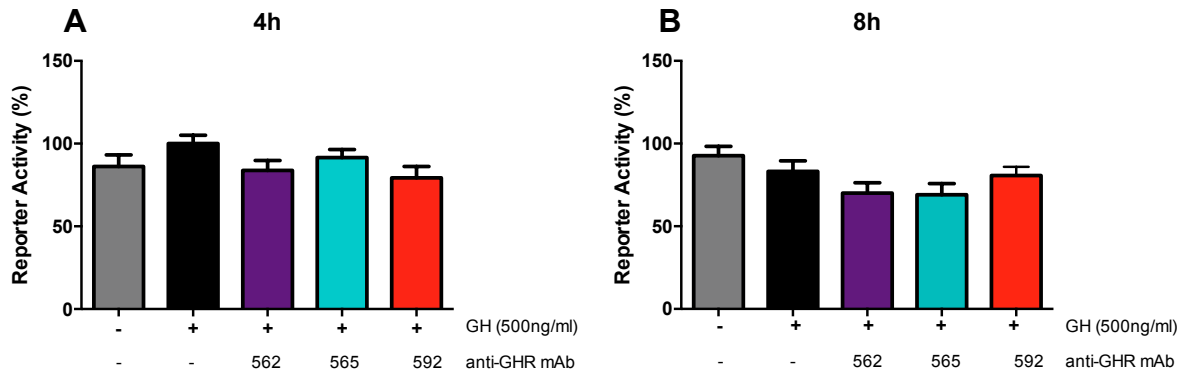

Fig. 3.12. IGF-1 promoter reporter activity in L cells.

Serum starved L cells were pre-treated with the corresponding α-GHR mAbs and then treated with GH for the indicated time points (4h and 8h) to induce IGF-1 promoter reporter activity. The dataset was analyzed by one-way ANOVA and represents the average of two independent experiments with multiple replicates ($P < 0.05$).

The assembled dataset shows that there is no significant downregulation of IGF-1 promoter reporter activation for each of the indicated time points (Fig. 3.12.). However, induction of reporter activity could be shown using GH for the 4h time point (Fig. 3.12.).

3.7. *In vivo* Testing of the mAbs

Functionality and effectiveness of the mAbs is especially crucial considering *in vivo* applications. The ability to reduce IGF-1 serum concentration levels to a level considered to be protective, would establish the basis for the respective drugs to be tested in clinical trials. This would mark a milestone. In the present project, each mAb has been tested for its ability to achieve the desired effects by intravenous injections in C57BL/6 mice over three consecutive days. However, in case of α-GHR592, the experiment had to be discontinued on day two of the experiment due to visible cytotoxic effects at the injection site. The mice were sacrificed and serum was collected to be tested for induced liver damage cytotoxicity (ALT) and a general immune response marker (SAP) to assess cytotoxicity (Fig. 3.13.). Serum ALT (alanine transaminase) levels were significantly elevated in the mAb treated group, and serum SAP (serum amyloid protein) levels were also increased, however not significantly (Fig. 3.13.).

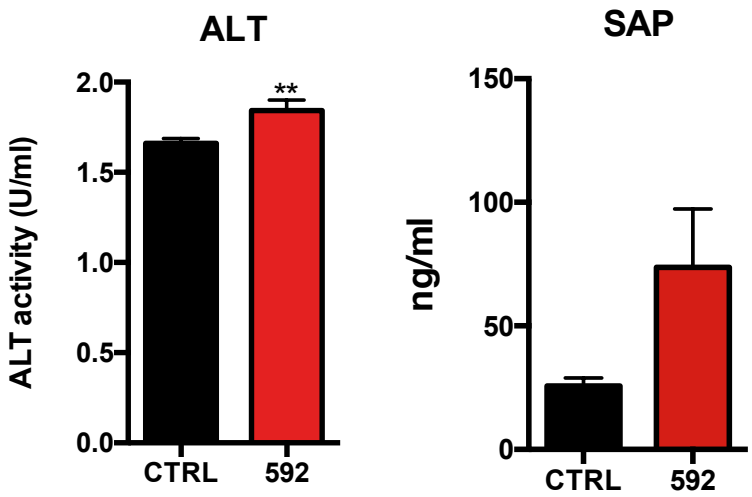

Fig. 3.13. Serum ALT and SAP levels in C57BL/6 mice treated with α-GHR592.
Serum ALT and and SAP levels were measured by commercial ELISA. The obtained data were statistically analyzed by an unpaired t-test (n = 3 mice/group; ALT: *p = 0.076*; SAP: *p = 0.0710*).

Since the monoclonal antibody α-GHR592 has now been eliminated from the study due to its cytotoxic features in the in vivo experiments, candidates α-GHR562 and α-GHR565 have further been evaluated for their ability to reduce serum IGF-1 concentrations. Serum of the treated mice was collected 24 hours after the last injection following a regimen of three consecutive days of intravenous injections. The serum was subjected to an ELISA assay to assess IGF-1 levels (Fig. 3.14.). Furthermore, biochemical analysis was performed by subjecting whole blood to a complete cell count (CBC) to determine any abnormalities to cell populations potentially caused by the treatment with the respective mAbs (Fig. 11.3.). However, no significant data could be obtained in any of the instance and measurement that were taken, questioning the applicability of the tested α-GHR mAbs.

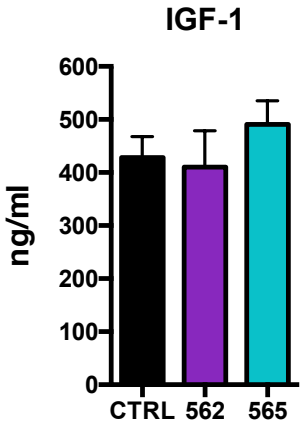

Fig. 3.14. Serum IGF-1 levels in C57BL/6 mice treated with α-GHR562 and/or α-GHR565.
IGF-1 serum concentrations were measured using a commercially available ELISA kit. The obtained data were statistically analyzed by one-way ANOVA (n = 4-6 mice/group).

4. Discussion

4.1. Evaluation of Bioinformatical Data

Evaluating sequence-based information and structural evidence provides a fundamental understanding of the conservation of function and shared evolutionary history between species of a protein of interest. In the present work, detailed *in silico* analysis of the GHR was carried out. This was achieved by applying bioinformatical algorithms to determine homology of the target between evolutionary divergent species and to identify potential targets for the development of α-GHR mAbs. The selected α-GHR mAbs would ideally have the ability to modulate GHR function in order to downregulate GHR downstream signaling.

Implementation of a multiple sequence alignment algorithm and calculating evolutionary distance between a variety of species showed that the GHR protein is persistently evolutionary conserved throughout the tested spectrum of species (see Fig. 3.1. and Fig. 3.2.). This is suggestive of a fundamental role of the GHR protein during evolution and implies that its function is essential for survival and/or is of certain selective advantage for the organism in a given environment. This is especially important since the structure of any given protein is better conserved than its sequence (Koonin and Galperin, 2003). Studies performed by Illergård *et al.* delivered experimental evidence that the three-dimensional structure is three to ten times more conserved than its sequence (Illergård *et al.,* 2009). This is due to the close structure-function relationship of a protein. Hence, the maintenance of the structure is of evolutionary advantage.

A proprietary algorithm was applied to identify antigenic determinants that would most likely yield α-GHR mAbs. Subsequently, five candidates were selected for further investigation and characterization (see Fig. 3.3.). Furthermore, the target sequences of these five candidates named α-GHR562, α-GHR565, α-GHR570, α-GHR576, and α-GHR592 were highlighted within the GHR crystal structure to gather further relevant information regarding functional implications to potentially modify GHR function (see Fig. 3.4). It is of important notice to mention that the developed α-GHR mAbs are mouse anti-mouse mAbs. This system has been chosen due to its broad and relatively easy applicability in murine *in vitro* and *in vivo*

systems. However, the present drug development project served ideally as a base for the potential establishment of clinical α-GHR mAbs for humans. Successful candidates were to be selected for humanization procedures. Nonetheless, the experimental data for the present project was only carried out in murine systems. Yet, pairwise sequence alignments between the murine and human target sequences of the candidates were performed (see table 3.3.). This represents an important step to be able to conclude for any relevance and/or significance of the mouse anti-mouse mAbs within the human system. Such sequence-based data provides insights on immunogenicity. Additionally, current literature proposes an alignment score of at least 85% between the epitope of any given mAb of a particular species with the homolog epitope of another species to qualify for cross-reactive experiments (Jones *et al.,* 2016). The sequence identity between the murine and the human version of the antigenic determinants for the α-GHR mAb candidates is 83% (α-GHR562), 70% (α-GHR565), 58% (α-GHR570), 86% (α-GHR576), and 100% (α-GHR592) (see table 3.3.). According to the threshold of ≥85%, this would theoretically disqualify α-GHR562, α-GHR565, and α-GHR570 as candidates to be tested in any cross-reactive experiments. This is especially significant for tests performed in any human systems. Although these candidates are hypothetically not applicable in human systems, they can still be of use as biochemical tools for the manipulation of GH signaling in murine systems.

4.2. Production of the α-GHR mAbs

Generation of the α-GHR mAbs represented an initial step prior to the experimental procedures carried out to characterize the respective mAbs. The production was carried out in an *in vivo* system due to the inadaptability of the hybridoma clones to the *in vitro* system. Production *in vitro* was simply not effective as a result of self-limiting growth characteristics of the hybridoma clones. Furthermore, only insignificant low yield nanogram-ranges of the α-GHR mAbs could be obtained from the cell culture supernatant. As a result, *in vivo* ascites production was chosen to obtain high titer levels.

For large-scale production purpose, Balb/c mice were primed and inoculated with the respective clones (see 2.4.1.). Three out of five clones succeeded the production procedure, while clones C570 and C576 clearly failed to produce ascites

(see Fig. 3.5. A). Changes in body weight and fluid content of the inoculated mice is providing experimental evidence. While there is a significant body weight and fluid content increase for mice inoculated with clones C562, C565, and C592, there are no changes observed for the mice inoculated with C570 and C576 (see Fig. 3.5. B and C). There are several parameters affecting ascites formation. A reason as to why these two clones failed to produce could be that they are hypothetically the most potent antagonistic candidates. Theoretically, GHR inhibition could have led to an impairment of hybridoma proliferation, and therefore failure of ascites production. A way to circumvent this potential issue could be the production in hollow fiber bioreactors. This constitutes an engineered cell culture technology that supports production. The hollow fibers represent semi-permeable membranes with an adjustable molecular weight cut-off. These fibers are bundled and arranged in a parallel way to form hollow fiber cartridges. Moreover, the cartridges are spatially divided into an extracapillary (EC) and in an intracapillary (IC) spot. Cells are seeded in the EC spot. Nutrients and oxygen are delivered through the IC spot with the cell culture medium, which is being pumped through the semi-permeable fibers. End products of metabolism and mAbs secreted in the cell culture medium can then be pumped away through the IC spot for accumulation. This eliminates toxicity of waste products and potential changes in the behavior of the hybridoma clones arising from effects of the α-GHR mAbs. Other ways to optimize ascites production could be the usage of male mice instead of female. Research has shown that production in males is significantly improved in males compared to females (Brodeur *et al.,* 1984). However, ascites production via the inoculation has been chosen for the project due to budget limitations, and candidates C570 and C576 were eliminated at this stage of the project.

A pre-experimental isotyping determination was carried out for the remaining three candidates (see Fig. 3.6.). This step was necessary for the subsequent titer determination due to the availability of IgG-specific titer assay kits. Titer determination gave a yield of 6-8 µg/µL for each of the three candidates (see Fig. 3.7. B). However, after purification a yield of approximately 2 µg/µL was obtained (see Fig. 3.7. C). The loss of 4-6 µg/µL of purified mAb could be due to the efficiency of the purification system that was chosen. A flow-through system was used instead of a binding-and-release support. According to the protocol, the purified antibody was collected in the flow-through fraction, while non-antibody proteins were bound by a proprietary ligand in the column. The loss is most likely due to unspecific binding of

the mAbs in the columns. However, the used system eliminated the need of harsh elution conditions, which are in place for Protein A and Protein G affinity methods. The harsh conditions in place for those methods could potentially have disrupted functionality of the purified mAbs, such as affinity interactions.

4.3. Binding of the α-GHR mAbs to the GHR

Testing binding of the α-GHR mAbs to their target was executed through two different approaches. Using the first approach, immunofluorescent staining followed by confocal microscopy was carried out (see 3.4.1.). For this purpose, the mAbs were incubated with increasing ratios of their antigenic determinants/peptides and then used to treat GHR-overexpressing L cells (see 2.2.5.). Images were taken using a confocal microscope and relative pixel intensity was analyzed (see Fig. 3.8. A and B). It could be demonstrated that α-GHR mAbs 562 and 565 display a significant decrease of pixel intensity at 1:1 ratio (antibody to peptide), indicating that cell surface binding of the mAbs is significantly reduced at this ratio (see Fig. 3.8. B). Interpretation of the data implies that the significant decline in relative pixel intensity was achieved as a result of saturation. Free mAbs were bound by their respective peptides they were designed against during the incubation time of the mixture before they were given onto the cells. Since there were theoretically not as many free mAbs available to bind to the GHR expressed on the cells, a decreased intensity could be observed at the highest ratio. These results imply specificity for the candidates α-GHR562 and α-GHR565. However, in case of α-GHR565 this interpretation is misleading due to the fact that not sufficient data points could be obtained for the highest ratio of 1:1. Measuring pixel intensity for this data point was always associated with complications since no green fluorescent signal could be detected. For, α-GHR592 a general trend of decreasing signal with increasing target peptide input could be observed implying a decline of specific binding. However, no significant changes were observed using this approach.

Due to the complications associated with this method, a more sophisticated method was chosen. The Biacore platform delivers data regarding kinetics in addition to binding. Data sets were assembled by making use of the surface plasmon resonance phenomenon (see 2.2.6.). KD values were recorded for α-GHR562 and α-GHR592, whereas for α-GHR565 no valuable data was reported (see Fig. 3.9. A-

C). This data reveals that α-GHR562 and α-GHR592 demonstrate binding affinity. However, K_{on} and K_{off} rates could not be determined. This could be the result of the binding affinity. High affinity interaction between the ligand and the analyte can result in very slow rates for K_{off} rendering equilibrium analysis incompatible. Sensorgrams for α-GHR565 clearly show no specificity, indicating that this mAb does not bind specifically to the GHR.

4.4. Evaluation of Intracellular Effects

Intracellular effects of the mAbs were evaluated by a STAT5 and ERK1/2 phosphorylation assay (see 2.3.1.). L cells were pre-treated with the respective α-GHR mAbs at increasing ratios, and then treated with GH to induce phosphorylation. A downregulation of phosphorylation would be indicative of antagonistic behavior, while an upregulation of phosphorylation would imply agonistic behavior of the tested α-GHR mAbs. Gathered datasets indicate a decrease in the phosphorylation of STAT5 using α-GHR562 at all three ratios, a decrease using a GH:α-GHR565 ratio of 1:10 and 1:20, and a decrease of STAT5 phosphorylation using a GH:α-GHR592 ratio of 1:20 (see Fig. 3.11. A, B, and C). However, no significant changes could be observed in the phosphorylation of ERK1/2 using any of the antibodies (see Fig. 3.11. A, B, and C). Furthermore, an IGF-1 Renilla luciferase reporter assay was performed to test the ability of the mAbs to induce changes in IGF-1 reporter activity (see 2.2.7.). It could be shown that no significant changes could be observed for the tested time points (see Fig. 3.12. A and B).

This data set reveals that α-GHR562 is the most promising candidate in the STAT5 phosphorylation assays. It significantly downregulates STAT5 phosphorylation. Monoclonal antibody α-GHR592 is only effective using the highest ratio and is therefore a less effective mAb at this stage of the project. Candidate α-GHR565 is effective in decreasing STAT5 phosphorylation, and is simultaneously inducing an insignificant increase the phosphorylation of ERK1/2. However, binding data revealed no specificity for GHR. This suggests that this mAb acts through a different signaling pathway, and not the GH signaling pathway.

4.5. *In vivo* Testing is Demonstrative of α-GHR592 Cytotoxicity

C57BL/6 mice were injected with the α-GHR mAbs for three consecutive days (see 2.4.2.). For α-GHR592, the experiment had to be terminated due to visible cytotoxic effects. Serum was collected and assessed for ALT and SAP markers. ALT levels were significantly increased (see Fig. 3.13.). This is indicative of induced liver damage. This is important considering that the GHR is mainly expressed by hepatic cells (see Fig. 1.1), suggesting GHR specificity. Serum SAP levels were also elevated, although not significantly (see Fig. 3.13.). Cytotoxicity could not be observed in the *in vitro* system, but *in vivo*. This is due to absence of the complement system in the mammalian cell culture system. The presence of the complement system *in vivo* might have triggered α-GHR592 cytotoxicity. At this stage, further processing of α-GHR592 should be taken into consideration to eliminate cytotoxicity. This could be achieved by generating F(ab) or F(ab')2 fragments of α-GHR592. On the other hand, monoclonal antibodies α-GHR562 and α-GHR565 did not exert any detectable liver toxicity, and the *in vivo* experiment was completed as outlined and designed previously. After three consecutive days of injection, serum was collected and serum IGF-1 levels were tested to deliver efficacy of the mAbs regarding their potency to decrease serum IGF-1. Data has shown that α-GHR562 did not induce any changes, whereas α-GHR565 induces an insignificant increase (see Fig. 3.14.). This is again supportive of the previous assumption that α-GHR565 is not specifically targeting GHR, and α-GHR562 or the protocol in place can be further engineered to achieve better results.

5. Perspectives

The project presented in this dissertation is focused on the generation and establishment of α-GHR mAbs regarding their ability to induce changes in GH signaling in *in vitro* and *in vivo* systems. The purpose of manipulating GH signaling is to ideally lower the expression of its effector, IGF-1. This represents the most important part of the project, since IGF-1 has been demonstrated to be a major risk factor for the development of age-related diseases. Hence, lowering IGF-1 levels is of certain interest for the prevention of age-related diseases and the augmentation of therapies implicated for age-related diseases.

Five candidates were initially chosen to be tested in various *in vitro* and *in vivo* systems. However, only three out of five candidates succeeded in the production part of the project: α-GHR562, α-GHR565, and α-GHR592. *In vitro* testing of the remaining three candidates was carried out in binding experiments, a STAT5 and ERK1/2 phosphorylation experiment, and an IGF-1 luciferase promoter reporter activity test. Experimental data showed that α-GHR562 and α-GHR592 bind to the GHR with a certain binding affinity, and that all three mAbs significantly downregulate STAT5 phosphorylation. However, no significant changes could be observed in the IGF-1 luciferase promoter reporter activity experiments. In contrast, the *in vivo* experiments showed α-GHR592-induced liver toxicity. Furthermore, no significant changes in circulating IGF-1 levels could be obtained using α-GHR562 or α-GHR565. Combining all the data sets it can be concluded that α-GHR592 might be the most promising candidate so far. Furthermore, the cytotoxic behavior observed in the *in vivo* setting can serve as an important indicator of mAb binding and subsequent liver cytotoxicity. To be able to draw final conclusions regarding the classification of α-GHR592 as a GHR antagonist, it can be further processed into F(ab) or F(ab')2 fragments to eliminate antibody-dependent cell-mediated cytotoxicity (ADCC). This represents a mechanism by which an effector cell of the immune system lyses a cell by binding to antibodies, which are in turn bound to their antigen on the cell surface of target cells to mark them for lysis. Testing of the α-GHR592 fragments could eliminate cytotoxicity and allow to test potential antagonistic behavior. If it can be proven that the α-GHR592 fragments are significantly lowering circulating IGF-1 levels, more sophisticated experimental settings can be taken into consideration. For example, studies where IGF-1 is associated with the proliferation and anti-apoptotic

events in the formation of breast cancer can serve as a basis for the design of *in vivo* experiments (Christopoulos *et al.,* 2015). Cancer cells can be injected into C57BL/6 mice and the ability of the α-GHR592 fragments to reduce proliferation of the tumor and/or induce lysis of the cells can be investigated. In case of α-GHR562, specificity and significant downregulation of STAT5 as immediate indicator could be shown, but no significant *in vivo* observation could be made questioning the applicability of this mAb for further testing. Monoclonal antibody α-GHR565 can be ruled out at this stage of the project, since especially no GHR specificity could be demonstrated. However, the development of novel antibodies targeting the GHR or the development of molecular compounds aimed at targeting GH signaling should also be included for further investigation.

6. Abstract

The development of monoclonal antibodies (mAbs) targeting the GHR aimed at lowering the expression of IGF-1 was the main focus of this dissertation. The significance of the project is based on the fact that IGF-1 is associated with a variety of age-related diseases. Hence, the development and characterization of mAbs targeting the GH-IGF-1 axis with the potential to downregulate IGF-1 expression could result in the prevention of such age-related diseases and the augmentation of therapeutic outcomes of age-related diseases.

The initial part of the project constituted the production of five selected hybridoma clones, which produce five individual α-GHR mAbs targeting different structures of the GHR. Three out of five clones were successfully produced and were the subject of further testing: α-GHR562, α-GHR565, and α-GHR592. *In vitro* experiments aimed at assessing binding specificity and affinity, the ability to downregulate STAT5 and ERK1/2 phosphorylation, as well as IGF-1 luciferase promoter reporter activity, showed variable characteristics of the tested mAbs. Binding affinity for candidates α-GHR562 and α-GHR592 could be determined, but no binding of α-GHR565 could be detected. Furthermore, all three mAbs significantly downregulated STAT5 phosphorylation, a marker tested for any immediate effects of mAbs on GH signaling. However, none of the tested mAbs induced any significant changes in the phosphorylation of ERK1/2 and the IGF-1 luciferase promoter reporter activity tests. Testing of the mAbs *in vivo* revealed no significant effect of α-GHR562 or α-GHR565 on circulating IGF-1 levels. On the other hand, significant increases in serum ALT (alanine transaminase) levels was observed after α-GHR592 treatment, indicative of induced liver toxicity. Additionally, an increase in the general immune response marker SAP (serum amyloid protein) was detected, however this increase was not significant. Interpretation of the compiled data set might indicate that, out of the tested mAbs, α-GHR592 might be the most promising candidate thus far in establishing a drug to manipulate GH signaling.

6.1. Zusammenfassung

Der Schwerpunkt der vorliegenden Dissertation war die Entwicklung von monoklonalen Antikörpern (moAks), die spezifisch den Somatotropin-Rezeptor (GHR) binden und somit theoretisch die Expression des insulinähnlichen Wachstumsfaktors IGF-1 herunterregulieren. Dies ist von besonderem Interesse, da erhöhte Konzentrationen von IGF-1 im Serum mit einer Vielzahl von altersbedingten Erkrankungen assoziiert ist. Aufgrund dessen könnte die Entwicklung von moAks die spezifisch den Somatotropin-Rezeptor binden und somit potentiell die Expression von IGF-1 herunterregulieren, zu einer Effektivitätssteigerung von Behandlungen und zur Prävention von altersbedingten Erkrankungen beitragen.

Der erste Teil des Projektes bestand in der Aszites Produktion von fünf individuellen α-GHR moAks, die unterschiedliche Strukturen des GHR binden. Die Produktion gelang in drei von fünf Fällen, und entsprechende moAks waren der Gegenstand weiterer Anwendungen: α-GHR562, α-GHR565, und α-GHR592. Eine Vielzahl von *in vitro* Experimenten wurden zwecks Charakterisierung der moAks ausgeführt. Diese Experimente beinhalteten unter anderem eine Charakterisierung bezüglich der Bindungsaffinität, bezüglich der Fähigkeit zur Herunterregulierung der Phosphorylierung von STAT5 und ERK1/2, sowie Teste bezüglich der IGF-1 Luciferase-Promoter-Reporteraktivität. Die Bindungsaffinität für die Kandidaten α-GHR562 und α-GHR592 konnten ermittelt werden, jedoch konnten keine bedeutenden Parameter für α-GHR565 erhalten werden. Darüber hinaus wurde die Phosphorylierung von STAT5 von allen drei moAks signifikant herunterreguliert. STAT5 stellt dabei einen Marker dar, der im Rahmen von unmittelbaren Effekten von moAks auf die Signalgebung durch den GHR getestet wird. Jedoch konnten keine signifikanten Änderungen in der Phosphorylierung von ERK1/2 und in den IGF-1 Luciferase-Promotor-Reporteraktivitätstests nachgewiesen werden. Das Testen der moAks α-GHR562 und α-GHR565 *in vivo* zeigte keine signifikanten Änderungen von IGF-1 Konzentrationen im Serum. Andererseits konnten zytotoxische Wirkungen von α-GHR592 nachgewiesen werden. Ein signifikanter Anstieg von ALT (Alanin-Aminotransferase), welcher einen induzierten Leberschaden andeutet, und ein Anstieg von SAP (Serum-Amyloid-Protein) Werten im Serum deutet Zytotoxizität an. Die Interpretation der Datensätze könnte somit darauf hinweisen, dass α-GHR592 den vielversprechendsten Kandidaten für die Etablierung eines moAks zur Beeinflussung der GH-Signalübertragung darstellt.

7. Abbreviations

AILME	Ailuroipoda melanoleuca (Giant panda)
AKT	protein kinase B
ALT	alanine transaminase
B1	batch 1
B2	batch 2
BAD	Bcl-2-associated death promoter
Bcl-2	B-cell lymphoma 2
BLAST	Basic Local Alignment Search Tool
BOSIN	Bos indicus (Zebu)
BOVIN	Bos taurus (Bovine)
bp	base pairs
C	constant region
C562	Hybridoma clone 562
C565	Hybridoma clone 565
C570	Hybridoma clone 570
C576	Hybridoma clone 576
C592	Hybridoma clone 592
CAVPO	Cavia porcellus (Guinea pig)
CBC	complete blood count
CHICK	Gallus gallus (Chicken)
CNLF	Canis lupus familiaris (Dog)
COLLI	Columba livia (Rock dove)
CR	calorie restriction
DMBA	dimethylbenz[a]anthracene
DMEM	Dulbecco's Modified Eagle's Medium
DMSO	dimethyl sulfoxide
DNA	deoxyribonucleic acid
EC	extracapillary
ECD	extracellular domain
ELISA	enzyme-linked immunnosorbent assay
ERK	extracellular signal-regulated kinase
F(ab)	antigen-binding fragment

FBS	fetal bovine serum
Fc	fragment crystallizable region
FFA	free fatty acids
Fig.	figure
FMD	fasting-mimicking diet
FNIII	fibronectin III like modules
FOXO	forkhead box proteins
GAS	interferon-α-sequence
GH	growth hormone
GHBP	growth hormone binding protein
GHI	GH insensitivity
GHIH	growth hormone inhibiting hormone
GHR	growth hormone receptor
GHRfl	full-length growth hormone receptor
GHRH	growth hormone releasing hormone
GLE	GAS-like response element
GLUT-4	Glucose transporter type 4
GRB2	growth factor receptor bound protein 2
GTP	guanosine tripohosphate
Gy	gray
H	heavy chain
HAT	hypoxanthine-aminopterin-thymidine
HDL	high-density lipoprotein
HGPRT	hypoxanthine-guanine phosphoribosyltransferase
hGH	human growth hormone
hGHR	human growth hormone receptor
HMM	hidden Markov model
HSL	hormone-sensitive-lipase
IACUC	Institutional Animal Care and Use Committee
IC	intracapillary
ICD	intracellular domain
ID	identifier
Ig	immunoglobulin
IGF-1	insulin-like growth factor I
IGF-1R	IGF-1 receptor

IGF-2R	IGF-2 receptor
IGFBP	insulin-like growth factor binding protein
INS	insulin
IR	insulin receptor
IRS	insulin receptor substrate
i.p.	intraperitoneal
i.v.	intravenous
JAK	Janus kinases
JM	juxtamembrane
KD	dissociation constant
kDA	kilo Dalton
L	light chain
LDL	low-density lipoprotein
M	marker
mA	milliampere
mAbs	monoclonal antibodies
MACMU	Macaca mulatta (Rhesus macaque)
MAPK	mitogen-activated protein kinase
MEGA7	molecular evolutionary genetics analysis 7
MEK	MAP-ERK kinase
moAk	monoklonale Antikörper
mTOR	mammalian target of rapamycin
mTORC1	mTOR complex 1
mTORC2	mTOR complex 2
NCBI	National Center for Biotechnology Information
NGS	normal goat serum
p27	cyclin-dependent kinase inhibitor 1B
pAbs	polyclonal antibodies
PAPAN	Papio Anubis (Olive baboon)
PDB	protein data bank
PDK	phosphoinositide-dependent kinase 1
PEG	polyethylene glycol
pI	isoelectric point
PI3K	phosphatidylinositol 3-kinase
PIP2	phosphatidylinositol 3,4-bisphosphate

PIP3	phosphatidylinositol 3,4,5-trisphosphate
PKB	protein kinase B
PLC	phospholipase C
PVDF	polyvinylidene fluoride
RAF	rapidly accelerated fibrosarcoma
RAS	small GTPase protein family member
RenSP	Renilla luminescent reporter gene
RPMI	Roswell Park Memorial Institute
RT	room temperature
RU	response unit
SAIBB	Saimiri boliviensis boliviensis (Bolivian squirrel monkey)
SAP	serum amyloid protein
SDS	sodium dodecyl sulfate
SDS-PAGE	SDS-polyacrylamide Gel Electrophoresis
SHC	Src homology 2 domain-containing
SH2	Src homology 2
SIE	sis-inducible element
spi2.1	serum protease inhibitor 2.1
SPR	surface plasmon resonance
SRIF	somatotropin release-inhibiting factor
STAT	signal transducer and activator of transcription
TMD	transmembrane domain
UbE	ubiquitination-dependent endocytosis
USC	University of Southern California
V	variable region
WT	wild type

8. Index of Figures

9. Index of Tables

10. Bibliography

Abs R, Verhelst J, Maiter D, Van Acker K, Nobels F, Coolens JL, Mahler C, Beckers A. Cabergoline in the treatment of acromegaly: a study in 64 patients. *J Clin Endocrinol Metab.* 1998 Feb;83(2):374-8. **PMID: 9467544.**

Abdel-Meguid SS, Shieh HS, Smith WW, Dayringer HE, Violand BN, Bentle LA. Three-dimensional structure of a genetically engineered variant of porcine growth hormone. *Proc Natl Acad Sci U S A.* 1987 Sep;84(18):6434-7. **PMID: 2819877.**

Aguiar-Oliveira MH, Oliveira FT, Pereira RM, Oliveira CR, Blackford A, Valenca EH, Santos EG, Gois-Junior MB, Meneguz-Moreno RA, Araujo VP, Oliveira-Neto LA, Almeida RP, Santos MA, Farias NT, Silveira DC, Cabral GW, Calazans FR, Seabra JD, Lopes TF, Rodrigues EO, Porto LA, Oliveira IP, Melo EV, Martari M, Salvatori R. Longevity in untreated congenital growth hormone deficiency due to a homozygous mutation in the GHRH receptor gene. *J Clin Endocrinol Metab.* 2010 Feb;95(2):714-21. doi: 10.1210/jc.2009-1879. Epub 2009 Dec 4. **PMID: 19965916.**

Arai KI, Lee F, Miyajima A, Miyatake S, Arai N, Yokota T. Cytokines: coordinators of immune and inflammatory responses. *Annu Rev Biochem*. 1990;59:783-836. **PMID: 1695833.**

Argente J, Chowen JA, Zeitler P, Clifton DK, Steiner RA. Sexual dimorphism of growth hormone-releasing hormone and somatostatin gene expression in the hypothalamus of the rat during development. *Endocrinology.* 1991 May;128(5):2369-75. **PMID: 1673430.**

Argetsinger LS, Campbell GS, Yang X, Witthuhn BA, Silvennoinen O, Ihle JN, Carter-Su C. Identification of JAK2 as a growth hormone-receptor associated tyrosine kinase. *Cell.* 1993 Jul 30;74(2):237-44. **PMID: 8343952.**

Attallah H, Friedlander AL, Nino-Murcia M, Hoffman AR. Effects of growth hormone and pioglitazone in viscerally obese adults with impaired glucose tolerance: a factorial clinical trial. *PLoS Clin Trials.* 2007 May 4;2(5):e21. **PMID: 17479164.**

Bachrach LK, Marcus R, Ott SM, Rosenbloom AL, Vasconez O, Martinez V, Martinez AL, Rosenfeld RG, Guevara-Aguirre J. Bone mineral, histomorphometry, and body composition in adults with growth hormone receptor deficiency. *J Bone Miner Res.* 1998 Mar;13(3):415-21. **PMID: 9525342.**

Ballesteros M, Leung KC, Ross RJ, Iismaa TP, Ho KK. Distribution and abundance of messenger ribonucleic acid for growth hormone receptor isoforms in human tissues. *J Clin Endocrinol Metab*. 2000 Aug;85(8):2865-71. **PMID: 10946895.**

Barclay JL, Kerr LM, Arthur L, Rowland JE, Nelson CN, Ishikawa M, d'Aniello EM, White M, Noakes PG, Waters MJ. In vivo targeting of the growth hormone receptor (GHR) Box1 sequence demonstrates that the GHR does not signal exclusively through JAK2. *Mol Endocrionol.* 2010 Jan;24(1):204-17. doi: 10.1210/me.2009-0233. Epub 2009 Nov 2. **PMID: 19884384.**

Barnard R, Waters MJ. The serum growth hormone binding protein: pregnant with possibilities. *J Endocrinol*. 1997 Apr;153(1):1-14. **PMID: 9135564.**

Bartke A. (2000) Delayed Aging in Ames Dwarf Mice. Relationships to Endocrine Function and Bdy Size. In: Hekimi S. (eds) The Molecular Genetics of Aging. Results and Problems in Cell Differentiation, vol 29. *Springer*, Berlin, Heidelberg. **ISBN: 978-3-642-53686-1.**

Bazan JF. Structural design and molecular evolution of a cytokine receptor superfamily. *Proc Natl Acad Sci* U S A. 1990 Sep;87(18):6934-8. **PMID: 2169613.**

Beauville M, Harant I, Crampes F, Riviere D, Tauber MT, Tauber JP, Garrigues M. Effect of long-term rhGH administration in GH-deficient adults on fat cell epinephrine response. *Am J Physiol.* 1992 Sep;263(3 Pt 1):E467-72. **PMID: 1415526.**

Berg MA, Guevara-Aguirre J, Rosenbloom AL, Rosenfeld RG, Francke U. Mutation creating a new splice site in the growth hormone receptor genes of 37 Ecuadorian patients with Laron syndrome. *Hum Mutat.* 1992;1(1):24-32. **PMID: 1284474**.

Bernat B, Pal G, Sun M, Kossiakoff AA. Determination of the energetics governing the regulatory step in growth hormone-induced receptor homodimerization. *Proc Natl Acad Sci U S A.* 2003 Feb 4;100(3):952-7. Epub 2003 Jan 27. **PMID: 12552121.**

Bevan JS, Atkin SL, Atkinson AB, Bouloux PM, Hanna F, Harris PE, James RA, McConnell M, Roberts GA, Scanlon MF, Stewart PM, Teasdale E, Turner HE, Wass JA, Wardlaw JM. Primary medical therapy for acromegaly: an open, prospective, multicenter study of the effects of subcutaneous and intramuscular slow-release octreotide on growth hormone, insulin-like growth factor-I, and tumor size. *J Clin Endocrinol Metab.* 2002 Oct;87(10):4554-63. **PMID: 12364434.**

Bodkin NL, Ortmeyer HK, Hansen BC. Long-term dietary restriction in older-aged rhesus monkeys: effects on insulin resistance. *J Gerontol A Biol Sci Med Sci.* 1995 May;50(3):B142-7. **PMID: 7743393.**

Bohlke K, Cramer DW, Trichopoulos D, Mantzoros CS. Insulin-like growth factor-I in relation to premenopausal ductal carcinoma in situ of the breast. *Epidemiology.* 1998 Sep;9(5):570-3. **PMID: 9730040.**

Bonkowski MS, Dominici FP, Arum O, Rocha JS, Al Regaiey KA, Westbrook R, Spong A, Panici J, Masternak MM, Kopchick JJ, Bartke A. Disruption of growth hormone receptor prevents calorie restriction from improving insulin action and longevity. *PLoS One*. 2009;4(2):e4567. doi: 10.1371/journal.pone.0004567. Epub 2009 Feb 23. **PMID: 19234595.**

Brada M, Burchell L, Ashley S, Traish D. The incidence of cerebrovascular accidents in patients with pituitary adenoma. *Int J Radiat Oncol Biol Phys*. 1999 Oct 1;45(3):693-8. **PMID: 10524424.**

Brandhorst S, Choi IY, Wei M, Cheng CW, Sedrakyan S, Navarrete G, Dubeau L, Yap LP, Park R, Vinciguerra M, Di Biase S, Mirzaei H, Mirisola MG, Childress P, Ji L, Groshen S, Penna F, Odetti P, Perin L, Conti PS, Ikeno Y, Kennedy BK, Cohen P, Morgan TE, Dorff TB, Longo VD. A Periodic Diet that Mimics Fasting Promotes Multi-System Regeneration, Enhanced Cognitive Performance, and Healthspan. *Cell Metab*. 2015 Jul 7;22(1):86-99. doi: 10.1016/j.cmet.2015.05.012. Epub 2015 Jun 18. **PMID: 26094889.**

Breese CR, Ingram RL, Sonntag WE. Influence of age and long-term dietary restriction on plasma insulin-like growth factor-1 (IGF-1), IGF-1 gene expression, and IGF-1 binding proteins. *J Gerontol.* 1991 Sep;46(5):B180-7. **PMID: 1716275.**

Brodeur BR, Tsang P, Larose Y. Parameters affecting ascites tumour formation in mice and monoclonal antibody production. J Immunol Methods. 1984 Jul 6;71(2):265-72. **PMID: 6736661.**

Brooks AJ, Dai W, O'Mara ML, Abankwa D, Chhabra Y, Pelekanos RA, Gardon O, Tunny KA, Blucher KM, Morton CJ, Parker MW, Sierecki E, Gambin Y, Gomez GA, Alexandrov K, Wilson IA, Doxastakis M, Mark AE, Waters MJ. Mechanism of activation of protein kinase JAK2 by the growth hormone receptor. *Science.* 2014 May 16;344(6185):1249783. doi: 10.1126/science.1249783. **PMID: 24833397.**

Brown RJ, Adams JJ, Pelekanos RA, Wan Y, McKinstry WJ, Palethorpe K, Seeber RM, Monks TA, Eidne KA, Parker MW, Waters MJ. Model for growth hormone receptor activation based on subunit rotation within a receptor dimer. *Nat Struct Mol Biol.* 2005 Sep;12(9):814-21. Epub 2005 Aug 21. **PMID: 16116438.**

Carboni JM, Wittman M, Yang Z, Lee F, Greer A, Hurlburt W, Hillerman S, Cao C, Cantor GH, Dell-John J, Chen C, Discenza L, Menard K, Li A, Trainor G, Vyas D, Kramer R, Attar RM, Gottardis MM. BMS-754807, a small molecule inhibitor of insulin-like growth-factor-1R/IR. *Mol Cancer Ther.* 2009 Dec;8(12):3341-9. doi: 10.1158/1535-7163.MCT-09-0499. **PMID: 19996272.**

Carlsson LM, Clark RG, Robinson IC. Sex difference in growth hormone feedback in the rat. *J Endocrinol*. 1990 Jul;126(1):27-35. **PMID: 2116494.**

Caron P, Beckers A, Cullen DR, Goth MI, Gutt B, Laurberg P, Pico AM, Valimaki M, Zgliczynski W. Efficacy of the new long-acting formulation of lanreotide (lanreotide Autogel) in the management of acromegaly. *J Clin Endocrinol Metab.* 2002 Jan;87(1):99-104. **PMID: 11788630.**

Carter-Su C, Rui L, Herrington J. Role of the tyrosine kinase JAK2 in signal transduction by growth hormone. *Pediatr Nephrol.* 2000 Jul;14(7):550-7. **PMID: 10912517.**

Carter-Su C, Smit LS. Signaling via JAK tyrosine kinases: growth hormone receptor as a model system. *Recent Prog Horm Res*. 1998;53:61-82; discussion 82-3. **PMID: 9769703.**

Chan JM, Stampfer MJ, Giovannucci E, Gann PH, Ma J, Wilkinson P, Hennekens CH, Pollak M. Plasma insulin-like growth factor-I and prostate cancer risk: a prospective study. *Science.* 1998 Jan 23;279(5350):563-6. **PMID: 9438850.**

Chanson P, Boerlin V, Ajzenberg C, Bachelot Y, Benito P, Bringer J, Caron P, Charbonnel B, Cortet C, Delemer B, Escobar-Jiménez F, Foubert L, Gaztambide S, Jockenhoevel F, Kuhn JM, Leclere J, Lorcy Y, Perlemuter L, Prestele H, Roger P, Rohmer V, Santen R, Sassolas G, Scherbaum WA, Schopohl J, Torres E, Varela C, Villamil F, Webb SM. Comparison of octreotide acetate LAR and lanreotide SR in patients with acromegaly. *Clin Endocrinol (Oxf).* 2000 Nov;53(5):577-86. **PMID: 11106918.**

Chanson P, Salenave S. Acromegaly. *Orphanet J Rare Dis*. 2008 Jun 25;3:17. doi: 10.1186/1750-1172-3-17. **PMID: 18578866.**

Chanson P, Timsit J, Harris AG. Clinical pharmacokinetics of octreotide. Therapeutic applications in patients with pituitary tumours. *Clin Pharmacokinet.* 1993 Nov;25(5):375-91. **PMID: 8287633.**

Chantalat, L., Jones N., Korber, F., Navaza, J., Pavlovsky, A.G. The Crystal-Structure of the wild-type Growth-Hormone at 2.5 Angstrom Resolution. (1995) *Protein Pept.Lett.* 2: 333-340. **UniProtKB AC: P01241.**

Chen C, Brinkworth R, Waters MJ. The role of receptor dimerization domain residues in growth hormone signaling. *J Biol Chem.* 1997 Feb 21;272(8):5133-40. **PMID: 9030580.**

Chen L, Veldhuis JD, Johnson ML, and Straume M. System-level analysis of physiological regulatory interactions controlling complex secretory dynamics of the growth hormone axis: a dynamical network model. In: *Methods in Neurosciences. New York: Academic*, 1995, p. 270–310.

Chen NY, Chen WY, Bellush L, Yang CW, Striker LJ, Striker GE, Kopchick JJ. Effects of streptozotocin treatment in growth hormone (GH) and GH antagonist transgenic mice. *Endocrinology.* 1995 Feb;136(2):660-7. **PMID: 7835300.**

Cheng CW, Adams GB, Perin L, Wei M, Zhou X, Lam BS, Da Sacco S, Mirisola M, Quinn DI, Dorff TB, Kopchick JJ, Longo VD. Prolonged fasting reduces IGF-1/PKA to promote hematopoietic-stem-cell based regeneration and reverse immunosuppression. *Cell Stem Cell.* 2014 Jun 5;14(6):810-23. doi: 10.1016/j.stem.2014.04.014. **PMID: 24905167.**

Choi IY, Piccio L, Childress P, Bollman B, Ghosh A, Brandhorst S, Suarez J, Michalsen A, Cross AH, Morgan TE, Wei M, Paul F, Bock M, Longo VD. A Diet Mimicking Fasting Promotes Regeneration and Reduces Autoimmunity and Multiple Sclerosis Symptoms. *Cell Rep*. 2016 Jun 7;15(10):2136-2146. doi: 10.1016/j.celrep.2016.05.009. Epub 2016 May 26. **PMID: 27239035.**

Chowen-Breed JA, Steiner RA, Clifton DK. Sexual dimorphism and testosterone-dependent regulation of somatostatin gene expression in the periventricular nucleus of the rat brain. *Endocrinology.* 1989 Jul;125(1):357-62. **PMID: 2567663.**

Christopoulos PF, Msaouel P, Koutsilieris M. The role of the insulin-like growth factor-1 system in breast cancer. Mol Cancer. 2015 Feb 15;14:43. doi: 10.1186/s12943-015-0291-7. **PMID: 25743390.**

Clackson T, Ultsch MH, Wells JA, de Vos AM. Structural and functional analysis of the 1:1 growth hormone:receptor complex revelas the molecular basis for receptor affinity. *J Mol Biol.* 1998 Apr 17;277(5):1111-28. **PMID: 9571026.**

Clayton RN. Cardiovascular function in acromegaly. *Endocr Rev*. 2003 Jun;24(3):272-7. **PMID: 12788799.**

Clark RG, Carlsson LM, Robinson IC. Growth hormone secretory profiles in conscious female rats. *J Endocrinol.* 1987 Sep;114(3):399-407. **PMID: 3668430.**

Clark RG, Carlsson LM, Robinson IC. Growth hormone (GH) secretion in the conscious rat: negative feedback of GH on its own release. *J Endocrinol.* 1988 Nov;119(2):201-9. **PMID: 2904475.**

Clark R, Olson K, Fuh G, Marian M, Mortensen D, Teshima G, Chang S, Chu H, Mukku V, Canova-Davis E, Somers T, Cronin M, Winkler M, Wells JA. Long-acting growth hormones produced by conjugation with polyethylene glycol. *J Biol Chem.* 1996 Sep 6;271(36):21969-77. **PMID: 8703002.**

Clark RG, Robinson IC. Growth hormone responses to multiple injections of a fragment of human growth hormone-releasing factor in conscious male and female rats. *J Endocrinol.* 1985 Sep;106(3):281-9. **PMID: 2864380.**

Cocchi D, Bianchi S, Moretti R, Raimondi L, Algeri S. Effect of lifelong hypocaloric diet on growth hormone secretion in adult and old male rats. *Neuroendocrinol Lett.* 1991;13:1–5.

Colao A, Ferone D, Marzullo P, Cappabianca P, Cirillo S, Boerlin V, Lancranjan I, Lombardi G. Long-term effects of depot long-acting somatostatin analog octreotide on hormone levels and tumor mass in acromegaly. *J Clin Endocrinol Metab*. 2001 Jun;86(6):2779-86. **PMID: 11397887.**

Copeland KC, Nair KS. Acute growth hormone effects on amino acid and lipid metabolism. *J Clin Endocrinol Metab.* 1994 May;78(5):1040-7. **PMID: 8175957.**

Coschigano KT, Clemmons D, Bellush LL, Kopchick JJ. Assessment of growth parameters and life span of GHR/BP gene-disrupted mice. *Endocrinology.* 2000 Jul;141(7):2608-13. **PMID: 10875265.**

Cosman D, Lyman SD, Idzerda RL, Beckmann MP, Park LS, Goodwin RG, March CJ. A new cytokine receptor superfamily. *Trends Biochem Sci*. 1990 Jul;15(7):265-70. **PMID: 2166365.**

Cunningham BC, Ultsch M, De Vos AM, Mulkerrin MG, Clauser KR, Wells JA. Dimerization of the extracellular domain of the human growth hormone receptor by a single hormone molecule. *Science.* 1991 Nov 8;254(5033):821-5. **PMID: 1948064.**

Dagenais GR, Tancredi RG, Zierler KL. Free fatty acid oxidation by forearn nuscle at rest, and evidence for an intramuscular lipid pool in the human forearm. *J Clin Invest.* 1976 Aug;58(2):421-31. **PMID: 956375.**

David A, Hwa V, Metherell LA, Netchine I, Camacho-Hübner C, Clark AJ, Rosenfeld RG, Savage MO. Evidence for a continuum of genetic, phenotypic, and biochemical abnormalities in children with growth hormone insensitivity. *Endocr Rev.* 2011 Aug;32(4):472-97. doi: 10.1210/er.2010-0023. Epub 2011 Apr 27. **PMID: 21525302.**

Dastot F, Sobrier ML, Duquesnoy P, Duriez B, Goossens M, Amselem S. Alternatively spliced forms in the cytoplasmic domain of the human growth hormone (GH) receptor regulate its ability to generate a soluble GH-binding protein. *Proc Natl Acad Sci U S A.* 1996 Oct 1;93(20):10723-8. **PMID: 8855247.**

Davis SL, Ohlson DL, Klindt J, Anfinson MS. Episodic growth hormone secretory patterns in sheep: relationship to gonadal steroid hormones. *Am J Physiol.* 1977 Dec;233(6):E519-23. **PMID: 596447.**

de Vos AM, Ultsch M, Kossiakoff AA. Human growth hormone and extracellular domain of its receptor: crystal structure of the complex. *Science*. 1992 Jan 17; 255(5042):306-12. **PMID: 1549776.**

Doi T, Striker LJ, Quaife C, Conti FG, Palmiter R, Behringer R, Brinster R, Striker GE. Progressive glomerulosclerosis develops in transgenic mice chronically expressing growth hormone and growth releasing factor but not in those expressing insulin like growth factor-1. *Am J Pathol.* 1988 Jun;131(3):398-403. **PMID: 3132856.**

Dunn SE, Kari FW, French J, Leininger JR, Travlos G, Wilson R, Barrett JC. Dietary restriction reduces insulin-like growth factor I levels, which modulates apoptosis, cell proliferation, and tumor progression in p53-deficient mice. *Cancer Res.* 1997 Nov 1;57(21):4667-72. **PMID: 9354418.**

Fang P, Girgis R, Little BM, Pratt KL, Guevara-Aguirre J, Hwa V, Rosenfeld RG. Growth hormone (GH) insensitivity and insulin-like growth factor-I deficiency in Inuit subjects and an Ecuadorian cohort: functional studies of two codon 180 GH receptor gene mutations. *J Clin Endocrinol Metab.* 2008 Mar;93(3):1030-7. Epub 2007 Dec 11. **PMID: 18073295.**

Farhy LS, Straume M, Johnson ML, Kovatchev B, Veldhuis JD. A construct of interactive feedback control of the GH axis in the male. *Am J Physiol Regul Integr Comp Physiol*. 2001 Jul;281(1):R38-51. **PMID: 11404277.**

Farhy LS, Straume M, Johnson ML, Kovatchev B, Veldhuis JD. Unequal autonegative feedback by GH models the sexual dimorphism in GH secretory dynamics. *Am J Physiol Regul Integr Comp Physiol.* 2002 Mar;282(3):R753-64. **PMID: 11832396.**

Flurkey K, Papaconstantinou J, Miller RA, Harrison DE. Lifespan extension and delayed immune and collagen aging in mutant mice with defects in growth hormone production. *Proc Natl Acad Sci U S A*. 2001 Jun 5;98(12):6736-41. Epub 2001 May 22. **PMID: 11371619.**

Flyvbjerg A. Growth factors and diabetic complications. *Diabet Med.* 1990 Jun;7(5):387-99. **PMID: 2142035.**

Foltz IN, Karow M, Wasserman SM. Evolution and emergence of therapeutic monoclonal antibodies: what cardiologists need to know. *Circulation*. 2013 Jun 4;127(22):2222-30. doi: 10.1161/CIRCULATIONAHA.113.002033. **PMID: 23733968.**

Freda PU. Somatostatin analogs in acromegaly. *J Clin Endocrionol Metab*. 2002 Jul;87(7):3013-8. **PMID: 12107192.**

Freda PU, Wardlaw SL, Post KD. Long-term endocrinological follow-up evaluation in 115 patients who underwent transphenoidalsurgery for acromegaly. *J Neurosurg*. 1998 Sep;89(3):353-8. **PMID: 9724106.**

Frohman LA, Downs TR, Chomczynski P. Regulation of growth hormone secretion. Front *Neuroendocrinol.* 1992 Oct;13(4):344-405. **PMID: 1360911.**

Fryburg DA, Gelfand RA, Barrett EJ. Growth hormone acutely stimulates forearm muscle protein synthesis in normal humans. *Am J Physiol.* 1991 Mar;260(3 Pt 1):E499-504. **PMID: 2003602.**

Fryburg DA, Louard RJ, Gerow KE, Gelfand RA, Barrett EJ. Growth hormone stimulates skeletal muscle protein synthesis and antagonizes insulin's antiproteolytic action in humans. *Diabetes.* 1992 Apr;41(4):424-9. **PMID: 1607069.**

Fuh G, Cunningham BC, Fukunaga R, Nagata S, Goeddel DV, Wells JA. Rational design of potent antagonists to the human growth hormone receptor. *Science.* 1992 Jun 19;256(5064):1677-80. **PMID: 1535167.**

Fuh G, Mulkerrin MG, Bass S, McFarland N, Brochier M, Bourell JH, Light DR, Wells JA. The human growth hormone receptor. Secretion from Escherichia coli and disulfide bonding pattern of the extracellular binding domain. *J Biol Chem.* 1990 Feb 25;265(6):3111-5. **PMID: 2406245.**

Fürstenberger G, Senn HJ. Insulin-like growth factors and cancer. *Lancet Oncol.* 2002 May;3(5):298-302. **PMID: 12067807.**

Ganzetti I, De Gennaro V, Redaelli M, Müller EE, Cocchi D. Effect of hypophysectomy and growth hormone replacement on hypothalamic GHRH. *Peptides.* 1986 Nov-Dec;7(6):1011-4. **PMID: 3550723.**

Gevers E, Pincus SM, Robinson IC, Veldhuis JD. Differential orderliness of the GH release process in castrate male and female rats. *Am J Physiol.* 1998 Feb;274(2 Pt 2):R437-44. **PMID: 9486302.**

Gillis JC, Noble S, Goa KL. Octreotide long-acting release (LAR). A review of its pharmacological properties and therapeutic use in the management of acromegaly. *Drugs.* 1997 Apr;53(4):681-99. **PMID: 9098666.**

Giustina A, Veldhuis JD. Pathophysiology of the neuroregulation of growth hormone secretion in experimental animals and the human. *Endocr Rev.* 1998 Dec;19(6):717-97. **PMID: 9861545.**

Glukhova XA, Prusakova OV, Trizna JA, Zaripov MM, Afanas'eva GV, Glukhov AS, Poltavtseva RA, Ivanov AA, Avila-Rodriguez M, Barreto GE, Aliev G, Beletsky IP. Updates on the Production of Therapeutic Antibodies Using Human Hybridoma Technique. *Curr Pharm Des*. 2016;22(7):870-8. **PMID: 26696411.**

Gonçalves FT, Fridman C, Pinto EM, Guevara-Aguirre J, Shevah O, Rosembloom AL, Hwa V, Cassorla F, Rosenfeld RG, Lins TS, Damiani D, Arnhold IJ, Laron Z, Jorge AA. The E180splice mutation in the GHR gene causing Laron syndrome: witness of a Sephardic Jewish exodus from the Iberian Jewish exodus from the Iberian Peninsula to the New World? *Am J Med Genet A*. 2014 May;164A(5):1204-8. doi: 10.1002/ajmg.a.36444. Epub 2014 Mar 24. **PMID: 24664892.**

Gravhølt CH, Schmitz O, Simonsen L, Bülow J, Christiansen JS, Møller N. Effects of a physiological GH pulse on interstitial glycerol in abdominal and femoral adipose tissue. Am J Physiol. 1999 Nov;277(5 Pt 1):E848-54. **PMID: 10567011.**

Guevara-Aguirre J, Balasubramanian P, Guevara-Aguirre M, Wei M, Madia F, Cheng CW, Hwang D, Martin-Montalvo A, Saavedra J, Ingles S, de Cabo R, Cohen P, Longo VD. Growth hormone receptor deficiency is associated with a major reduction in pro-aging signaling, cancer, and diabetes in humans. *Sci Transl Med.* 2011 Feb 16;3(70):70ra13. doi: 10.1126/scitranslmed.3001845. **PMID: 21325617.**

Guevara-Aguirre J, Rosenbloom AL, Fielder PJ, Diamond FB Jr, Rosenfeld RG. Growth hormone receptor deficiency in Ecuador: clinical and biochemical phenotype in two populations. *J Clin Endocrinol Metab.* 1993 Feb;76(2):417-23. **PMID: 7679400.**

Hansel TT, Kropshofer H, Singer T, Mitchell JA, George AJ. The safety and side effects of monoclonal antibodies. *Nat Rev Drug Discov*. 2010 Apr;9(4):325-38. doi: 10.1038/nrd3003. Epub 2010 Mar 22. **PMID: 20305665.**

Hansen TK, Gravholt CH, ØRskov H, Rasmussen MH, Christiansen JS, Jørgensen JO. Dose dependency of the pharmacokinetics and acute lipolytic actions of growth hormone. *J Clin Endocrinol Metab*. 2002 Oct;87(10):4691-8. **PMID: 12364460.**

Hartman ML, Faria AC, Vance ML, Johnson ML, Thorner MO, Veldhuis JD. Temporal structure of in vivo growth hormone secretory events in humans. *Am J Physiol.* 1991 Jan;260(1 Pt 1):E101-10. **PMID: 1987784.**

Hartman, M.L., Veldhuis, J.D., Thorner, M.O. (1993). Normal control of growth hormone secretion. *Horm Res* 40: 37–47. **PMID: 8300049.**

Herrington J, Carter-Su C. Signaling pathways activated by the growth hormone receptor. *Trends Endocrinol Metab.* 2001 Aug;12(6):252-7. **PMID: 11445442.**

Hochholzer W, Giugliano RP. Lipid lowering goals: back to nature? *Ther Adv Cardiovasc Dis.* 2010 Jun;4(3):185-91. doi: 10.1177/1753944710368206. Epub 2010 Apr 16. **PMID: 20400493.**

Horber FF, Haymond MW. Human growth hormone prevents the protein catabolic side effects of prednisone in humans. *J Clin Invest.* 1990 Jul;86(1):265-72. **PMID: 2195062.**

Hursting SD, Switzer BR, French JE, Kari FW. The growth hormone: insulin-like growth factor 1 axis is a mediator of diet restriction-induced inhibition of mononuclear cell leukemia in Fischer rats. *Cancer Res.* 1993 Jun 15;53(12):2750-7. **PMID: 8389243.**

Ikeno Y, Bronson RT, Hubbard GB, Lee S, Bartke A. Delayed occurence of fatal neoplastic diseases in ames dwarf mice: correlation to extended longevity. *J Gerontol A Biol Sci Med Sci*. 2003 Apr;58(4):291-6. **PMID: 12663691.**

Illergård K, Ardell DH, Elofsson A. Structure is three to ten times more conserved than sequence--a study of structural response in protein cores. *Proteins.* 2009 Nov 15;77(3):499-508. doi: 10.1002/prot.22458. **PMID: 19507241.**

Jansson JO, Edén S, Isaksson O. Sexual dimorphism in the control of growth hormone secretion. *Endocr Rev*. 1985 Spring;6(2):128-50. **PMID: 2861084.**

Jenkins PJ, Mukherjee A, Shalet SM. Does growth hormone cause cancer? Clinical Endocrinol (Oxf). 2006 Feb;64(2):115-21. **PMID: 16430706.**

Jones TD, Carter PJ, Plückthun A, Vásquez M, Holgate RG, Hötzel I, Popplewell AG, Parren PW, Enzelberger M, Rademaker HJ, Clark MR, Lowe DC, Dahiyat BI, Smith V, Lambert JM, Wu H, Reilly M, Haurum JS, Dübel S, Huston JS, Schirrmann T, Janssen RA, Steegmaier M, Gross JA, Bradbury AR, Burton DR, Dimitrov DS, Chester KA, Glennie MJ, Davies J, Walker A, Martin S, McCafferty J, Baker MP. The INNs and out of antibody nonproprietary names. MAbs. 2016,8(1):1-9. doi: 10.1080/19420862.2015.1114320. **PMID: 26716992.**

Keizer RJ, Huitema AD, Schellens JH, Beijnen JH. Clinical pharmacokinetics of therapeutic monoclonal antibodies. *Clin Pharmacokinet.* 2010 Aug;49(8):493-507. doi: 10.2165/11531280-000000000-00000. **PMID: 20608753.**

Koonin EV, Galperin MY. Sequence - Evolution - Function: Computational Approaches in Comparative Genomics. Boston: Kluwer Academic; 2003. **PMID: 21089240.**

Kopchick JJ, Bellush LL, Coschigano KT. Transgenic models of growth hormone action. *Annu Rev Nutr.* 1999;19:437-61. **PMID: 10448532.**

Kopchick JJ, Parkinson C, Stevens EC, Trainer PJ. Growth hormone receptor antagonists: discovery, development, and use in patients with acromegaly. *Endocr Rev*. 2002 Oct;23(5):623-46. **PMID: 12372843.**

Kolar GR, Capra JD. Immunoglobulins: structure and function. In: Paul WE, ed. *Fundamental Immunology.* 5th ed. Philadelphia, Pa: Lippincott Williams & Wilkins; 2003:47-68.

Köhler G, Milstein C. Continuous cultures of fused cells secreting antibody of predefined specificity. *Nature.* 1975 Aug 7;256(5517):495-7. **PMID: 1172191.**

Krag MB, Gormsen LC, Guo Z, Christiansen JS, Jensen MD, Nielsen S, Jørgensen JO. Growth hormone-induced insulin resistance is associated with increased intramyocellular triglyceride content but unaltered VLDL-triglyceride kinetics. *Am J Physiol Endocrinol Metab.* 2007 Mar;292(3):E920-7. Epub 2006 Nov 28. **PMID: 17132823.**

Kubatzky KF, Liu W, Goldgraben K, Simmerling C, Smith SO, Constantinescu SN. Structural requirements of the extracellular to transmembrane domain junction for erythropoietin receptor function. *J Biol Chem.* 2005 Apr 15;280(15):14844-54. Epub 2005 Jan 18. **PMID: 15657048.**

Lane MA, Black A, Ingram DK, and Roth GS. Calorie Restriction in Nonhuman Primates: Implications for Age-Related Disease Risk. *Journal of Anti-Aging Medicine*. January 2009, 1(4): 315-326. https://doi.org/10.1089/rej.1.1998.1.315.

Laron Z. Laron syndrome (primary growth hormone resistance or insensitivity): the personal experience 1958-2003. *J Clin Endocrinol Metab.* 2004 Mar;89(3):1031-44. **PMID: 15001582.**

Lee B, Richards FM. The interpretation of protein structures: estimation of static accessibility. *J Mol Biol.* 1971 Feb 14;55(3):379-400. **PMID: 5551392.**

Le Marchand-Brustel Y, Tanti JF, Cormont M, Ricort JM, Grémeaux T, Grillo S. From insulin receptor signalling to Glut 4 translocation abnormalities in obesity and insulin resistance. *J Recept Signal Transduct Res.* 1999 Jan-Jul;19(1-4):217-28. **PMID: 10071760.**

Lichanska AM, Waters MJ. How growth hormone controls growth, obesity and sexual dimorphism. *Trends Genet.* 2008 Jan;24(1):41-7. Epub 2007 Dec 3. **PMID: 18063438.**

Lonberg N. Human antibodies from transgenic animals. *Nat Biotechnol.* 2005 Sep;23(9):1117-25. **PMID: 16151405.**

Lonberg N. Fully human antibodies from transgenic mouse and phage display platforms. *Curr Opin Immunol*. 2008 Aug;20(4):450-9. doi: 10.1016/j.coi.2008.06.004. Epub 2008 Jul 21. **PMID: 18606226.**

Longo VD, Mattson MP. Fasting: molecular mechanisms and clinical applications. *Cell Metab.* 2014 Feb 4;19(2):181-92. doi: 10.1016/j.cmet.2013.12.008. Epub 2014 Jan 16. **PMID: 24440038.**

Longo VD, Panda S. Fasting, Circadian Rhythms, and Time-Restricted Feeding in Healthy Lifespan. *Cell Metab.* 2016 Jun 14;23(6):1048-1059. doi: 10.1016/j.cmet.2016.06.001. **PMID: 27304506.**

Maiter DM, Gabriel SM, Koenig JI, Russell WE, Martin JB. Sexual differentiation of growth hormone feedback effects on hypothalamic growth hormone-releasing hormone and somatostatin. *Neuroendocrinology.* 1990 Feb;51(2):174-80. **PMID: 1968235.**

Maiter D, Koenig JI, Kaplan LM. Sexually dimorphic expression of the growth hormone-releasing hormone gene is not mediated by circulating gonadal hormones in the adult rat. *Endocrinology*. 1991 Apr;128(4):1709-16. **PMID: 2004597.**

Meites J. Aging: hypothalamic catecholamines neuroendocrine-immune interactions, and dietary restriction. *Proc Soc Exp Biol Med.* 1990 Dec;195(3):304-11. **PMID: 2259700.**

Michnick SW, Sidhu SS. Submitting antibodies to binding arbitration. *Nat Chem Biol.* 2008 Jun;4(6):326-9. doi: 10.1038/nchembio0608-326. **PMID: 18488004.**

Milman S, Atzmon G, Huffman DM, Wan J, Crandall JP, Cohen P, Barzilai N. Lown insulin-like growth factor-1 level predicts survival in humans with exceptional longevity. *Aging Cell.* 2014 Aug;13(4):769-71. doi: 10.1111/acel.12213. Epub 2014 Mar 12. **PMID: 24618355.**

Møller N, Jørgensen JO. Effects of growth hormone on glucose, lipid, and protein metabolism in human subjects. *Endocr Rev*. 2009 Apr;30(2):152-77. doi: 10.1210/er.2008-0027. Epub 2009 Feb 24. **PMID: 19240267.**

Møller N, Jørgensen JO, Alberti KG, Flyvbjerg A, Schmitz O. Short-term effects of growth hormone on fuel oxidation and regional substrate metabolism in normal man. *J Clin Endocrinol Metab.* 1990 Apr;70(4):1179-86. **PMID: 2318938.**

Møller N, Jørgensen JO, Schmitz O, Møller J, Christiansen J, Alberti KG, Orskov H. Effects of a growth hormone pulse on total and forearm substrate fluxes in humans. *Am J Physiol*. 1990 Jan;258(1 Pt 1):E86-91. **PMID: 2405702.**

Møller N, Schmitz O, Pørksen N, Møller J, Jørgensen JO. Dose-response studies on the metabolic effects of a growth hormone pulse in humans. *Metabolism.* 1992 Feb;41(2):172-5. **PMID: 1736039.**

Mueller EE, Locatelli V, Cocchi D. Neuroendocrine control of growth hormone secretion. *Physiol Rev.* 1999 Apr;79(2):511-607. **PMID: 10221989**.

Newman CB. Medical therapy for acromegaly. *Endocrinol Metab Clin North Am*. 1999 Mar;28(1):171-90. **PMID: 10207690.**

Newman CB, Melmed S, George A, Torigian D, Duhaney M, Snyder P, Young W, Klibanski A, Molitch ME, Gagel R, Sheeler L, Cook D, Malarkey W, Jackson I, Vance ML, Barkan A, Frohman L, Kleinberg DL. Octreotide as primary therapy for acromegaly. *J Clin Endocrinol Metab.* 1998 Sep;83(9):3034-40. **PMID: 9745397.**

Nielsen S, Møller N, Christiansen JS, Jørgensen JO. Pharmacological antilipolysis restores insulin sensitivity during growth hormone exposure. *Diabetes.* 2001 Oct;50(10):2301-8. PMID: 11574412.

Nørrelund H, Nielsen S, Christiansen JS, Jørgensen JO, Møller N. Modulation of basal glucose metabolism and insulin sensitivity by growth hormone and free fatty acid during short-term fasting. *Eur J Endocrinol.* 2004 Jun;150(6):779-87. **PMID: 15191347.**

Okada S, Kopchick JJ. Biological effects of growth hormone and its antagonist. *Trends Mol Med*. 2001 Mar;7(3):126-32. **PMID: 11286784.**

Olson K, Gehant R, Mukku V, O'Connell K, Tomlinson B, Totpal K, Winkler M. Preparation and Characterization of Poly(ethylene glycol)ylated Human Growth Hormone Antagonist. *Poly(ethylene glycol).* Chapter 12, pp 170–181. Chapter DOI: 10.1021/bk-1997-0680.ch012. *ACS Symposium Series*, Vol. 680. Publication Date (Print): August 05, 1997. Copyright © 1997 American Chemical Society. **ISBN13: 9780841235373 eISBN: 9780841216440**.

Ono M, Miki N, Demura H. effect of antiserum rat growth hormone (GH)-releasing factor on physiological Gh secretion in the female rat. *Endocrinology.* 1991 Oct;129(4):1791-6. **PMID: 1915068.**

Ono M, Miki N, Murata Y, Osaki E, Tamitsu K, Ri T, Yamada M, Demura H. Sexually dimorphic expression of pituitary growth hormone-releasing factor receptor in the rat. *Biochem Biophys Res Commun.* 1995 Nov 22;216(3):1060-6. **PMID: 7488180.**

Painson JC, Thorner MO, Krieg RJ, Tannenbaum GS. Short-term adult exposure to estradiol feminizes the male pattern of spontaneous and growth hormone-releasing factor-stimulated growth hormone secretion in the rat. *Endocrinology.* 1992 Jan;130(1):511-9. **PMID: 1345780.**

Painson JC, Veldhuis JD, Tannenbaum GS. Single exposure to testosterone in adulthood rapidly induces regularity in the growth hormone release process. *Am J Physiol Endocrinol Metab.* 2000 May;278(5):E933-40. **PMID: 10780951.**

Parr T. Insulin exposure controls the rate of mammalian aging. *Mech Ageing Dev.* 1996 Jul 5;88(1-2):75-82. **PMID: 8803924.**

Piatti PM, Monti LD, Caumo A, Conti M, Magni F, Galli-Kienle M, Fochesato E, Pizzini A, Baldi L, Valsecchi G, Pontiroli AE. Mediation of the hepatic effects of growth hormone by its lypolitic activity. *J Clin Endocrinol Metab.* 1999 May;84(5):1658-63. **PMID: 10323396.**

Pincus SM, Gevers EF, Robinson IC, van den Berg G, Roelfsema F, Hartman ML, Veldhuis JD. Females secrete growth hormone with more process irregularity than males in both humans and rats. *Am J Physiol*. 1996 Jan;270(1 Pt 1):E107-15. **PMID: 8772482.**

Plotsky PM, Vale W. Patterns of growth hormone-releasing factor and somatostatin secretion into the hypophysial-circulation of the rat. *Science.* 1985 Oct 25;230(4724):461-3. **PMID: 2864742.**

Poger D, Mark AE. Turning the growth hormone receptor on: evidence that hormone binding induces subunit rotation. *Proteins.* 2010 Apr;78(5):1163-74. doi: 10.1002/prot.22636. **PMID: 19927328.**

Pollak M, Blouin MJ, Zhang JC, Kopchick JJ. Reduced mammary gland carcinogenesis in transgenic mice expressing a growth hormone antagonist. *Br J Cancer.* 2001 Aug 3;85(3):428-30. **PMID: 11487276.**

Press M. Growth hormone and metabolism. *Diabetes Metab Rev*. 1988 Jun;4(4):391-414. **PMID: 3292176.**

Quigley K, Goya R, Nachreiner R, Meites J. Effects of underfeeding and refeeding on GH and thyroid hormone secretion in young, middle-aged, and old rats. *Exp Gerontol*. 1990;25(5):447-57. **PMID: 2257891.**

Rabinowitz D, Klassen GA, Zierler KL. Effect of human growth hormone on muscle and adipose tissue metabolism in the forearm of man. *J Clin Invest.* 1965 Jan;44:51-61. **PMID: 14254256.**

Robinson IC. The growth hormone secretory pattern: a response to neuroendocrine signals. *Acta Paediatr Scand Suppl.* 1991;372:70-8; discussion 79-80. **PMID: 1681678.**

Rogers SA, Miller SB, Hammerman MR. Growth hormone stimulates IGF I gene expression in isolated rat renal collecting duct. *Am J Physiol.* 1990 Sep;259(3 Pt 2):F474-9. **PMID: 2396672.**

Rosenbloom AL, Guevara Aguirre J, Rosenfeld RG, Fielder PJ. The little women of Loja--growth hormone-receptor deficiency in an inbred population of southern Ecuador. *N Engl J Med.* 1990 Nov 15;323(20):1367-74. **PMID: 2233903.**

Roshan,S.Y., McCutcheon,I.E., Bennett,W.F., Hill,H.L., Scarlett,J.A., Flyvbjerg,A. and Friend,K.E. (1999) The growth hormone receptor antagonist B2036PEG (Trovert) inhibits the growth of breast cancer xenografts in nude mice. *In The Endocrine Society's 84th Annual Meeting.* Abstract, pp. P2–P122. Endocrine Society, San Diego, CA.

Ross RJ, Esposito N, Shen XY, Von Laue S, Chew SL, Dobson PR, Postel-Vinay MC, Finidori J. A short isoform of the human growth hormone receptor functions as a dominant negative inhibitor of the full-length receptor and generates large amounts of binding protein. *Mol Endocrinol.* 1997 Mar;11(3):265-73. **PMID: 9058373.**

Saeed AF, Wang R, Ling S, Wang S. Antibody Engineering for Pursuing a Healthier Future. *Front Microbiol.* 2017 Mar 28;8:495. doi: 10.3389/fmicb.2017.00495. eCollection 2017. **PMID: 28400756.**

Sassolas G, Harris AG, James-Deidier A. Long term effect of incremental doses of the somatostatin analog SMS 201-995 in 58 acromegalic patients. French SMS 201-995 approximately equal to Acromegaly Study Group. *J Clin Endocrinol Metab.* 1990 Aug;71(2):391-7. **PMID: 2199479.**

Segerlantz M, Bramnert M, Manhem P, Laurila E, Groop LC. Inhibition of the rise in FFA by Acipimox partially prevents GH-induced insulin resistance in GH-deficient adults. *J Clin Endocrinol Metab.* 2001 Dec;86(12):5813-8. **PMID: 11739444.**

Shaneyfelt T, Husein R, Bubley G, Mantzoros CS. Hormonal predictors of prostate cancer: a meta-analysis. *J Clin Oncol*. 2000 Feb;18(4):847-53. **PMID: 10673527.**

Shevah O, Laron Z. 2011. Genetic aspects. In: Laron Z, Kopchick JJ, editors. Laron syndrome - From man to mouse. Berlin, Heidelberg: *Springer-Verlag*. p 29–52. **ISBN: 978-3-642-11183-9.**

Shimizu M, Dickhoff WW. Circulating insulin-like growth factor binding proteins in fish: Their identities and physiological regulation. *Gen Comp Endocrinol*. 2017 Oct 1;252:150-161. doi: 10.1016/j.ygcen.2017.08.002. Epub 2017 Aug 4. **PMID: 28782538.**

Smit LS, Meyer DJ, Billestrup N, Norstedt G, Schwartz J, Carter-Su C. The role of the growth hormone (GH) receptor and JAK1 and JAK2 kinases in the activation of Stats 1, 3, and 5 by GH. *Mol Endocrinol.* 1996 May;10(5):519-33. **PMID: 8732683.**

Smith LE, Kopchick JJ, Chen W, Knapp J, Kinose F, Daley D, Foley E, Smith RG, Schaeffer JM. Essential role of growth hormone in ischemia-induced retinal neovascularization. *Science.* 1997 Jun 13;276(5319):1706-9. **PMID: 9180082.**

Sonntag WE, Lynch CD, Cefalu WT, Ingram RL, Bennett SA, Thornton PL, Khan AS. Pleiotropic effects of growth hormone and insulin-like growth factor (IGF)-1 on biological aging: inferences from moderate caloric-restricted animals. *J Gerontol A Biol Sci Med Sci*. 1999 Dec;54(12):B521-38. **PMID: 10647962.**

Sonntag WE, Xu X, Ingram RL, D'Costa A. Moderate caloric restriction alters the subcellular distribution of somatostatin mRNA and increases growth hormone pulse amplitude in aged animals. *Neuroendocrinology*. 1995 May;61(5):601-8. **PMID: 7617139.**

Souza SC, Frick GP, Yip R, Lobo RB, Tai LR, Goodman HM. Growth hormone stimulates tyrosine phosphorylation of insulin receptor substrate-1**. J Biol Chem.** 1994 Dec 2;269(48):30085-8. **PMID: 7527025.**

Söding, J. Protein homology detection by HMM-HMM comparison. *Bioinformatics.* 2005 Apr 1; 21(7):951-60. Epub 2004 Nov 5. **PMID: 15531603.**

Sönksen PH, Russell-Jones D, Jones RH. Growth hormone and diabetes mellitus. A review of sixty-three years of medical research and a glimpse into the future? *Horm Res.* 1993;40(1-3):68-79. **PMID: 8300053.**

Steiner RA, Stewart JK, Barber J, Koerker D, Goodner CJ, Brown A, Illner P, Gale CC. Somatostatin: a physiological role in the regulation of growth hormone secretion in the adolescent male baboon. *Endocrinology.* 1978 May;102(5):1587-94. **PMID: 105879.**

Suh Y, Atzmon G, Cho MO, Hwang D, Liu B, Leahy DJ, Barzilai N, Cohen P. Functionally significant insulin-like growth factor I receptor mutations in centenarians. *Proc Natl Acad Sci U S A*. 2008 Mar 4;105(9):3438-42. doi: 10.1073/pnas.0705467105. Epub 2008 Mar 3. **PMID: 18316725.**

Tannenbaum GS. Neuroendocrine control of growth hormone secretion. *Acta Paediatr Scand Suppl.* 1991;372:5-16. **PMID: 1681677.**

Tannenbaum GS, Ling N. The interrelationship of growth hormone (GH)-releasing factor and somatostatin in generation of the ultradian rhythm of GH secretion. *Endocrinology.* 1984 Nov;115(5):1952-7. **PMID: 6149116.**

Terry LC, Martin JB. The effects of lateral hypothalamic-medial forebrain stimulation and somatostatin antiserum on pulsatile growth hormone secretion in freely behaving rats: evidence for a dual regulatory mechanism. *Endocrinology.* 1981 Aug;109(2):622-7. **PMID: 7250062.**

Trainer PJ, Drake WM, Katznelson L, Freda PU, Herman-Bonert V, van der Lely AJ, Dimaraki EV, Stewart PM, Friend KE, Vance ML, Besser GM, Scarlett JA, Thorner MO, Parkinson C, Klibanski A, Powell JS, Barkan AL, Sheppard MC, Malsonado M, Rose DR, Clemmons DR, Johannsson G, Bengtsson BA, Stavrou S, Kleinberg DL, Cook DM, Phillips LS, Bidlingmaier M, Strasburger CJ, Hackett S, Zib K, Bennett WF, Davis RJ. Treatment of acromegaly with the growth hormone-receptor antagonist pegvisomant. *N Engl J Med.* 2000 Apr 20;342(16):1171-7. **PMID: 10770982.**

Tsukazaki T, Matsumoto T, Enomoto H, Usa T, Ohtsuru A, Namba H, Iwasaki K, Yamashita S. Growth hormone directly and indirectly stimulates articular chondrocyte cell growth. *Osteoarthritis Cartilage.* 1994 Dec;2(4):259-67. **PMID: 11550711.**

Uchiyama, T., H. Abe, S. Shakutsui, S. Ohashi, T. Fujita, and K. Chihara. Sexual dimorphism in hypothalamic GRF and somatostatin mRNA and pituitary GH mRNA levels in rats (Abstract). *Proc. Annu. Meet. Endocr. Soc.* 72nd Atlanta GA 1990, p. 50

Vanderkuur JA, Butch ER, Waters SB, Pessin JE, Guan KL, Carter-Su C. Signaling molecules involved in coupling growth hormone receptor to mitogen-activated protein kinase activation. *Endocrinology.* 1997 Oct;138(10):4301-7**. PMID: 9322943.**

Veldhuis JD, Roemmich JN, Rogol AD. Gender and sexual maturation-dependent contrasts in the neuroregulation of growth hormone secretion in prepubertal and late adolescent males and females—a general clinical research center-based study. *J Clin Endocrinol Metab.* 2000 Jul;85(7):2385-94. **PMID: 10902783.**

Verdery RB, Walford RL. Changes in plasma lipids and lipoproteins in humans during a 2-year period of dietary restriction in Biosphere 2*. Arch Intern Med.* 1998 Apr 27;158(8):900-6. **PMID: 9570177.**

Walford RL. Biosphere 2 as Voyage of Discovery: The Serendipity from Inside. *BioScience*, Volume 52, Issue 3, 1 March 2002, Pages 259-263,https://doi.org/10.1641/0006-3568(2002)052[0259:BAVODT]2.0.CO;2.
Published: 01 March 2002. **ISSN 0006-3568. EISSN 1525-3244.**

Walford RL, Bechtel R, MacCallum T, Paglia DE, Weber LJ. "Biospheric medicine" as viewed from the two-year first closure of Biosphere 2. *Aviat Space Environ Med.* 1996 Jul;67(7):609-17. **PMID: 8830939.**

Walford RL, Mock D, Verdery R, MacCallum T. Calorie restriction in biosphere 2: alterations in physiologic, hematologic, hormonal, and biochemical parameters in humans restricted for a 2-year period. *J Gerontol A Biol Sci Med Sci.* 2002 Jun;57(6):B211-24. **PMID: 12023257.**

Warshamana-Greene GS, Litz J, Buchdunger E, García-Echeverría C, Hofmann F, Krystal GW. The insulin-like growth factor-I receptor kinase inhibitor, NVP-ADW742, sensitizes small cell lung cancer cell lines to the effects of chemotherapy. *Clin Cancer Res.* 2005 Feb 15;11(4):1563-71. **PMID: 15746061.**

Waters MJ. The growth hormone receptor. *Growth Horm IGF Res*. 2016 Jun;28:6-10. doi: 10.1016/j.ghir.2015.06.001. Epub 2015 Jun 7. **PMID: 26059750.**

Waters MJ, Shang CA, Behncken SN, Tam SP, Li H, Shen B, Lobie PE. Growth hormone as a cytokine. *Clin Exp Pharmacol Physiol.* 1999 Oct;26(10):760-4. **PMID: 10549398.**

Wehrenberg WB, Baird A, Ying SY, Ling N. The effects of testosterone and estrogen on the pituitary growth hormone response to growth hormone-releasing factor. *Biol Reprod.* 1985 Mar;32(2):369-75. **PMID: 3921073.**

Wehrenberg WB, Brazeau P, Luben R, Böhlen P, Guillemin R. Inhibition of the pulsatile secretion of growth hormone by monoclonal antibodies to the hypothalamic growth hormone releasing factor (GRF). *Endocrinology.* 1982 Dec;111(6):2147-8. **PMID: 6128220.**

Wei M, Brandhorst S, Shelehchi M, Mirzaei H, Cheng CW, Budniak J, Groshen S, Mack WJ, Guen E, Di Biase S, Cohen P, Morgan TE, Dorff T, Hong K, Michalsen A, Laviano A, Longo VD. Fasting-mimicking diet and markers/risk factors for aging, diabetes, cancer, and cardiovascular disease. *Sci Transl Med.* 2017 Feb 15;9(377). pii: eaai8700. doi: 10.1126/scitranslmed.aai8700. **PMID: 28202779.**

Weindruch R, Walford RL. The Retardation of Aging and Disease by Dietary Restriction. *Springfield,* IL: Charles C Thomas; 1988. **ISBN-13: 978-0398054960. ISBN-10: 0398054967.**

Weiner LM. Fully human therapeutic monoclonal antibodies. *J Immunother.* 2006 Jan-Feb;29(1):1-9. **PMID: 16365595**.

Yamauchi T, Kaburagi Y, Ueki K, Tsuji Y, Stark GR, Kerr IM, Tsushima T, Akanuma Y, Komuro I, Tobe K, Yazaki Y, Kadowaki T. Growth hormone and prolactin stimulate tyrosine phosphorylation of insulin receptor substrate-1, -2, and -3, their association with p85 phosphatidylinositol 3-kinase (PI3-kinase), and concomitantly PI3-kinase activation via JAK2 kinase. *J Biol Chem.* 1998 Jun 19;273(25):15719-26. **PMID: 9624169.**

Yang CW, Striker LJ, Kopchick JJ, Chen WY, Pesce CM, Peten EP, Striker GE. Glomerulosclerosis in mice transgenic for native or mutated bovine growth hormone gene. *Kidney Int Suppl.* 1993 Jan;39:S90-4. **PMID: 8468934.**

Yang XD, Jia XC, Corvalan JR, Wang P, Davis CG. Development of ABX-EGF, a fully human anti-EGF receptor monoclonal antibody, for cancer therapy. *Crit Rev Oncol Hematol.* 2001 Apr;38(1):17-23. **PMID: 11255078.**

Yarasheski KE, Campbell JA, Smith K, Rennie MJ, Holloszy JO, Bier DM. Effect of growth hormone and resistance exercise on muscle growth in young men. *Am J Physiol*. 1992 Mar;262(3 Pt 1):E261-7. **PMID: 1550219.**

Zha J, LAckner MR. Targeting the insulin-like growth factor receptor-1R pathway for cancer therapy. *Clin Cancer Res.* 2010 May 1;16(9):2512-7. doi: 10.1158/1078-0432.CCR-09-2232. Epub 2010 Apr 13. **PMID: 20388853.**

Zhou Y, Xu BC, Maheshwari HG, He L, Reed M, Lozykowski M, Okada S, Cataldo L, Coschigamo K, Wagner TE, Baumann G, Kopchick JJ. A mammalian model for Laron syndrome produced by targeted disruption of the mouse growth hormone receptor/binding protein gene (the Laron mouse). *Proc Natl Acad Sci U S A.* 1997 Nov 25;94(24):13215-20. **PMID: 9371826.**

Zierler KL, Rabinowitz D. Roles of insulin and growth hormone, based on studies of forearm metabolism in man. *Medicine (Baltimore).* 1963 Nov;42:385-402. **PMID: 14085535.**

11. Appendix

```
GHR_HUMAN      MDLWQLLLTLALAGSSDAFSGSEATAAILSRAPWSLQSVNPGLKTNSSKEPKFTKCRSPE  60
GHR_PAPAN      MDLWQLLLTLALAGSSDAFSGSEPTAAILSRASWSLQSVNPGLKTNSSKEPKFTKCRSPE  60
GHR_MACMU      ------------------------------------------------------------  0
GHR_SAIBB      MDLWQLLLTLALAGSSDAFSGRETTAAVLSRVSQSLLSVNPGLKTNSSKEPKFTKCRSPE  60
GHR_RAT        MDLWRVFLTLALAVSSDMFPGSGATPATLGKASPVLQRINPSLRESSSGKPRFTKCRSPE  60
GHR_MOUSE      MDLCQVFLTLALAVTSSTFSGSEATPATLGKASPVLQRINPSLGTSSSGKPRFTKCRSPE  60
GHR_CAVPO      MDLWQLLLTLAVVGSSNAFVGREAVTVTLNRANLSLQRVNASLETNSSGNPKFTKCRSPE  60
GHR_RABIT      MDLWQLLLTVALAGSSDAFSGSEATPATLGRASESVQRVHPGLGTNSSGKPKFTKCRSPE  60
GHR_BOSIN      MDLWQLLLTLAVAGSSDAFSGSEATPAFLVRASQSLQILYPVLETNSSGNPKFTKCRSPE  60
GHR_BOVIN      MDLWQLLLTLAVAGSSDAFSGSEATPAFLVRASQSLQILYPVLETNSSGNPKFTKCRSPE  60
GHR_SHEEP      MDLWQLLLTLAVAGSSDAFSGSEATPAFFVRASQSLQILYPGLETNSSGNLKFTKCRSPE  60
GHR_PIG        MDLWQLLLTLAVAGSSDAFSGSEATPAVLVRASQSLQRVHPGLETNSSGKPKFTKCRSPE  60
GHR_CANLF      MDLWQLLLTLAVAGSGSAFSGSEATPTILGSASQSLQRVNPGLGTNSSEKPKFTKCRSPE  60
GHR_AILME      MDLWQLLLTLAVAGSGNAVSGSEATPAILGRASQSLQRVNPGPGTNPSGKPQFTKCRSPE  60
GHR_CHICK      MDLRHLLFTLALVCANDSLSASDD----------------------LLQWPQISKCRSPE  38
GHR_COLLI      MDLRHLLLTLVLVCANDSLSASDD----------------------VLRLPQISKCRSPE  38

GHR_HUMAN      RETFSCHWTDEVHHGTKNLGPIQLFYTRRN--------TQEWTQEWKECPDYVSAGENSC  112
GHR_PAPAN      RETFSCHWTDAVHHGSKSLGPIQLFYTRRN--------IQEWTQEWKECPDYVSAGENSC  112
GHR_MACMU      ----------AVHHGSKSLGPIQLFYTRRN--------IQGQTQEWKECPDYVSAGENSC  42
GHR_SAIBB      LETFSCRWTDAVHHGLKSPGPIQLFYTRRN--------TQEGTQEWKECPDYVSAGENSC  112
GHR_RAT        LETFSCYWTEGDDHNLKVPGSIQLYYAR--------RIAHEWTPEWKECPDYVSAGANSC  112
GHR_MOUSE      LETFSCYWTEGDNPDLKTPGSIQLYYAKRESQRQAARIAHEWTQEWKECPDYVSAGKNSC  120
GHR_CAVPO      LETFSCHWTDEGHHGLKSTGFIQMFYTKRN--------SQEQNQEWKECPDYVSAGENSC  112
GHR_RABIT      LETFSCHWTDGVHHGLKSPGSVQLFYIRRN--------TQEWTQEWKECPDYVSAGENSC  112
GHR_BOSIN      LETFSCHWTDGANHSLQSPGSVQMFYIRRD--------IQ----EWKECPDYVSAGENSC  108
GHR_BOVIN      LETFSCHWTDGANHSLQSPGSVQMFYIRRD--------IQ----EWKECPDYVSAGENSC  108
GHR_SHEEP      LETFSCHWTDGANHSLQSPGSVQMFYIRRD--------IQ----EWKECPDYVSAGENSC  108
GHR_PIG        LETFSCHWTDGVRHGLQSPGSIQLFYIRRS--------TQEWTQEWKECPDYVSAGENSC  112
GHR_CANLF      LETFSCHWTDGVRHGLKNAGSVQLFYIRRS--------TQEWTQEWKECPDYVSAGENSC  112
GHR_AILME      LETFSCHWTEGVHHGVKNPGSIQLFYIRRS--------TQEWTPEWKECPDYVSAGENSC  112
GHR_CHICK      LETFSCYWTDGKV---TTSGTIQLLYMKRS------------DEDWKECPDYITAGENSC  83
GHR_COLLI      LETFSCYWTDGNFYNLSAPGTIQLLYMKRN------------DEDWKECPDYITAGENSC  86
                              * :*: * :               :*******::** ***

GHR_HUMAN      YFNSSFTSIWIPYCIKLTSNGGTVDEKCFSVDEIVQPDPPIALNWTLLNVSLTGIHADIQ  172
GHR_PAPAN      YFNSSFTSVWIPYCIKLTSNGDTVDGKCFSVDEIVQPDPPIALNWTLLNVSLTGIHADIQ  172
GHR_MACMU      YFNSSFTSVWIPYCIKLTSNGDTVDGKCFSVDEIVQPDPPIALNWTLLNVSLTGIHADIL  102
GHR_SAIBB      YFNSSFTSIWIPYCIKLTSNGGTVDEKCFSVDQIVQPDPPIALNWTLLNISLTGVHADIQ  172
GHR_RAT        YFNSSYTSIWIPYCIKLTTNGDLLDEKCFTVDEIVQPDPPIGLNWTLLNISLPGIRGDIQ  172
GHR_MOUSE      YFNSSYTSIWIPYCIKLTTNGDLLDQKCFTVDEIVQPDPPIGLNWTLLNISLTGIRGDIQ  180
GHR_CAVPO      YFNSSYTSIWKPYCVKLTSNGGKVDEKCFYVEEIVQPDPPTGLNWTLMNTSATAIYGDIQ  172
GHR_RABIT      YFNSSYTSIWIPYCIKLTNNGGMVDQKCFSVEEIVQPDPPIGLNWTLLNVSLTGIHADIQ  172
GHR_BOSIN      YFNSSYTSVWTPYCIKLTSNGGIVDHKCFSVEDIVQPDPPVGLNWTLLNISLTEIHADIL  168
GHR_BOVIN      YFNSSYTSVWTPYCIKLTSNGGIVDHKCFSVEDIVQPDPPVGLNWTLLNISLTEIHADIL  168
GHR_SHEEP      YFNSSYTSVWTPYCIKLTSNGGIVDHKCFSVEDIVQPDPPVGLNWTLLNISLTEIHADIL  168
GHR_PIG        YFNSSYTSIWIPYCIKLTSNGGTVDQKCFSVEEIVQPDPPIGLNWTLLNISLTGIHADIQ  172
GHR_CANLF      YFNSSYTSIWIPYCIKLTSNGGTVDQKCFSVEEIVQPDPPIGLNWTLLNISLTGIHADIQ  172
GHR_AILME      YFNSSYTSIWIPYCIKLTSNGDTVDQKCFSVEEIVQPDPPIGLNWTLLNISLTGIHADIQ  172
GHR_CHICK      YFNTSYTSIWIPYCVKLANKDEVFDEKCFSVDEIVLPDPPVHLNWTLLNTSQTGIHGDIQ  143
GHR_COLLI      YFNTSYTSIWIPYCVKLVNKDEVFDEKCFSVDEIVLPDPPVHLNWTLLNTSQTGIHGDIQ  146
               ***:*:**:* ***:**..:.  .* *** *::** ****  *****:* *   : .**

GHR_HUMAN      VRWEAPRNADIQKGWMVLEYELQYKEVNETKWKMMDPILTTSVPVYSLKVDKEYEVRVRS  232
GHR_PAPAN      VRWEAPPNADIQKGWMVLEYELQYKEVNETKWKMMDPILSTSVPVYSLKVDKEYEVRVRS  232
GHR_MACMU      VRWEAPPNADIQKGWMVLEYELQYKEVNETKWKMMDPILSTSVPVYSLKVDKEYEVLVRS  162
GHR_SAIBB      VRWEAPPNADIQKGWMVLEYELQYKEVNETQWKMMDPILSTSVPLYSLRVDKEYEVRVRS  232
GHR_RAT        VSWQPPPSADVLKGWIILEYEIQYKEVNETKWKTMSPIWSTSVPLYSLRLDKEHEVRVRS  232
GHR_MOUSE      VSWQPPPNADVLKGWIILEYEIQYKEVNESKWKVMGPIWLTYCPVYSLRMDKEHEVRVRS  240
GHR_CAVPO      VRWKPPRSADVKKGWIMLDYELQIKQTNETQWKMMDPVTSTSVPLYSLRLDKEYEVRIRS  232
GHR_RABIT      VRWEPPPNADVQKGWIVLEYELQYKEVNETQWKMMDPVLSTSVPVYSLRLDKEYEVRVRS  232
GHR_BOSIN      VKWEPPPNTDVKMGWIILEYELHYKELNETQWKMMDPLMVTSVPMYSLRLDKEYEVRVRT  228
GHR_BOVIN      VKWEPPPNTDVKMGWIILEYELHYKELNETQWKMMDPLMVTSVPMYSLRLDKEYEVRVRT  228
GHR_SHEEP      VKWEPPPNTDVKMGWIILEYELHYKELNETQWKMMDPLLVTSVPMYSLRLDKEYEVRVRT  228
GHR_PIG        VRWEPPPNADVQKGWIVLEYELQYKEVNETQWKMMDPVLSTSVPVYSLRLDKEYEVRVRS  232
```

```
GHR_CANLF      VRWEPPPNADVQKGWIVLKYELQYKEVNESQWKMMDPVSATSVPVYSLRLDKEYEVRVRS 232
GHR_AILME      VRWEPPPNADVQKGWIVLEYELQYKEVNESQWKMMDPVLSTSVPVYSLRLDKEYEVRVRS 232
GHR_CHICK      VRWDPPPTADVQKGWITLEYELQYKEVNETKWKELEPRLSTVVPLYSLKMGRDYEIRVRS 203
GHR_COLLI      VRWDPPPTADVQKGWITLEYELQYKEVNETKWKELEPRLSTMVPLYSLKIGRDYEIRVRS 206
               * *. * .:*:  **: *.**:: *: **::** : *   *  *:***::.:::*: :*:

GHR_HUMAN      KQRNSGNYGEFSEVLYVTLPQMS-QF-TCEEDFYFPWLLIIIFGIFGLTVMLFVFLFSKQ 290
GHR_PAPAN      KRRNSGNYGEFSEVLYVTLPQMN-QF-TCEEDFYFPWLLIIIFGIFGLTVMLFVFLFSKQ 290
GHR_MACMU      KRRNSRNYGEFSEVLYVTLPQMN-QF-TCEEDFYFPWLLIIIFGIFGLTVMLFVFLFSKQ 220
GHR_SAIBB      RQRKSENYGEFSEVLYVKLPQMS-QF-TCEEDFYYPWLLIIIFGISGLTVMLFVFLFSKQ 290
GHR_RAT        RQRSFEKYSEFSEVLRVTFPQMD-TLAACEEDFRFPWFLIIIFGIFGVAVMLFVVIFSKQ 291
GHR_MOUSE      RQRSFEKYSEFSEVLRVIFPQTN-ILEACEEDIQFPWFLIIIFGIFGVAVMLFVVIFSKQ 299
GHR_CAVPO      RLQNSDKYGEFSEILYITLPQSS-PF-TCEEEFQFPWFLIMIFGIFGLTVMLLVVMFSKQ 290
GHR_RABIT      RQRSSEKYGEFSEVLYVTLPQMS-PF-TCEEDFRFPWFLIIIFGIFGLTVMLFVFIFSKQ 290
GHR_BOSIN      RQRNTEKYGKFSEVLLITFPQMN-PS-ACEEDFQFPWFLIIMFGILGLAVTLFLLIFSKQ 286
GHR_BOVIN      RQRNTEKYGKFSEVLLITFPQMN-PS-ACEEDFQFPWFLIIIFGILGLAVTLYLLIFSKQ 286
GHR_SHEEP      RQRNTEKYGKFSEVLLITFPQMN-PS-ACEEDFQFPWFLIIIFGILGLTVTLFLLIFSKQ 286
GHR_PIG        RQRNSEKYGEFSEVLYVTLPQMS-PF-ACEEDFRFPWFLIIIFGIFGLTVILFLLIFSKQ 290
GHR_CANLF      RQRNSEKYGEFSEALYVTLPQMS-PF-ACEEDFQFPWFLIIIFGIFGLTMILFLFIFSKQ 290
GHR_AILME      RQRNSEKYGEFSEVLYVALPQMS-PF-ACEEDFQFPWFLIIIFGIFGLTMILFLFIFSKQ 290
GHR_CHICK      RQRTSEKFGEFSEILYVSFTQAGIEFVHCAEEIEFPWFLVVVFGVCGLAVTAILILLSKQ 263
GHR_COLLI      RQRTSEKFGEFSEILYVSFSQAGIEFVHCAEEIEFPWFLVVIFGACGLAVTVILILLSKQ 266
               : :.  ::.:*** * : : * .     * *:: :**:*:::**  *:::   :.::***

GHR_HUMAN      QRIKMLILPPVPVPKIKGIDPDLLKEGKLEEVNTILAIHDSYKPEFHSDDSWVEFIELDI 350
GHR_PAPAN      QRIKMLILPPVPVPKIKGIDPDLLKEGKLEEVNTILAIHDSYKPEFHSDDSWVEFIELDI 350
GHR_MACMU      QRIKMLILPPVPVPKIKGINPDLLKEGKLEEVNAILAIHDSYKPEFHSDDSWVEFIELDI 280
GHR_SAIBB      QRIKMLILPPVPVPKIKGIDPDLLKEGKLEEVNTILAIHDSYKPEFHSDDSWVEFIELDI 350
GHR_RAT        QRIKMLILPPVPVPKIKGIDPDLLKEGKLEEVNTILGIHDNYKPDFYNDDSWVEFIELDI 351
GHR_MOUSE      QRIKMLILPPVPVPKIKGIDPDLLKEGKLEEVNTILGIHDNYKPDFYNDDSWVEFIELDI 359
GHR_CAVPO      QRIKMLILPPVPVPKIKGVDPDLLKEGKLEEVNTILAIHDNSKPQFYNDDSWVEFIELDI 350
GHR_RABIT      QRIKMLILPPVPVPKIKGIDPDLLKEGKLEEVNTILAIQDSYKPEFYNDDSWVEFIELDI 350
GHR_BOSIN      QRIKMLILPPVPVPKIKGIDPDLLKEGKLEEVNTILAIHDNYKHEFYNDDSWVEFIELDI 346
GHR_BOVIN      QRIKMLILPPVPVPKIKGIDPDLLKEGKLEEVNTILAIHDNYKHEFYNDDSWVEFIELDI 346
GHR_SHEEP      QRIKMLILPPVPVPKIKGIDPDLLKEGKLEEVNTILAIHDNYKHEFYNDDSWVEFIELDI 346
GHR_PIG        QRIKMLILPPVPVPKIKGIDPDLLKEGKLEEVNTILAIHDNYKHEFYSDDSWVEFIELDI 350
GHR_CANLF      QRIKMLILPPVPVPKIKGIDPDLLKEGKLEEVNTILAIHDNYKPEFYNDDSWVEFIELDI 350
GHR_AILME      QRIKMLILPPVPVPKIKGIDSDLLKEGKLEEVSTILAIHDNYKPEFYNDDSWVEFIELDI 350
GHR_CHICK      PRLKMLIFPPVPVPKIKGIDPDLLKKGKLDEVNSILASHDNYKTQLYNDDLWVEFIELDI 323
GHR_COLLI      SRLKMLIFPPVPVPKIKGIDPDLLKKGKLDEVNSILASHDNYKTQLYNDDLWVEFIELDI 326
                *:****:**********:: ****:***:**.:**. :*. * :::.** *********

GHR_HUMAN      DEP--DEKTEESDTDRLLSSDHEKSHSNLGVKDGDSGRTSCCEPDILETDFNANDIHEGT 408
GHR_PAPAN      DEP--DEKNEGSDTDRLLSSDHQKSHSNLGVKDGDSGRTSCYEPDILETDFNANNIHEGT 408
GHR_MACMU      DEP--DEKNEGSDTDRLLSSDHQKSHSNLGVKDGDSGRTSCYEPDILETDFNANNIHEGT 338
GHR_SAIBB      EDP--DEKTEGLDTDRLLSSDHEKSRSNLGVKDGDSGRTSCYEPDMLETDFNANDIHDGT 408
GHR_RAT        DDA--DEKTEESDTDRLLSDDQEKSAGILGAKDDDSGRTSCYDPDILDTDFHTSDMCDGT 409
GHR_MOUSE      DEADVDEKTEGSDTDRLLSNDHEKSAGILGAKDDDSGRTSCYDPDILDTDFHTSDMCDGT 419
GHR_CAVPO      DDS--DEKIEGSDTDRLLSSDHQKSLNILGAKDGDSGRTSCYEPDILEADFNAND---GT 405
GHR_RABIT      DDP--DEKTEGSDTDRLLSNSHQKSLSVLAAKDDDSGRTSCYEPDILENDFNASDGCDGN 408
GHR_BOSIN      DDP--DEKTEGSDTDRLLSNDHEKSLNIFGAKDDDSGRTSCYEPDILEADFHVSDMCDGT 404
GHR_BOVIN      DDP--DEKTEGSDTDRLLSNDHEKSLNIFGAKDDDSGRTSCYEPDILEADFHVSDMCDGT 404
GHR_SHEEP      DDP--DEKTEGSDTDRLLSNDHEKSLSIFGAKDDDSGRTSCYEPDILETDFHVSDMCDGT 404
GHR_PIG        DDP--DEKTEGSDTDRLLNNDHEKSLTILGAKEDDSGRTSCYEPDILETDFNANDVCDGT 408
GHR_CANLF      DDL--DEKTEGSDTDRLLSNDHEKSLNILGAKDDDSGRTSCYEPDILETDFNASDVCDGT 408
GHR_AILME      DDP--DEKTEGSDTDRLLSNDHEKSLNILGAKDDDSGRTSCYEPDILETDFNASDVCDGT 408
GHR_CHICK      DDS--DEKNRVSDTDRLLSDDHLKSHSCLGAKDDDSGRASCYEPDIPETDFSASDTCDAI 381
GHR_COLLI      EDP--DEKNRVSDTDRLLSEDHLKSHSCLGAKDDDSGRASCCEPDIPETDFSASDTCDAI 384
               ::   *** .  ******...: **   :..*:.****:** :**: : ** ..:   .

GHR_HUMAN      SEVAQPQRLK-GEADLLCLDQKNQNNSPYHDACPATQQP-SVIQAEKNKPQPLPTEGAES 466
GHR_PAPAN      SEVAQPQRLK-GEADLLCLDQKNQNKSPYHDACPAAQQS-SVIQAEKNKPQPLPTDGAES 466
GHR_MACMU      SEVAQPQRLK-GEADLLCLDQKNQNKSPYHDACPATQQP-SVIQAEKNKPQPLPTDGAES 396
GHR_SAIBB      SEVVQPQRLK-GEADLLCLDQKNQNNSPYHDACPAIHQP-SVIQAEKNKPQPLLIDGAES 466
GHR_RAT        SEFAQPQKLK-AEADLLCLDQKNLKNSPYDASLGSLHPS-ITLTM-EDKPQPLLGSETES 466
GHR_MOUSE      LKFRQSQKLN-MEADLLCLDQKNLKNLPYDASLGSLHPS-ITQTVEENKPQPLLSSETEA 477
GHR_CAVPO      SEDVQPDKLK-EEADLLCLDEKNQNNSPC-DAPPDPQQA-LVIPPEEEKPQPLLIGKTES 462
GHR_RABIT      SEVAQPQRLK-GEADLLCLDQKNQNNSPYHDVSPAAQQP-EVVLAEEDKPRPLLTGEIES 466
GHR_BOSIN      SEVAQPQRLK-GEADISCLDQKNQNNSPSNDAAPANQQP-SVIHVEENKPRPLLIGGTES 462
GHR_BOVIN      SEVAQPQRLK-GEADISCLDQKNQNNSPSNDAAPASQQP-SVILVEENKPRPLLIGGTES 462
GHR_SHEEP      SEVAQPQRLK-GEADILCLDQKNQNNSPSNDAAPASQQP-SVILVEENKPRPLPIGGTES 462
```

```
GHR_PIG         AEVAQPQRLK-GEADLLCLDQKNQNNSPSNDAAPATQQP-SVILAEENKPRPLIISGTDS  466
GHR_CANLF       SEVAQPQRLK-GEVDLLCLDQKNQNNSPSTDTTPTTQQP-SIILAKENKPRPLLISGTES  466
GHR_AILME       SEVAQPQRLK-GEIDLLCLDQKNQSNSPSTDTAPNTQQP-GVILAKENKPRPLLISGTES  466
GHR_CHICK       SDIDQFKKVTEKEEDLLCLHRKDDVEALQSLANTDTQQPHTSTQSESRESWPPFADSTDS  441
GHR_COLLI       SDIDQFKKVTEKEEDLLCLGRKDNDESLPSLANTDTQQPRMSTRPENSQPWPPFADSIDA  444
                 .  * .::.  * *: ** .*:  :          :         . :  *      ::

GHR_HUMAN       THQAAHIQLSNPSSLSNIDFYAQVSDITPAGSVVLSPGQKNKAGMSQCDMHPEMVSLCQE  526
GHR_PAPAN       THQAAHIQLSNPSSLANIDFYAQVSDITPAGSVVLSPGQKNKAGMSQCDMHLEMVSLCQE  526
GHR_MACMU       THQAAHIQLSNPSSLANIDFYAQVSDITPAGSVVLSPGQKNKAGMSQCDMHLEMVSLCQE  456
GHR_SAIBB       THQAAHIQLSNPSSLANIDFYAQVSDITPAGSVVLSPGQKNNGGMSQWDMHPEVVSLCQA  526
GHR_RAT         THQLPSTPMSSPVSLANIDFYAQVSDITPAGGVVLSPGQKIKAGLAQGNTQLEVAAPCQE  526
GHR_MOUSE       THQLASTPMSNPTSLANIDFYAQVSDITPAGGDVLSPGQKIKAGIAQGNTQREVATPCQE  537
GHR_CAVPO       TNQDAPNQISNPISLANMDFYAQVSDITPAGSVVLSPGQKNKAGLSQCEAHPE------A  516
GHR_RABIT       TLQAAPSQLSNPNSLANIDFYAQVSDITPAGSVVLSPGQKNKAGNSQCDAHPEVVSLCQT  526
GHR_BOSIN       THQAVHHQLSNPSSLANIDFYAQVSDITPAGNVVLSPGQKNKTGNPQCDTHPEVVTSCQA  522
GHR_BOVIN       THQAVHTQLSNPSSLANIDFYAQVSDITPAGNVVLSPGQKNKTGNPQCDTHPEVVTPCQA  522
GHR_SHEEP       THQAVHTQLSNPSSLANIDFYAQVSDITPAGNVVLSPGQKNKTGNPQCDTHPEVVTPSQA  522
GHR_PIG         THQTAHTQLSNPSSLANIDFYAQVSDITPAGSVVLSPGQKNKAGISQCDMHLEVVSPCPA  526
GHR_CANLF       TQQAAHTQLSNPSSLANIDFYAQVSDITLAGSVVLSPGQKNKAGISPCDMPPEVASLCQA  526
GHR_AILME       THQAAHPQLSNPSSLANIDFYAQVSDITPAGSVVLSPGQKNKAGIAPCDMPPEVVSLCQA  526
GHR_CHICK       ANPSVQTQLSNQNSLTNTDFYAQVSDITPAGSVVLSPGQKSKVGRAQCESCTE------Q  495
GHR_COLLI       ASPSAHNQLSNQNSLRNTDFYAQVSDITPAGSVVLSPGQKSKVARARCEFCTE------Q  498
                :       :*.  ** * ********** **. ******* : .    :   *

GHR_HUMAN       NFLMDNAYFCEADAKKCIPVAPHIKVESHIQPSLNQEDIYITTESLTTAAGRPG-TGEHV  585
GHR_PAPAN       DFIMDNAYFCEADAKKCIPVAPHIKVESHIEPSFNQEDIYITTESLTTTAGRPG-TTEHI  585
GHR_MACMU       DFIMDNAYFCEADAKKCIPVAPHIKVESHIEPSFNQEDIYITTESLTTTAGRPG-TTEHI  515
GHR_SAIBB       NFIMDNAYFCEADAKKCIPVTPHIKVESHTEPSFNQEDIYITTESLTTTARRPG-TAEHV  585
GHR_RAT         NYSMNSAYFCESDAKKCIAAAPHMEATTCVKPSFNQEDIYITTESLTTTARMSE-TADTA  585
GHR_MOUSE       NYSMNSAYFCESDAKKCIAVARRMEATSCIKPSFNQEDIYITTESLTTTAQMSE-TADIA  596
GHR_CAVPO       NFVKDNACFFKGDAKNPDVMTPHIEVKSHEEPSFKQEDPYITTESLTTAAEKSG-PPEQS  575
GHR_RABIT       NFIMDNAYFCEADAKKCIAVAPHVDVESRVEPSFNQEDIYITTESLTTTAERSG-TAEDA  585
GHR_BOSIN       NFIVDNAYFCEVDAKKYIALAPHVEAESHVEPSFNQEDIYITTESLTTTAGRSG-TAEHV  581
GHR_BOVIN       NFIVDNAYFCEVDAKKYIALAPHVEAESHVEPSFNQEDIYITTESLTTTAGRSG-TAEHV  581
GHR_SHEEP       DFIVDSAYFCEVDAKKYIALAPDVEAESHIEPSFNQEDIYITTESLTTTAGRSG-TAENV  581
GHR_PIG         NFIMDNAYFCEADAKKCIAMAPHVEVESRLAPSFNQEDIYITTESLTTTAGRSA-TAECA  585
GHR_CANLF       NFIMDNAYFCEADAKKCITVAPHVEAESRVEPSFNQEDIYITTESLTTTAGQSG-TTERA  585
GHR_AILME       NFIMDNAYFCEADAKKCITVAPHVEAESRGEPSFNQEDIYITTESLTTVAGQPG-TAERA  585
GHR_CHICK       NFTMDNAYFCEADVKKCIAVISQEEDEPRVQEQSCNEDTYFTTESLTTTGINLGASMAET  555
GHR_COLLI       NFTLDNAYFCEADVKKCIAVISHEEDEPRVQAQICNEDTYFTTESLTTTGISLGASTAET  558
                ::  :.* * : *.*:        .       .  :** *:*******..

GHR_HUMAN       PGSEMPVPDYTSIHIVQSPQGLILNATALPLPDK-EFLSSCGYVSTDQLNKIMP        638
GHR_PAPAN       PGSEMPVPDYTSIHIVQSPQGLILNATALPLPGK-EFLSSCGYVSTDQLNKIMP        638
GHR_MACMU       PGSEMPVPDYTSIHIVQSPQGLILNATALPLPGK-EFLSSCGYVSTDQLNKIMP        568
GHR_SAIBB       PGSEMPVPDYTSIHIVQSPQGLILNATALPLPDK-EFLSSCGYVAQTN------        632
GHR_RAT         PDAE-PVPDYTTVHTVKSPRGLILNATALPLPDKKKFLSSCGYVSTDQLNKIMQ        638
GHR_MOUSE       PDAEMSVPDYTTVHTVQSPRGLILNATALPLPDKKNFPSSCGYVSTDQLNKIMQ        650
GHR_CAVPO       PSSEMALPDYTSIHIVQSPQGLILNAAALPLPDK-EFLSSCGYVSTDQLNKIML        628
GHR_RABIT       PGSEMPVPDYTSIHLVQSPQGLVLNAATLPLPDK-EFLSSCGYVSTDQLNKILP        638
GHR_BOSIN       PSSEIPVPDYTSIHIVQSPQGLVLNATALPLPDK-EFLSSCGYVSTDQLNKIMP        634
GHR_BOVIN       PSSEIPVPDYTSIHIVQSPQGLVLNATALPLPDK-EFLSSCGYVSTDQLNKIMP        634
GHR_SHEEP       PSSEIPVPDYTSIHIVQSPQGLVLNATALPLPDK-EFLSSCGYVSTDQLNKIMP        634
GHR_PIG         PSSEMPVPDYTSIHIVQSPQGLVLNATALPLPDK-EFLSSCGYVSTDQLNKIMP        638
GHR_CANLF       VSSEMPVPDYTSIHIIQSPRGLVLNATALPLPDK-EFLSSCGYVSTDQLNKIMP        638
GHR_AILME       PSSEIPVPDYTSIHIVQSPRGLVLNATALPLPDK-EFLSSCGYVSTDQLNKIMP        638
GHR_CHICK       PSMEMPVPDYTSIHIVHSPQGLVLNATALPVPEK-EFNMSCGYVSTDQLNKIMP        608
GHR_COLLI       PSPEVPVPDYTSIHIVHSPQGLVLNATALPVPDK-EFNMSCGYVSTDQLNKIMP        611
                 . *  :****::* ::**:**:***::**:* * :*  *****:  :
```

Fig. 11.1. Multiple sequence alignment of the GHR.

Protein sequences of the GHR of multiple species were aligned using the Clustal Omega tool to assess for homology and evolutionary correlation. An asterisk (*) symbolizes fully conserved amino acid residues. A colon (:) stands for conserved amino acid groups sharing strongly similar features, while a period (.) stands for conserved amino acid groups sharing weakly similar features. (GHR_HUMAN: Homo sapiens [Human], UniProt ID: P10912; GHR_PAPAN: Papio Anubis [Olive

baboon], UniProtID: Q9XSZ1; GHR_MACMU: Macaca mulatta [Rhesus macaque], UniProt ID: P79194; GHR_SAIBB: Saimiri boliviensis boliviensis [Bolivian squirrel monkey], UniProt ID: Q95ML5; GHR_RAT: Rattus norvegicus [Rat], UniProt ID: P16310; GHR_MOUSE: Mus musculus [Mouse], UniProt ID: P16882; GHR_CAVPO: Cavia porcellus [Guinea pig], UniProt ID: Q9JI97; GHR_RABIT: Oryctolagus cuniculus [Rabbit], UniProt ID: P19941; GHR_BOSIN: Bos indicus [Zebu], UniProt ID: P79108; GHR_BOVIN: Bos taurus [Bovine], UniProt ID: O46600; GHR_SHEEP: Ovis aries [Sheep], UniProt ID: Q28575; GHR_PIG: Sus scrofa [Pig], UniProt ID: P19756; GHR_CNLF: Canis lupus familiaris [Dog], UniProt: Q9TU69; GHR_AILME: Ailuropoda melanoleuca [Giant panda], UniProt ID: Q96JF2; GHR_CHICK: Gallus gallus [Chicken], UniProt ID: Q02092; GHR_COLLI: Columba livia [Rock dove], UniProt ID: Q90375).

Table 11.1. Percentage identity matrix of the GHR between species.

Homologous relationships of the GHR protein between different species were calculated by applying the hidden Markov model (HMM) algorithm described by Söding (Söding, 2005). The scored values are presented in a percentage identity matrix.

(%)	GHR_HUMAN	GHR_PAPAN	GHR_MACMU	GHR_SAIBB	GHR_RAT	GHR_MOUSE	GHR_CAVPO	GHR_RABIT	GHR_BOSIN	GHR_BOVIN	GHR_SHEEP	GHR_PIG	GHR_CANLF	GHR_AILME	GHR_CHICK	GHR_COLLI
GHR_HUMAN	100.00	94.98	93.84	90.51	69.56	68.34	74.68	83.70	77.13	77.13	77.44	84.17	82.29	82.45	61.36	61.55
GHR_PAPAN	94.98	100.00	98.42	90.19	69.40	68.50	73.89	83.70	77.29	77.29	77.92	83.70	81.35	81.66	61.03	60.89
GHR_MACMU	93.84	98.42	100.00	89.68	68.97	67.78	73.48	82.92	76.77	76.77	77.66	83.10	80.81	81.69	61.26	61.11
GHR_SAIBB	90.51	90.19	89.68	100.00	69.11	67.41	73.95	83.07	77.55	77.55	77.39	83.70	81.01	81.49	59.63	60.17
GHR_RAT	69.56	69.40	68.97	69.11	100.00	89.34	66.67	73.97	71.75	72.06	71.43	74.45	73.50	74.13	58.50	58.04
GHR_MOUSE	68.34	68.50	67.78	67.41	89.34	100.00	64.81	72.26	70.35	70.66	70.50	73.04	73.20	73.35	57.95	57.17
GHR_CAVPO	74.68	73.89	73.48	73.95	66.67	64.81	100.00	76.75	74.36	74.52	73.56	77.07	75.80	75.00	59.10	58.97
GHR_RABIT	83.70	83.70	82.92	83.07	73.97	72.26	76.75	100.00	82.02	82.18	81.86	88.71	87.15	86.83	62.69	63.04
GHR_BOSIN	77.13	77.29	76.77	77.55	71.75	70.35	74.36	82.02	100.00	99.05	96.85	86.12	83.28	83.28	60.23	60.10
GHR_BOVIN	77.13	77.29	76.77	77.55	72.06	70.66	74.52	82.18	99.05	100.00	97.48	86.59	83.60	83.44	60.40	60.26
GHR_SHEEP	77.44	77.92	77.66	77.39	71.43	70.50	73.56	81.86	96.85	97.48	100.00	86.59	82.97	83.12	60.23	59.93
GHR_PIG	84.17	83.70	83.10	83.70	74.45	73.04	77.07	88.71	86.12	86.59	86.59	100.00	90.75	90.60	64.01	63.70
GHR_CANLF	82.29	81.35	80.81	81.01	73.50	73.20	75.80	87.15	83.28	83.60	82.97	90.75	100.00	93.57	62.69	62.38
GHR_AILME	82.45	81.66	81.69	81.49	74.13	73.35	75.00	86.83	83.28	83.44	83.12	90.60	93.57	100.00	63.02	63.04
GHR_CHICK	61.36	61.03	61.26	59.63	58.50	57.95	59.10	62.69	60.23	60.40	60.23	64.01	62.69	63.02	100.00	90.95
GHR_COLLI	61.55	60.89	61.11	60.17	58.04	57.17	58.97	63.04	60.10	60.26	59.93	63.70	62.38	63.04	90.95	100.00

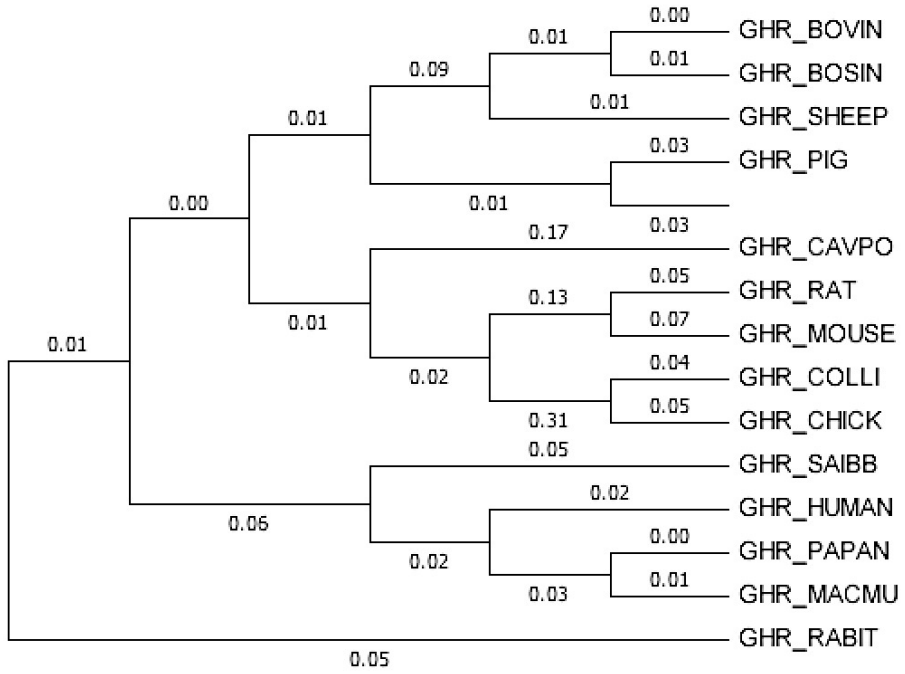

Fig. 11.2. Phylogenetic tree of the GHR between species.

Evolutionary origins of the GHR were calculated in MEGA7 (molecular evolutionary genetics analysis 7) software using the Neighbor-Joining method with Poisson correction. (GHR_HUMAN: Homo sapiens [Human], UniProt ID: P10912; GHR_PAPAN: Papio Anubis [Olive baboon], UniProtID: Q9XSZ1; GHR_MACMU: Macaca mulatta [Rhesus macaque], UniProt ID: P79194; GHR_SAIBB: Saimiri boliviensis boliviensis [Bolivian squirrel monkey], UniProt ID: Q95ML5; GHR_RAT: Rattus norvegicus [Rat], UniProt ID: P16310; GHR_MOUSE: Mus musculus [Mouse], UniProt ID: P16882; GHR_CAVPO: Cavia porcellus [Guinea pig], UniProt ID: Q9JI97; GHR_RABIT: Oryctolagus cuniculus [Rabbit], UniProt ID: P19941; GHR_BOSIN: Bos indicus [Zebu], UniProt ID: P79108; GHR_BOVIN: Bos taurus [Bovine], UniProt ID: O46600; GHR_SHEEP: Ovis aries [Sheep], UniProt ID: Q28575; GHR_PIG: Sus scrofa [Pig], UniProt ID: P19756; GHR_CNLF: Canis lupus familiaris [Dog], UniProt: Q9TU69; GHR_AILME: Ailuropoda melanoleuca [Giant panda], UniProt ID: Q96JF2; GHR_CHICK: Gallus gallus [Chicken], UniProt ID: Q02092; GHR_COLLI: Columba livia [Rock dove], UniProt ID: Q90375).

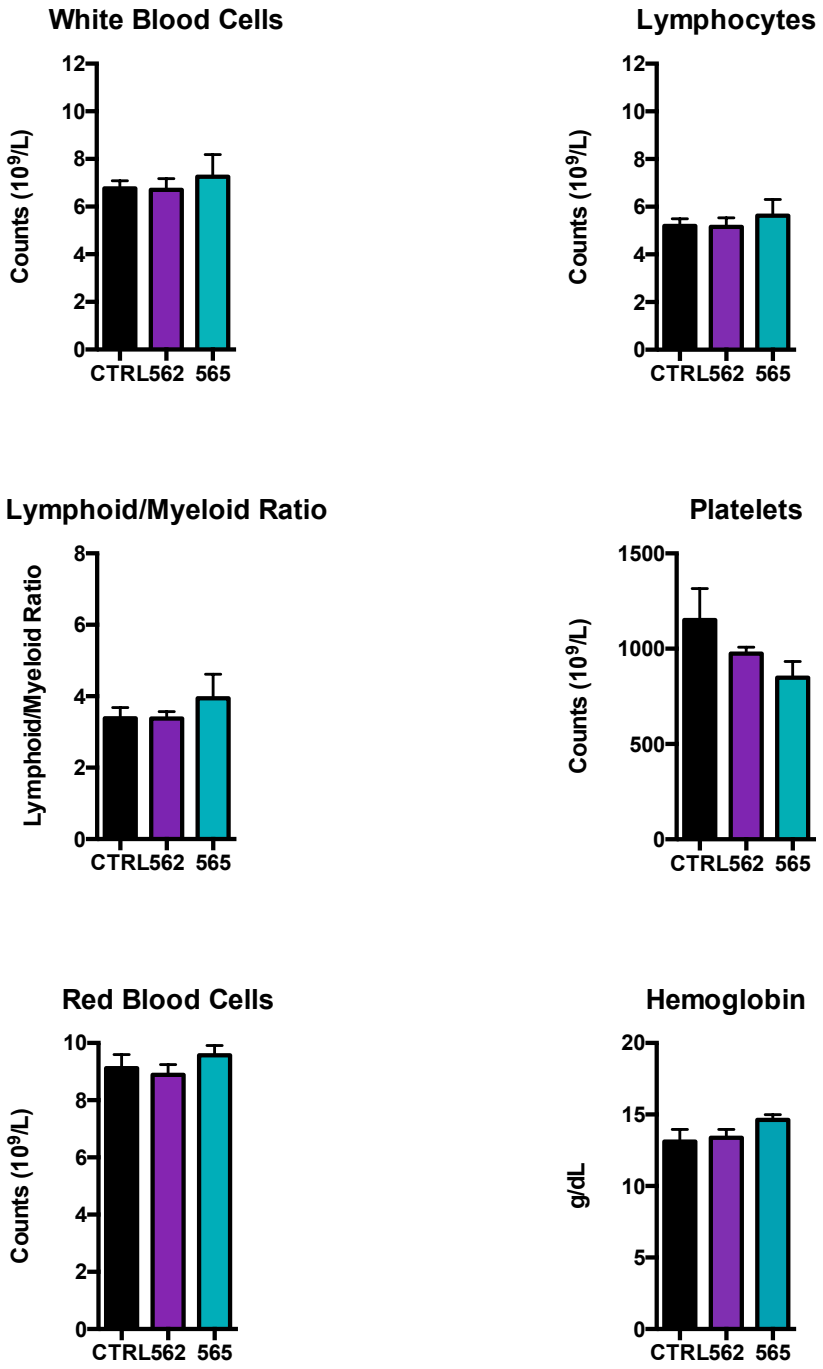

Fig. 11.3. CBC of C57BL/6 mice treated with α-GHR562 and/or α-GHR565.

Complete blood count of mice after treatment with the respective mAbs. Whole blood was collected, processed and subjected to analysis. White blood cells, lymphocytes, lymphoid/myeloid ratio, platelets, red blood cells, as well as hemoglobin levels were assessed. Data was analyzed by an unpaired t-test. However, no significance could be determined.

12. Acknowledgements

Undergoing this journey has been a mind-changing process with ups and downs. Nonetheless, it taught me how to persevere and not to be afraid of change during times when I did not feel in control of life. The determination to overcome tough obstacles of any kind and the realization that embracing the challenge provides strength was key to achieve goals.

I would like to express my sincere gratitude to my advisor Dr. Shirley Knauer for the continuous support, patience, encouragement, and motivation during my research studies. Her guidance helped me to broaden my horizon and overcome challenges. My sincere thanks also goes to Dr. Valter Longo, who provided me an opportunity to join his laboratory at USC and conduct this research. I would like to thank Dr. Min Wei for his supervision and reading the manuscript, and Dr. Hong Seok Shim for the countless discussions and critical questioning which incented me to widen my research focus. I want to thank my fellow labmates Drs. Chia-Wei Cheng, Hamed Mirzaei, Novella Guidi, Roberta Buono, and Sebastian Brandhorst for being part of this journey. I especially want to thank Gerardo Navarrete and Priya Rangan for all the talks, advice, inspiration and laughs we have had during the past few years. Patty, thank you for always lending a helping hand, listening when I needed someone to talk to, and putting a smile on my face.

Chris, Dem, Yani, and Jordan: Thank you for always making me feel welcome and cared for, and being family over the past few years. I appreciate you for being such an important part of my life. I am blessed to have had the chance to get to know you. Thank you for giving me advice, supporting me through every circumstance that I had to face, and smiling with me during the highs of my life. Molly, thank you for always being there for me, for understanding me, and accepting me for who I am.

Last but not least, I want to thank my amazing parents and siblings for supporting me throughout this journey and my life. I am beyond glad to be part of this wonderful family.

13. Curriculum Vitae

Der Lebenslauf ist in der Online-Version aus Gründen des Datenschutzes nicht enthalten.

14. Eidesstattliche Erklärungen

Erklärung:

Hiermit erkläre ich, gem. § 7 Abs. (2) d) + f) der Promotionsordnung der Fakultät für Biologie zur Erlangung des Dr. rer. nat., dass ich die vorliegende Dissertation selbständig verfasst und mich keiner anderen als der angegebenen Hilfsmittel bedient, bei der Abfassung der Dissertation nur die angegeben Hilfsmittel benutzt und alle wörtlich oder inhaltlich übernommenen Stellen als solche gekennzeichnet habe.

Werne, den _____ _____

Unterschrift des/r Doktoranden/in

Erklärung:

Hiermit erkläre ich, gem. § 7 Abs. (2) e) + g) der Promotionsordnung der Fakultät für Biologie zur Erlangung des Dr. rer. nat., dass ich keine anderen Promotionen bzw. Promotionsversuche in der Vergangenheit durchgeführt habe und dass diese Arbeit von keiner anderen Fakultät/Fachbereich abgelehnt worden ist.

Werne, den _____ _____

Unterschrift des/r Doktoranden/in

Erklärung:

Hiermit erkläre ich, gem. § 6 Abs. (2) g) der Promotionsordnung der Fakultät für Biologie, Chemie und Mathematik zur Erlangung des Dr. rer. nat., dass ich das Arbeitsgebiet, dem das Thema „Investigation of Monoclonal Antibodies Generated against the Growth Hormone Receptor on Growth Hormone Signaling“ zuzuordnen ist, in Forschung und Lehre vertrete und den Antrag von Esra Guen befürworte und die Betreuung auch im Falle eines Weggangs, wenn nicht wichtige Gründe dem entgegenstehen, weiterführen werde.

Essen, den _____ _____

Unterschrift eines Mitglieds der Universität Duisburg-Essen